Rainfall in West Central Africa

By
Samuel Mbele-Mbong

Department of Atmospheric Science
Colorado State University
Fort Collins, Colorado

This progress report was prepared with support from the National Science Foundation
(Contract No. GA-29147)
Principal investigator: E.R. Reiter
April 1974

Colorado State University

Department of Atmospheric Science

Paper No. 222

RAINFALL IN WEST CENTRAL AFRICA

By

SAMUEL MBELE-MBONG

This progress report was prepared with support from
The National Science Foundation
(Contract No. GA 29147)
Principal Investigator: E. R. Reiter

Department of Atmospheric Science
Colorado State University
Fort Collins, Colorado

April, 1974

Atmospheric Science Paper No. 222

ABSTRACT

An estimation of the relative importance of various factors to the rainfall in West Central Africa has been attempted. The factors considered were tropical waves, monsoon depressions, the position of the intertropical discontinuity (ITD) and the tropical easterly jet stream (TEJ) of summer. Eleven years (1954-1964) of daily rainfall amounts at 20 stations in Cameroun, Central African Republic, Congo, Gabon and Tchad were analyzed using spectral and cross spectral methods.

The spectral results revealed the presence, at nearly all stations, of wavelike oscillations with periods ranging from 2.03 to 10.25 days, and periods of about 40 days or longer. Oscillations with periods 2.58 to 4.21 days and those with periods 40 days or longer showed significant coherence magnitudes and propagated from East to West with approximate wave lengths of 500 and 2000 km, respectively. Oscillations with periods 2.58 to 4.21 days have been interpreted as cloud clusters, very likely of the "disturbance line" type which usually associate with easterly waves. Oscillations with period 40 days have been tentatively interpreted as major rain-generating disturbances, perhaps of the monsoon depression type which are observed over the region in the summer months (June through September) when most of the rains fall.

Preliminary indications are that the dominant factors in the rainfall of this part of Africa are the position of the ITD and the presence and speed oscillations of the TEJ.

Samuel Mbele-Mbong
Atmospheric Science Department
Colorado State University
Fort Collins, Colorado 80521

TABLE OF CONTENTS

TABLE OF CONTENTS - Continued

LIST OF TABLES

LIST OF FIGURES

LIST OF FIGURES - Continued

LIST OF FIGURES - Continued

Chapter 1

INTRODUCTION

1.1 Relevance of rainfall studies

The primary atmospheric process in tropical latitudes is convection. According to Yanai (1971), most of the atmospheric eddy kinetic energy is derived by conversion from eddy available potential energy, $-\overline{(\alpha'\omega')}$, where α is the specific volume and ω the vertical p-velocity. The source of this potential energy, neglecting storage, is given by

$$-\overline{(\alpha'\omega')} = -\frac{f}{s}\frac{\partial \bar{u}}{\partial p}\overline{(v'\alpha')} + \frac{R}{C_p s}\overline{(\alpha'Q')} \qquad (1)$$

where s is the stability, Q the diabatic heating rate per unit mass of air and the other symbols follow convention. The first term on the right hand side is the baroclinic term, the second term the convective term, since most of the diabatic heating derives from the release of the latent heat of condensation. The baroclinic term prevails in middle latitudes as a consequence of the strong meridional temperature gradients; the convective term predominates in the tropical latitudes (Nitta, 1970) as a result of the widespread presence of conditional instability.

In addition to providing kinetic energy to the disturbances--as further verified by numerical experiments which showed that the tropical tropospheric circulation is many times more intense with than without it (Manabe, Holloway and Stone, 1970) -- the release of the latent heat

of condensation possibly plays a significant role in the vertical structure of the disturbances (Wallace, 1972).

Furthermore, rainfall amounts and rates are known to be related to the life cycle of individual convective clouds comprising meso- and synoptic-scale disturbance systems (Garstang, 1966). Although the nature of this relation remains one of the outstanding problems in tropical meteorology to date, rainfall studies should give some indication of the zone of maximum convection activity--perhaps orographically enhanced--and its time variation.

The time and space distributions of rainfall affect the agricultural production, the livestock, the water supply, indeed the whole economy of a region, and the whole existence of its people. That rainfall variability can become critical, and sometimes disastrous is illustrated by a report (GICAM, 1969) on the agricultural production in Cameroun for the year 1967-68, and dramatized by the recent drought in, among other parts, the Sahelian zone of West and Central Africa.

The report read in part:

> The Arabica coffee season of 1967-68. . . unfavorably influenced by the drought from December 1966 to March 1967. . . produced 4000 tons in West Cameroun (6000 tons in 1966-67) and 8000 tons in East Cameroun 14200 tons in 1966-67). The cotton season of 1967-68 registered a new decrease in production (49,085 tons of grain against 55,810 in 1966-67 and 57,444 in 1965-66 due to the shortest rainy season recorded in 24 years . . . The production of industrial palm oil in East Cameroun decreased from 1523 tons in 1965 to 1426 tons in 1966 and 1384 tons in 1967, and that of palm-nuts from 1126 tons to 1107 tons and 1047 tons, respectively, in consequence of a bad distribution of the rains in 1967.

The Sahel is a 2600-mile (3000 km) stretch of Africa bordering the southern edge of the Sahara Desert. It includes parts of six countries with an estimated population of 30 million: Mauritania, Senegal, Mali, Upper Volta, Niger, Tchad (Fig. 1). Droughts have afflicted the Sahel before, e.g., in 1910-1914, and in 1941-42; but the current one which has also hit a one-thousand-mile-long belt in Northern Nigeria, and whose effects have been felt in Northern Cameroun and as far east as Ethiopia, has been going on for more than five years, and has been characterized as "the worst in 60 years, perhaps ever" (Rosenthal, 1973a, Winstanley, 1973).

One immediate effect has been a near crippling of the economies of the area. For example, estimates were that the six nations have lost half of their GNP, and that reaching previous levels of economic growth may take at least five years. At the height of the drought, Senegal harvested only one-third of its normal crops and about 40 percent of its livestock died. Upper Volta lost some 35 percent of its livestock, Mauritania about 60 percent of its herds, and latest reports (1973) were that about 35 to 80 percent of all animals in the Sahel have perished. Another short range effect was the depletion of the water resources of the region. The Niger River reached its lowest level in nearly 40 years to the extent that water barges and boats which supply Tombouctou with food and other essentials could not reach the city in the desert; and at Niamey, the Niger could be crossed on foot for the first time in history. Lake Tchad had less water in it than at any time since 1943 (Rosenthal, 1973b; Derrick, 1973, Skinner, 1973).

The result has been widespread famine, malnourishment and death. An FAO official for African Affairs estimated in May 1973 that "out of the population of 30 million in the six countries, about one-third are now weakened by hunger and malnutrition, and some people are dying" (Bryson, 1973, p. 2). A regional director of the UN Economic Commission for Africa feared that "if the problem is not solved in two months, nearly six million people may die" (Newsweek, June 4, 1973). According to the latest reports, one million men, women and children may be already dead (Skinner, 1973).

Because "it has been very difficult to bring aid to the more remote areas, millions of people have been forced to move elsewhere to avoid starvation in what is the greatest migration in recent African history" (Derrick, 1974, p. 50).

From a long-range standpoint, one of the worst effects of the drought has been the accelerated southward advance of the Sahara Desert made possible by the destruction of trees by herdsmen to supply leaves to their hungry livestock, and by the slowed or killed growth of the trees and scanty vegetation due to the lack of moisture. AID experts estimate that more than 250,000 square kilometers of arable land have been forfeited in the last 50 years to the Desert which, in some parts of the Sahelian zone, has moved south at the frightening rate of 30 miles per year (Rosenthal, 1973b).

From the above, it is seen that characteristics of the rainfall in West and Central Africa may be viewed as relevant potentials for guidance not only in future studies of convective systems and fixed atmospheric volumes over the region, but above all, in agricultural development and hydrologic design, in planning the utilization and

protection of water and land resources, and social activities, and in many other problems for which rainfall climatologic information is valuable (Cochemé and Franquin, 1967).

1.2. Review of literature on primary features of the large-scale circulation and disturbances of West Central Africa

1.2.1. Primary features of large-scale circulation of West Central Africa

Large-scale features of the tropospheric circulation of this part of the tropics have been identified by researchers working, or interested, in West Central Africa. The following sections briefly summarize the present knowledge of phenomena and problem areas of interest to the rainfall activity in the region.

Figure 2 shows the location of the study area. The locations of the rainfall stations are seen in Figure 3 and in Appendix II. The summer and wintertime tropospheric circulation features in the area are depicted by average maps of resultant winds (Fig. 4), meridional cross sections of zonal winds (Fig. 5), sea-level pressure and prevailing air currents (Fig. 6), and of rainfall (Fig. 7).

The primary entities of the large-scale circulation, as depicted, are the following: (1) the semi-permanent and quasi-stationary subtropical anticyclones; (2) the Intertropical Discontinuity (ITD) and associated air currents; (3) the mid-tropospheric easterly wind maximum; and (4) the upper-tropospheric easterly jet stream (Germain, 1956).

1.2.1.1. Subtropical anticyclones

The mean surface positions of the subtropical anticyclones are seen in Figures 8 and 9, together with the associated air-mass boundaries (Dhonneur, 1971). The Azores High is located farthest south in January-February, and reaches its northernmost position in July-August.

The Sahara High, absent below 700 mb in summer when a heat low replaces it over that Desert, is permanent above the 700 mb level and often combines with that of the Azores when the flow over Northern Africa is little perturbed (Fig. 9). The Saint Helena high has smaller variations in pressure and seasonal movement than the other two. Its average position, nearer to the equator, is such that this center always affects the coastal areas of the Golf of Guinea, being farthest to the south and to the north in January and in July, respectively (Fig. 9).

A relationship has been established between the latitude of the Azores-Sahara anticyclone and that of the ITD (Fig. 10). The anticyclones are present at 850 mb both in January and July (Fig. 4, a and b). At 200 mb, they are well defined and located more over the continent (Fig. 4, c and d). It is a current feeling that the Sahara anticyclone at 200 mb during summer forms as a consequence of the blocking influence of the Tibetan thermal high on the mean zonal flow (Krishnamurti, et al., 1973).

1.2.1.2. Intertropical Discontinuity (ITD)

Changes in the extent and positions of the subtropical anticyclones directly affect the movement, as well as the characteristics of the intertropical discontiniuty.

Over tropical oceanic regions lies a trough of low pressures between the subtropical high pressure belts, which is called "the intertropical trough (ITT)." It extends approximately east-west, with the northeast trades to its north, and the southeast trades to its south. When the two trades meet and converge, as they do over ocean

areas, the ITT becomes a narrow zone of convergence, the Intertropical Convergence Zone (ITCZ). However, over large land masses such as Africa and Asia, no narrow zone of low pressure is found where the trades meet. Instead, one finds a wide belt of thermal lows with a definite cyclonic circulation. Studies of conditions over Africa (Soliman, 1960) reveal that the air mass forming the thermal lows is very hot and dry. This belt of hot air is separated on its south from relatively cool and moist air of Southern hemisphere origin by a discontinuity line known as the "Intertropical Discontinuity." The southeast trades, after crossing the equator, blow as southwest winds (southwest monsoon). The ITD is therefore the northern boundary of the southwest monsoon. The surface position of the boundary is regularly drawn on synoptic charts in three distinct parts identified on the basis of the properties of the air masses present (Fig. 11). The ITD slopes upward toward the equator (Fig. 12). Located on the surface at about 22^{o}N in July - August, the ITD is at 15^{o}N at 850 mb, and at 700 mb at approximately 5^{o}N. This represents a mean slope of about 1 in 500. To the north of the front winds are easterly at all levels, whereas to the south of it, winds are southwesterly or westerly (monsoon) at low levels (up to 700 mb).

The ITD undergoes "three distinct and superimposed movements. . . differing both in amplitude and duration" (Sansom, 1965, p. 96).

The diurnal movements consist of shifts southward during the morning and northward in the afternoon with an average amplitude of about 200 km. Nevière (1959a) has associated this oscillation with the differential diurnal heating cycle which causes significant local changes in the surface pressure distribution.

The seasonal migration has been linked to the thermally induced equatorial surface pressure trough. This trough moves through greater distances over continents than over oceans. But in West Africa, its movement is restricted by the absence of land masses south of the equator. Accordingly, at these longitudes, the ITD does not follow the sun into the southern hemisphere; instead, it oscillates between about 3^{o} N in January and 20^{o} N in July - August (Adejokun, 1963; Clackson, 1957; Obasi, 1965; Gleave and White, 1969; Hubert, et al., 1969; Surand, 1954). The characteristics of this seasonal movement vary considerably from year to year, and differ somewhat over the study area (Fig. 13).

Soliman (1960, p. 140-141), has given additional features of the seasonal evolution of the ITD at the surface:

> In winter the northeast winds over northern Africa penetrate to about 20^{o} N where they turn to easterly and are separated from the very hot air forming the thermal low by the subtropical Front (STF) (Fig. 14a). The hot air forming the thermal low originates as a southeast/east current from the Gulf of Aden, then completes its cyclonic curculation around the Sudan trough to northeast, and flows as hot easterly winds over the Sahara. . . The ITF is least marked and active, being more a "humidity" discontinuity over the south coast of West Africa.
>
> In spring the area of thermal lows shifts northward over Africa with the apparent movement of the sun, and the prevailing air currents and location of the ITF . . . are as shown in Fig. 14b. . . .The baroclinity of the ITF is more than in winter.
>
> In summer the huge Asiatic low sets in while the low pressure over Africa suffers further northward shift (Fig. 14, c and d). The baroclinity of the ITF is large . . . In consequence, an easterly jet is formed just south of the ITF. . . The temperature field suggests one jet stream from India to Africa passing south of Aden. . . .

> In autumn. . . the conditions are very similar to those in spring, with the only difference that the average location of the thermal belt, and in consequence the ITF, are a little farther north in autumn (Fig. 14e).

The intermediate oscillations, with an amplitude around an average seasonal position of several hundred kilometers and a duration of several days have been associated with pressure perturbations on a synoptic scale. This movement is often observed during northern hemisphere winter months when temperate-latitude upper westerlies are blocked over Europe and baroclinic disturbances propagate eastward across northern Africa (Johnson, 1964, 1965; Haudecoeur, 1965).

French meteorologists working in Equatorial Africa have identified two other discontiniuty lines, namely the front intertropical sud (FIT sud), and the front équatorial Africain (FEA). A scheme by Tschirhart (1959) shows the surface positions of the three African discontiniuties in the extreme seasons (Fig. 15). During northern hemisphere summer when it is most marked, the FIT sud or ITD south separates the humid westerlies from the drier easterlies of the Kalahari Desert. The FEA is the boundary between two air masses of oceanic origin, one from the Atlantic Ocean, the other from the Indian Ocean. This discontiniuty has been reported to be often active and to move seasonally from west to east, its extreme positions being 15^{o} E in January, and 35^{o} E in July (Dhonneur, 1971; Soliman, 1960). It is worth repeating that the ITD as described above is found only over the African continent (Soliman, 1960). It differs from the Intertropical Convergence Zone (ITCZ) whose formation and location have been the subject of recent theoretical studies (Bates, 1970;

Charney, 1969, 1972; Chang, 1973; Kuo, 1973). According to these authors the ITCZ is a narrow (about 100 km) east-west zone, roughly parallel to the equator, but lying some distance (usually 5-10^{o} away) from it. In this zone air from one hemisphere converges against air from the other hemisphere to produce deep, intense, concentrated cumulus and cumulonimbus convection extending to the tropopause as seen from meteorological satellite photographs, together with heavy precipitation.

The zone of rainfall-producing, rising motions concentrated in vigorous Cb convection is, over Africa, found within the monsoon flow, some distance south of the surface position of the ITD (Sadler, 1972).

1.2.1.3. Monsoon

In West and Central Africa, the air of southern hemisphere origin of which the ITD forms the northern boundary, is called the monsoon (Walker, 1960). It is part of the equatorial west wind zone also found over the Philippines and north of New Guinea.

In West Africa, the southeast trades crossing the equator flow continuously from high pressure in the southern hemisphere (Saint Helena High) to low pressure in the northern hemisphere. Hence, they turn and appear as westerlies in the northern hemisphere. The turning is consistent with the dynamic principle of conservation of absolute vorticity (Schmidt, 1951).

The monsoon circulation, present all year over the coastal fringes, becomes particularly established during the summer months when it reaches quite far to the north (Tucker, 1964, Struning and Flohn, 1960).

It has been shown (Flohn, 1960, 1964) that for tropical latitudes ($\phi<23^{o}$), winds with westerly and/or poleward components have a statistical tendency for lifting, and accordingly for thermal instability and for high rainfall frequency.

1.2.1.4. Mid-tropospheric easterly wind maximum

Surface temperature reach a maximum over the Sahara Desert during July - August, but change very little from season to season near 5^{o}N over West Africa, due in part to oceanic influence (Thompson, 1965; Berrit, 1961, 1962; Burpee, 1972). The meridional surface temperature gradient accordingly, is strongest during the summer months. Meridional cross sections show that the temperature in the middle troposphere is nearly uniform from the equator to 25^{o}N. On the other hand, a latitudinal cross section of monthly mean zonal winds near $10\text{-}15^{o}$N (figs. 5 and 16), reveals a westerly shear of the wind from 600 to 400 mb. By geostrophic inference, this shear indicates the presence of warm air equatorward and cool air poleward of $10\text{-}15^{o}$N. In response to the surface baroclinic zone and the reversal of the temperature gradient in the middle troposphere an easterly wind maximum develops near 600 mb (Burpee, 1972). According to Nevière (1959b), this easterly wind maximum is found on the average at a height of about 3-6 km and a distance of the order of 100-200 km south of the ITD; it is about 1500 km long, 2-6 degrees of latitude wide and 2-3 km deep; longitudinal (east-west) and normal shears are about 1.5 and 10 m sec^{-1}/500 km, respectively.

A certain relationship with the weather sequence and rainfall seems to exist (Nevière, 1959b).

1.2.1.5. Tropical Easterly jet stream (TEJ)

As is evident from cross sections of the zonal wind along 10°E (Fig. 5) a well developed easterly jet stream is found over West and Central Africa near 150 mb (Soliman, 1960). The magnitude of the mean wind vector at this level is, on the average, about 20 m sec^{-1} in July. Figure 17 shows an analysis of the 100-mb isotachs and streamlines for a particular day in July 1955. According to this analysis, an easterly, jet stream maximum with velocities of 30m sec^{-1} (60 knots) appears over the African West Coast (Koteswaram, in Reiter, 1961; see also Altantawy, 1964; Flohn, 1964).

The presence of this jet stream on mean charts indicates its quasi-stationary character. Furthermore, it is considerably intense only during summer. During winter months, only an easterly wind maximum with zonal speeds of the order 10 m sec^{-1} is found over West Central Africa, with the axis close to the equator (Fig. 5). This locally and seasonally confined existence of the easterly jet stream over Africa points to an association with the West African summer monsoon and with theITD which in summer is displaced far to the north. It seems likely that the easterly jet stream draws its kinetic energy from the Sahara anticyclone on the eastern slopes of which air masses flowing south carry along easterly angular momentum (Reiter, 1963), and from the latent heat released by wave disturbances (Carlson, 1971). Similar mechanisms have been proposed for the maintenance of the easterly jet stream over India (Flohn, 1964).

1.2.2 Disturbances of West Central Africa

In relation to the large-scale features of the mean tropospheric circulation described above, meteorologists working in or studying this part of Africa have identified several synoptic- and meso-scale weather systems. In the zone to the south of the ITD are found the following disturbances: the eastward-moving thundery formations of the Congo Basin associated with the FEA; the westward-moving disturbance lines, cyclonic vortices and easterly waves in association with the depth and strength of the monsoon, the mid-tropospheric easterly wind maximum and the easterly jet stream. To the north of the ITD troughs in the upper subtropical westerlies occasionally move eastward in conjunction with flow conditions in the temperate-latitude upper westerlies (Obasi, 1966).

1.2.2.1. Eastward-moving thundery systems

In the scheme illustrated in Figure 15, the equatorial African discontinuity (FEA) is indicated as dividing moist westerlies from moist easterlies. Jeandidier and Rainteau (1957) call this divide the boundary of the monsoon and report that eastward-moving thundery disturbances often develop, either near it, or within the westerly flow as a result of a surge in the monsoon (strengthening of the westerlies) in conjunction with the intensification of the Saint Helena High.

1.2.2.2. Westward-moving disturbance lines (DL)

Of the disturbances in the zone to the south of the ITD, the best known is the "disturbance line" (DL, ligne de grains), also called squall line and fast wave (Dhonneur, 1971; Eldridge, 1957, Hamilton and Archbold, 1945; Johnson, 1964; Nevière, 1959b; Tschirhart, 1958).

It consists of a line of thunderstorms, 300-500 km in length, oriented roughly north-south, and moving westwards against the low-level monsoon in which it is imbedded. Near the coast, the gusts in the squall are 30-40 knots (Okulaja, 1970), but they may reach up to 60 knots in the north where, with a dry surface, they raise a curtain of dust (harmattan haze). The speeds of movement are fairly uniform, being of the order of 25 knots, i.e., the speed of the easterlies near 700 mb (Sadler, 1972). The disturbed upper-level wind field (Fig. 18) is such that ahead of the disturbance speeds are light in the middle troposphere (600-400 mb) and high in the upper troposphere (300-200 mb). The reverse is observed to the rear of the squall line.

Disturbance lines occur in all months. But in the coastal latitudes, the most vigorous ones develop in May-June and September-October, being rare in July-August. Farther north, for instance in the Lake Tchad area, peak frequency is reached in July-August (Johnson, 1964). These differences are easily resolved if it is noted that DL's are more frequent and most developed in those areas where the monsoon is neither too shallow, nor too deep. During those months when the southwest monsoon extends farthest north, the lower-level southwesterlies are overlain by dry and hot winds from the Sahara, with easterlies in the high troposphere (Fig. 4). Near its northern limits (e.g., Lake Tchad area in May-June and September-October), the monsoon is normally too shallow for significant convection to occur, while farther south (e.g., Guinea Coast in July-August) the moist layer is too deep for marked instability to be present. The DL's occur between these two positions, "where moderately deep moist air is available and, with the

dry overrunning current, pronounced convective instability is present" (Palmen and Newton, 1969, p. 464).

While the exact mechanism of the formation of the DL's has not been established, development from afternoon convection is not uncommon; some persist through the night and a few start at night (Eldridge, 1957; Bisseck, 1968). DL's have been related to westward-moving pressure waves. (Johnson, 1964). Bernet (1968) has shown that the following synoptic conditions are favorable to the formation of DL's in Central Africa: (i) a particular streamline configuration near 700 mb in relation to that near 500 mb; (ii) the acceleration of the 700-mb current, (iii) a marked static stability of the air masses. Hamilton and Archbold (1945) were the first to suggest that the DL's propagate as gravity waves, with speeds depending on the height and intensity of the interface between the moist layer and the overlying drier and warmer air. Barrefors (1966) drew a parallel between the moist monsoon flow within which the DL's form and a shallow water flow. Then using shock wave theory, he derived a one-dimensional quantitative model of DL's as gravity waves on the ITD.

Okulaja (1970) has suggested a dependence of the disturbance line on the amplitude of an easterly wave near 700 mb, wherein thunderstorm activity along the line decreases as soon as the "sustaining parent wave" at 700 mb breaks or collapses. According to this view, the disturbance line is a "linear perturbation forming an integral part of the easterly wave perturbation" (p. 667) which, once formed, moves faster than the wave.

Sadler (1972) has related the formation of disturbance lines to the circulation associated with cyclonic vortices which continually form on the upper level ITD where the slope of the front attains its maximum value, i.e., near 700 mb. When the circulation associated with the vortices inject sufficient moisture into the overlying dry easterlies, disturbance lines result which, if sufficiently strong, will penetrate down to the surface.

1.2.2.3. Westward-moving tropical waves

Traced on satellite and wind data, waves in the low troposphere propagate westwards across West-Central Africa into the Atlantic Ocean between May and October, and occasionally reach the eastern Pacific (Carlson, 1969a, 1969b, 1971; Burpee, 1972; Arnold, 1966; Erickson, 1963).

By power-spectrum analysis of the zonal and meridional winds at Khartoum (15°36'N, 32°33'E), Fort Lamy (12°8'N, 15°2'E), and Dakar (14°44'N, 17°31'W), Burpee (1972) studied the energy source, the region of origin, and the structure of these waves. His analysis of five years of data showed that these low tropospheric disturbances, which form in conjunction with the low troposphere east winds maximum, produce a significant spectral peak in the meridional wind at periods 3-5 days with a maximum aplitude of 1-2 m sec $^{-1}$near 700 mb. The waves originate "east of 30°E" (Okulaja, 1970), between Khartoum and Fort Lamy, and from the phase difference between neighboring stations, were found to have a wavelength of about 4000 km. However, from both synoptic analysis and satellite pictures, other investigators have estimated the wavelength at 2000 km (Carlson, 1969a; Okulaja, 1970). Burpee attributed the disagreement between the two wavelengths to the lack of uniformity in the propagation of the waves. By computing the phase difference of the 700 mb wind component between Fort Lamy and Bangui (4°23'N, 18°34' E) and between Niamey (13°29'N, 2°10' E) and Lagos (6°35'N, 3°29;E), Burpee found that the trough axis of the wave tilts eastward with height, and cold air is behind it, up to 700 mb; the trough axis tilts westward with height and warm air is behind it

above 700 mb. The horizontal axis of the disturbance was determined to be directed from southwest to northeast in the southern part of the zone of maximum activity.

Charney and Stern (1962) have shown that where the meridional gradient of potential temperature (θ) vanishes at the ground, the vanishing of the mean potential vorticity along an isentropic surface is a necessary condition for instability of the zonal flow.

Burpee estimated the potential vorticity on an isentropic surface using:

$$P = -\left(\frac{\partial u}{\partial y}\right) + f\, g\frac{\partial \theta}{\partial p}$$

where P is the mean potential vorticity, f the Coriolis parameter, g the acceleration of gravity, u the zonal component of velocity, θ the potential temperature, and y the south-north distance. He found that P was a maximum along the isentropes at 5^{o}E on the equatorward side of the midtroposphere wind maximum from June to October, thereby establishing the necessary condition for instability at the same season and in the same zone where the waves were found.

Burpee further determined a transport of easterly momentum from the low-level easterly wind maximum and a transport of heat down the temperature gradient by the waves. These transports led him to suggest that both the vertical and horizontal shears of the mean zonal wind may be the energy source for the waves.

The integral criterion derived by Charney and Stern requires that $\frac{\partial P}{\partial y}$ change sign somewhere in the fluid. Burpee made estimates of the individual terms in the meridional gradient of P using terms evaluated at 700 mb from the monthly mean cross sections for August at 5^{o}E. The

results showed that, in those latitudes where waves were observed, both the vertical and horizontal shear terms were negative and greater than β, thereby indicating that both the vertical and horizontal shear of the mean flow could be a source of energy.

Krishnamurti (1972) has suggested a combined barotropic baroclinic instability to be the energy source.

1.2.2.4. Eastward-moving troughs in the upper-subtropical westerlies

Eastward-moving troughs in the upper-subtropical westerlies to the north of the ITF are most likely during those winter periods when temperate-latitude westerlies are blocked over Europe. At 500 mb, the troughs sometimes penetrate as far south as 10^{o}N. In many cases, the associated surface lows track eastward over North Africa, weakening the subtropical high pressure center and activating heat lows over the Sahara.

In response, the ITF shifts several kilometers northwards of its average seasonal position, the dry surface north-easterlies being replaced for several days by moister south-westerlies. Unseasonable thunderstorm activity often results.

1.2.3. Summary and problem to be studied

The primary features of the mean tropospheric circulation above West Central Africa include:

(1) at the surface and in the lower troposphere, the semi-permanent and quasi-stationary subtropical pressure centers which, during part of the year act in concert, and during the other part, oppose each other, the influence of one or the other predominating according to the season (Fig. 16). The first of the two centers is the Saint Helena Anticyclone, well defined in all seasons. Found near that island, it moves southward in winter, and northward in summer at which time it reaches well into the Golf of Guinea to direct toward the interior of the continent, a southwesterly, very moist current called the "monsoon." In contrast, the pressure center over most of the Sahara Desert changes its nature according to the season. In summer, when the Sahara is heated, the center is a thermal low, while in winter it becomes a strong anticyclone from which a very hot northeasterly continental current, the "harmattan," flows toward the equator. The boundary between the two currents is called the Intertropical convergence zone (ITCZ) over the ocean, and the Intertropical Discontinuity (ITD) over the continent. The surface of the ITD slopes gradually upward toward the south, so that the monsoon--rarely more than 2000 meters deep--overlies the harmattan. While maintaining its roughly east-west orientation, the ITD undergoes three distinct and superimposed north-south oscillations, the most important of which is seasonal in duration. The average seasonal extreme positions of the ITD (20^{o}N in July-August, 3^{o}N in January) are reached, respectively, when the Sahara heat low, very deep, and the Saint Helena high, in its

northernmost position, act in conert; and when the Sahara high is very well defined and a very strong and steady harmattan is established, while the monsoon is weak, occasionally absent, the Saint Helena high having retreated to its southernmost latitude;

(2) in mid-troposphere, the easterly wind maximum near 600 mb, found on the average at a distance of 100-200 km south of the ITD during the summer months;

(3) in the upper troposphere (200 mb), two African highs in summer (Fig. 4c), one in winter (Fig. 4d); the tropical easterly jet stream in summer and the subtropical westerly jet stream in winter.

Several rain-producing disturbances have been identified in relation to the above entites, although the relationship remains to be clarified. Among these systems are the eastward-moving thundery systems of the Congo basin, the westward-propagating disturbance lines, 850 mb cyclonic vortices, and, on occasions, troughs in the upper subtropical westerlies. With the exception of the latter, these disturbances are confined to the south of the surface position of the ITD, suggesting a dependence of their formation on the depth of the monsoon flow. The mechanisms of this formation, however, have not been established; in fact, little is understood about either the physical nature of the disturbances or their role in the rainfall activity, which in this region, is confined mainly to the months from June to September.

The purpose of this study is (1) to investigate the characteristics (periods, horizontal wavelengths, direction of horizontal propagation) of oscillations which appear in the time series of daily rainfall amounts; (2) in view of what is known about the ITD, the monsoon flow,

tropical waves and the Tropical Easterly Jet Stream (TEJ) over West Central Africa, to infer from the above characteristics the relative roles of these physical entities in the generation and/or modulation of the daily rainfall activity. The inference will be entirely qualitative, since no data on the ITD, the monsoon, tropical waves, and TEJ were available to us. Also, because of this lack of data, no attempt has been made to study the physical nature of the oscillations present in the time series of rainfall.

The statistical analysis is carried out with the aid of the spectrum and cross spectrum techniques described in the second section of Chapter 2. The next section of that chapter describes the data set used in the study. The results of the analysis are summarized in Section 4. Using these results, inferences as to the possible roles of tropical waves and the TEJ are given in Chapter 3 which also contains the conclusions and outlook for further research.

CHAPTER 2

SPECTRAL AND CROSS SPECTRAL ANALYSIS AND RESULTS

2.1. Introduction

The object of this Chapter is to present a simplified account of the technique of spectral and cross spectral analysis and to give the results of the application of the method to the time series of daily rainfall amounts at 20 stations in West Central Africa for the years 1954 through 1964.

The chapter is divided into four sections. After the introduction, the general considerations in the analysis of spectra are presented in Section 2, including the statement of the problem, the definition and physical meaning of the spectrum, the estimation of the spectral density, the evaluation of the spectral peaks, and the cross spectra. The rainfall data set is described in Section 3, and the results of the analysis are summarized in Section 4.

Spectral analysis has recently come into wide use as a basic analytical tool in the estimation of relations between time series and in the evaluation of the mechanisms which contribute to the generation of such series (Doberitz, 1969; Sikdar, et al., 1972).

The method has also helped to document the existence over Africa, at 700 mb, of fluctuations in the meridional wind field with periods of the order 3-5 days, and horizontal wavelength in the range 1000-4000 kilometers (Burpee, 1972). IT was used to detect, in the daily

rainfall near the ITC zone in the Pacific, disturbances with period ranges 2.78-3.57, 3.57-5.56, 5.56-16.67 days and respective horizontal wavelengths of 1000, 2000 and 10,000 kilometers (Murakami, 1971).

2.2. General Considerations in the Analysis of Spectra

2.2.1. Statement of the problem

The starting point in any spectral analysis is a function of time $X(t)$ defined in an interval $0 \leq t \leq T$ relative to an arbitrary origin. In general, $X(t)$ exhibits fluctuating properties to the eye and is called a time-series.

Roughly speaking, spectral analysis is concerned with an examination of $X(t)$ from the point of view of its frequency content. More generally, the cross spectral analysis between $X_i(t)$ and $X_j(t)$ is concerned with interactions or correlations between such pairs of variables at each frequency.

2.2.2. Definition and physical meaning of the spectrum.

In classical statistical problems, one is faced with observations which are independent because the experiments which generate these measurements are themselves physically independent. It is then usually assumed that the errors have a common, though generally unknown distribution, the variability of which is characterized by its variance

$$\sigma^2 = E(X-\mu)^2 = \int_{-\infty}^{\infty} (X-\mu)^2 p(X)\,dX \qquad (2.1)$$

where $E(X) = \mu$ is the mean value of X, assumed constant and $p(X)$ is the probability density function of the errors. If the errors are Gaussian or normal, then μ and σ^2 characterize the distribution completely.

When X becomes $X(t)$, a function of time or space, consecutive or contiguous values of $X(t)$ are correlated, so that in addition to μ and σ^2, one needs to specify the covariances between the values of $X(t)$ at different times. If attention is focused on n time points

$t_1, t_2, \ldots, t_n$, this involves the calculation of $\binom{n}{2}$ covariances, γ_{ij}, i.e.,

$$\gamma_{ij} = E[X_i-\mu)(X_j-\mu)] = E[(X(t_i)-\mu)(X(t_j)-\mu)] \qquad (2.2)$$

If a single series is to give meaningful information about the ensemble averages (2.1) and (2.2), it is necessary to assume stationarity, i.e., all statistical properties depend on differences t_i-t_j, rather than t_i and t_j themselves. Then the number of covariances to be estimated reduces to (n-1). These are the auto-covariances

$$\gamma_k = E(X_i-\mu)(X_{i+k}-\mu)$$

If it is legitimate to assume that, in addition to stationarity, the statistical properties of X(t) are governed by a Gaussian (normal) process, i.e., the joint distribution of X(t) at any time $t_1, t_2, \ldots, t_n$ is a multivariate normal distribution, then μ, $\sigma^2$and γ_k are sufficient to characterize the behavior of X(t) completely.

If X(t) is a more general statistical function, i.e., the behavior of X(t) at different times is governed by given probability laws, then it may be shown (Jenkins, 1961) that if X(t) is a mathematical function of time of the form

$$X(t) = A + B \cos(\omega t + \phi) \qquad (2.3)$$

where A is the mean value, B the amplitude, ω the frequency and ϕ the phase, then

$$\sigma^2 = \int_0^\infty F(\omega)d\omega + 1/2 \sum_{j=0}^{\infty} B_j^2$$

It is seen that in addition to the components of variance due to genuine periodic terms ($1/2\ B_j^2$), there is a further term representing contributions to the total variance from a continuous spectrum of frequencies. If a decomposition of the form (2.4) is possible, i.e., there are lines in the spectrum corresponding to

genuine periodic terms together with a continuous distribution of frequency, then the spectrum is said to be mixed.

If there are no lines, then (2.4) may be written as

$$1 = \int_0^\infty \frac{F(\omega)}{\sigma^2} d\omega \tag{2.5}$$

where $f(\omega) = \frac{F(\omega)}{\sigma^2}$ is called the spectral density function and $F(\omega) = \sigma^2 f(\omega)$ is the variance spectrum.

Therefore the spectral density function is analogous to the probability density function, and the line spectrum (if suitably normalized) corresponds to a probability mass function or discrete probability distribution. If both lines and continuous spectra are present, one may calculate the integrated spectrum $H(\omega)$ which represents the total variance in the frequency interval $(0, \omega)$ so that $\sigma^2 = H(\omega)$, and by normalizing, define $h(\omega) = \frac{H(\omega)}{\sigma^2}$ so that $h(\omega) = 1$.

It may be shown that a stationary Gaussian series is completely characterized by its integrated spectrum $H(\omega)$, and by its spectral density function $f(\omega)$ if no lines are present. If follows, therefore that a relation must exist between $f(\omega)$ and the autocovariances $\rho(k)$. In fact, they turn out to be Fourier transforms of one another (Yevjevich, 1972), i.e.,

$$g(\omega) = \frac{1}{\pi} \int_{-\infty}^{\infty} \frac{\rho(k)}{\sigma^2} \cos\omega k dk \tag{2.6}$$

where $\rho(k) = \gamma(k)/\sigma^2$ are the autocorrelations, satisfying the property $\rho(k) = \rho(-k)$ and $\rho(0) = 1$ since $\gamma(0) = \sigma^2$.

For a discrete series S_t, the autocorreltation function $\rho(k)$ is discrete, so that (2.6) becomes

$$g(f) = 2[\ 1+2 \sum_{k=1}^{\infty} \rho(k) \cos 2\pi fk] \qquad (2.7)$$

in which ρ_o is replaced by unity, k is the lag and $f = \frac{1}{\omega}$.

The expected sum on the right of (2.7) is zero for an independent random variable (Yevjevich, 1972), so that the sum of g(f) over the range $0 \leq f \leq 0.5$ is unity. Because the smallest frequency $f_{min} = \frac{1}{N}$, where N is the length of record, f_{min} tends to zero as N tends to infinity. The largest frequency, $f_{max} = \frac{1}{2\Delta t}$ is called the Nyquist or folding frequency. For Δt = one time unit, $f_{max} = 0.5$. If the series is finite, f_{min} depends on the sample size. To avoid this dependence, f_{min} is usually taken as zero.

2.2.3. Estimation of the spectral density

Several difficulties arise in the estimation of the spectral density, particularly the selection of the range of frequencies, the approximation of the continuous spectral density by a sequence of discrete spectral densities, and the smoothing of large variations about the expected population spectral density of estimated sample densities.

If the ordinary frequencies, $f = \frac{1}{\omega}$, are used, the range is from 0 to 0.5. But the estimates of the variance densities between f = 0 and $f = \frac{1}{N}$ are unreliable, since the fact that a series has values X_t observed at or averaged over Δt does not imply that the variance spectral densities for f>0.5 are zeros. These densities can be neglected only if the fluctuation of X_t inside Δt is minimal, or if the series is so defined that the properties inside Δt are not

relevant. If the properties of the series inside Δt are relevant, the sample variance densities of the range $0 \leq f \leq 0.5$ are greater than the expected or population variance densities; they are said to be biased.

To estimate a continuous spectral density in the given range of frequencies, the latter is divided into intervales, Δf, such that the number of density ordinates to be computed is $m = 1 + \frac{0.5}{\Delta f}$. If equation (2.7) is used, the procedure is equivalent to determining m values of g(f). The estimates are both biased and inefficient, i.e.,

$$E[g(f) - \gamma(f))] = \Delta g \qquad (2.8)$$

where $\gamma(f)$ is the population spectral density, is different from zero instead of zero as it should be for an unbiased estimate, and

$$\text{var } g(f) = E[g(f) - \gamma(f)]^2$$

is not a minimum as it should be in the case of an efficient estimate.

To obtain unbiased and efficient estimates, either the $\rho(k)$ function of (2.7) is smoothed prior to the estimation of g(f), or the computed g(f) estimates for a limited number of frequencies are smoothed. In this latter case, a finite spectral density with $k_{max} = N-1$ for a series of size N is smoothed with a smoothing function D(k) to give (Yevjevich, 1972, p. 93)

$$g(f) = 2[1 + 2 \sum_{k=1}^{N-1} D(k)\ P(k)\ \cos 2\pi fk] \qquad (2.10)$$

The function D(k) in the lag domain has an equivalent smoothing function or kernel, S(f), in the frequency domain which is a Fourier transform of D(k). The kernel S(f) consists of discrete symmetrical weights for consecutive values of equation (2.7). Two such functions are the Hann window, named after the Austrian meteorologist Julius von Hahn, and the Hamm window, after R. W. Hamming of the Bell

Telephone Laboratories (Muller, 1966, p. 14). They are, respectively,

$$S(f_j) = 0.25\ g(f_{j-1}) + 0.5\ g(f_j) + 0.25\ g(f_{j+1}) \qquad (2.11)$$

and

$$S(f_j) = 0.23\ g(f_{j-1}) + 0.54\ g(f_j) + 0.23\ g(f_{j+1}) \qquad (2.12)$$

where $S(f_j)$ is the resulting value of $S(f)$ at the position f_j.

One estimation procedure used in practice because of the availability of computer programs is the so-called Tukey-Hanning procedure. In this method, a value m of the maximum number of lags is chosen, so that the autocorreltaion coefficients ρ_k need to be computed only from ρ_1 to ρ_m.

Usually, $m < \frac{N}{3}$ is selected. The estimates $g(f)$ by equation (2.7) with $\rho(k)$ estimated by ρ_k, $k = 1, 2, 3, \ldots, m$, are obtained at discrete points $f_j = \frac{j}{2m}$, $j = 1, 2, 3, \ldots, m$, so that equal intervals between discrete estimates are $f = \frac{1}{2m}$. These raw estimates are then smoothed by the smoothing function of Eq. (2.11), with $f_1 = f_{-1}$, and $f_{m+1} = f_{m-1}$.

2.2.4. Evaluation of spectral peaks

One method for the evaluation of the statistical significance of spectral peaks has been given by Mitchell, et al. (1966, p. 36-46). In this method, a null or theoretical spectrum, S_k, is hypothesized. Next the confidence limits of S_k are derived by first computing the degrees of freedom $n = \frac{2N - m/2}{m}$ where m is the maximum lag and N the sample size. Then, since the ratio of the magnitude of the spectral estimate to the local magnitude of S_k follows the χ^2/n distribution (Blackman and Tukey, 1958), the α% point, where α is the confidence level, of the χ^2/n distribution is determined. The

percent point value is then multiplied by the ordinate value of S_k at each lag k to locate (1-α) percent confidence limit. The meaning of the (1-α) percent confidence limit is that if the "population" or true spectral density at lag K were S_k, then the probability would be 1 - (1- α) that a sample may show an estimate of $\frac{\chi^2\alpha(n)}{n} S_k$ or larger.

If no spectral estimate exceeds $\frac{\chi^2\alpha(n)}{n} S_k$, then the conclusion is that the sample spectral density is indeed that of the hypothesized model. If any spectral estimate exceeds the (1-α) percent confidence limit of S_k, then the decision as to what this exceedence means depends on one of two cases: (a) the estimate corresponds in wavelength or frequency to an oscillation suspected à priori to exist in the series; then the estimate is interpreted as being significant at the (1-α) percent confidence level; (b) the estimate corresponds to a frequency which has not been observed in previous studies of other series, and/or is not related to a known physical process; then the test of significance is as before, except that the appropriate percentage point, P_d, is given by $P_d = \frac{100m + (1-\alpha)}{m + 1}$

2.2.5. Cross spectra

The variance spectral density is based on the behavior at a single station of the stochastic variable X. In order to examine correlation between the fluctuations of the field of X at different locations, it is necessary to consider cross spectral information defined in terms of coherence magnitudes and phases.

The coherence magnitude, $CH^2(f)$, is understood to be the length of the "vector" in the co- and quadrature spectra plane, normalized by the geometric mean of the spectral densities, i.e.,

$$CH^2(f) = \frac{Co^2(f) + Q^2(f)}{g_1(f)g_2(f)}$$

where co(f) is the cospectrum, a measure of the contribution of oscillations of different frequencies to the total covariance between the series at location 1 and the series at location 2 for lag zero; Q(f) is the quadrature spectrum, a measure of the contribution of the different harmonics to the total covariance of the series obtained when the harmonics of the series at location 1 are delayed by one quarter period while the series at location 2 remains unchanged; $g_1(f)$ and $g_2(f)$ are the spectral density functions at locations 1 and 2, respectively.

The coherence, $CH^2(f)$, is analogous to the square of the correlation coefficient between the fluctuations in a given frequency band, independently of the phase relationship between the locations. It may therefore be visualized as the fraction of the variance of one series (within a given frequency band) which may be explained or predicted in terms of the other series (Wallace, 1971).

Chances are that even though the true coherence is zero, a coherence equal to or greater than a given value may be found. The approximate formula for the limiting coherence, β, at probability level P is (Panofski and Brier, 1958, p. 158)

$$\beta=[1-(P^{\frac{1}{n-1}})]^{1/2}$$

where $n=\frac{2N-m/2}{m}$ is the number of degrees of freedom. This value of β is used to evaluate the significance of coherence magnitudes, $CH^2(f)$.

CHAPTER 3

INTERPRETATIONS, CONCLUSIONS AND OUTLOOK

3.1. Interpretations

1. The spectral results, assuming a second order auto regressive model, showed that oscillations in deviations of daily rainfall amounts from the eleven-year mean amounts did not occur at random. Rather it was found that in addition to second order Markov-type persistence, at least one other form of non-randomness was present at 19 of the 20 stations.

This other non-randomness is interpreted as the forcing by wave-like atmospheric disturbances having a variety of periods. Because of this forcing, variance was concentrated in significant spectral peaks at periods corresponding to those of the disturbances and ranging from 2.03 days to 10.5 days (Table I). Significant spectral peaks were also found for periods of about 40 days or longer (Fig. 19).

With the exception of periods shorter than 2.78 days, and equal to or greater than 40.0 days, the above results agree well with those obtained by Murakami (1971) for the region near the ITCZ in the tropical Pacific. Periods in the range 3.81 to 5.56 days also correspond well with those of fluctuations in the meridional wind component over North Africa in summer (Burpee, 1971) as well as they do with the range of periods of 43 African tropical waves followed by Burpee, from 20-25E to the West Coast of Africa for the summers of 1968 and 1969 (Burpee, 1974, p. 15).

Table III shows the mean rainfall and number of rainy days by month and by year for the years 1930-1963 at Douala, Cameroun. Also shown in the table are the magnitudes of rainfall amounts and number of rainy days observed with thunder activity. The last line shows the average number of squall lines. From this table, it is possible to estimate the long-time average periods of rainy days with and without thunder activity both for the year and for the months of June, July, August and September (these months are hereafter referred to as the summer monsoon or rainy season). These average periods are shown in Table IV where it can be seen that for the year, the periods fall within the limits of those shown in Table I.

2. Oscillations with periods 2.58 to 4.21 days showed significant coherence magnitudes although the number of significant magnitudes was somewhat small (Table II). These oscillations were found to propagate Westward, with a wavelength of about 500 km. From Table V, it may be inferred that the wavelength of these oscillations falls within the wavelength range of cloud clusters.

It is known (Sawyer, 1971) that "the major tropical rainfall is produced by convection. . .However convection does not occur at random, and satellite pictures show that a major part of the convection occurs in organized 'cloud clusters' with dimensions from 100 to 1,000 km. . . Disturbances of the equatorial wind field. . .exist on a larger scale."

In addition, synoptic experience has shown that the rains in West Central Africa are of two types: isolated scales C and D (Table V) patterns, and organized scales A and B systems (Dhonneur, 1971). While isolated rain may be associated with daily, localized developments and

falls from cumulonimbus in the form of violent, short-lived storms, we think that organized rain systems are associated with "cloud clusters" and larger scale systems. Oscillations detected in the rainfall with periods 2.58 to 4.21 days propagating westwards with a wavelength of the order 500 km are, accordingly, interpreted as "cloud clusters", possibly imbedded within wind disturbances on a larger scale (Table VI). The "cloud clusters" are probably of the squall line type known in West Central Africa as disturbance lines (DL) which may be viewed as "part of the easterly wave perturbations" (Okulaja, 1971, p. 667).

3. However, the small number of significant coherence magnitudes for the period range 2.58 - 4.21 days and of significant coherence magnitudes for the other short periods suggest that by themselves, small scale systems embedded in large scale wind disturbances (wave disturbances) probably contribute little, in the long run, to the rainfall in the area. This suggestion is strengthened by the following consideration. From Table IV, assuming that the squall lines indicate the presence of wave disturbances, the latter contribute about 35% to the rainfall on disturbed days at Douala (the disturbed character is assumed to be indicated by thunder activity). From Table VII rainfall on disturbed days account for 34% of the total rainfall for the year and 30% for the rainy season. Subject to the above assumptions, wave disturbances are then seen to contribute only 12% of the total annual rainfall, and 11% to the rainfall during the rainy season at Douala.

The small contribution of wave disturbances to the rainfall is not surprising if account is taken of the low-level moisture and temperature advections over West Central Africa. In most parts of

the World, temperature and moisture advections are in phase and precipitation occurs in conjunction with the advection of warm, moist air. In West Central Africa the low-level moisture and temperature advection have a negative correlation. The warmer desert harmattan air is dry and stable, while the cooler maritime monsoon air is moist and conditionally unstable.

This complicates the rainfall patterns on the scale of the waves, since for instance, the advection of hot but very dry air will not likely lead to saturation. "The negative correlation between temperature and moisture advections may inhibit the ability of the waves to influence. . . the rainfall patterns" (Burpee, 1974, p. 23).

4. We feel that the rainfall over West Central Africa is mainly dependent upon the position of the ITD and the presence of the Tropical Easterly Jet Stream (TEJ), or more precisely, the oscillations of that upper tropospheric high velocity current.

The controlling influence of the ITD is seen in the fact that little or no rain falls at its surface position, in part because of the extreme dryness of the air in its poleward side, in part because the discontinuity lies beneath a region of subsidence dominated by anticyclones at 850 and 700 mb (Burpee, 1972; Sansom, 1965). These anticyclones are not stationary, however, and rainfall occurs whenever the ITD assumes a more vertical structure between 850 or 700 mb and 500 mb, thus allowing convergence and vertical motion to develop through a reasonable depth of the atmosphere. Since such movement of the upper trough can occur with little or no movement of the surface ITD, there may be no connection between the surface position of the trough and the area in which rain falls (Sansom, 1965).

Nonetheless, the normal structure of the ITD, being such that a warm, dry easterly or northeasterly continental air mass overlies a cooler, moist and very shallow maritime airstream, inhibits the formation of rain at the discontinuity itself since any cloud forming in the shallow monsoon air and penetrating through the discontinuity zone becomes dessicated. Accordingly, "only in those regions far enough removed from the [discontinuity] to possess sufficiently deep layers of moist unstable air can cumulonimbus clouds become fully developed. Thus, there exists a line approximately 200 miles south of the [discontinuity] which marks the northern limit of precipitation" (Sansom, 1965, p. 95).

Indeed four rainfall zones accompany the ITD in its seasonal meridional oscillations. These zones are, from north to south (Fig. 9) Zone A: immediately north of the ITD, with clear skies, or rare cirriform clouds and no rain; Zone B: immediately south of the ITD, few small cumuli and no rain; Zone C: farther south, about 1200 km wide, with overcast or very cloudy skies by cumuli or cumulonimbi, rain and thunderstorms, disturbance lines; Zone D: still farther south, with stratiform clouds, and less abundant rains. The season are controlled by the latitudinal displacement of these four zones. Zones A (or B) and Zones C and D correspond, respectively, when they affect a given area, to the major dry season, the major rainy season and the minor dry season. North of the average northernmost position of the southern limit of Zone C, stations (such as M, for Maroua, Cameroun, in Fig. 9) experience one dry and one rainy season; while south of that position, stations (such as Y for Yaoundé, Cameroun) experience two dry and two rainy seasons.

Ilesanmi (1971) has derived a statistical relationship between the latitude of the surface position of the ITD and rainfall in Nigeria and adjacent countries. For mean annual data, he found the following regression equation with a standard error of 14.6 inches and a coefficient of determination equal to 0.69

$$Y = 24.92 + 7.15\ (\phi - \phi)_{\text{ITD Station}}$$

Where Y is the rainfall in inches, and ϕ is the latitude. This relation shows that for each degeree of latitude that the surface position of the ITD is south of a station in Nigeria and nearby countries, the annual mean rainfall is decreased by nearly one third.

Mandengué (1965) also reports a relation between rainfall in the Douala area and the depth of the moist monsoon layer which depends on the surface position of the ITD.

Thus although the ITD itself is a region of fair or fine weather, its surface position by controlling the depth of the monsoon air to the south, limits the monsoon rainy zone to a distance south of it. It is in this zone, where the depth of the unstable monsoon attains suitable values that convection rains are normal.

In West Central Africa, these rains fall mainly in the rainy season (June-September) when the monsoon flow, present all year over the coastal fringes, becomes particularly established and reaches quite far to the North (Johnsoon, 1964; Fig. 7). For example, monsoon rains account for 63 and 75 percent of the average annual rainfalls at Douala and Garoua, Cameroun, respectively (Tables VII and VIII; see also Fig. 25).

Thus, rainfall over this part of the continent reaches its annual peak during the northern summer when the Tropical Easterly Jet Stream (TEJ) is present in the upper atmosphere. During these summer months, disturbance lines, and consequently wave disturbances are rare near the coast (Table III), while they reach peak frequency in the Lake Tchad area. The TEJ is then well developed, extending without interruption from India. As it flows across Africa from East to West near 10-15° N, it slowly decreases in speed.

From dynamical considerations (Reiter, 1961, p. 136) this jet stream pattern implies an ageostropic cross circulation in West Central Africa--the exit region of the TEJ--with divergence aloft, tropospheric lifting, low-level convergence and cyclogenesis on the southern flank; and convergence aloft, tropospheric subsidence and low-level divergence on the northern flank of the TEJ axis, near the surface position of the ITD. The strong divergence in the exit region of the TEJ, together with the corresponding convergence of unstable monsoon air, and cyclogenesis would offer a dynamically justifiable explanation for the marked convective activity in the monsoon depressions which are observed near the coastal areas during the rainy season, and in the disturbance lines farther to the north.

The situation during the monsoon season is thus similar to that in the northern Bay of Bengal (Ramage, 1971, p. 43-47) where rain-generating monsoon depressions are linked with oscillations in the Tropical easterly jet stream. Similar oscillations could be invoked to explain the low-level (850 mb) cyclonic voctices which, during the West African monsoon season, are observed to develop with the humid

unstable southwesterly flow well to the south of the ITD. With the passage of these vortices, the monsoon current over the coastal parts of West Central Africa deepen, and the deepening of the westerly is accompanied by outbreaks of monsoon rains. The closed, 850-mb cyclonic vortices are sometimes preceded by the passage of disturbance lines (Johnson, 1964).

Oscillations of the TEJ could be brought about by changes in the meridional temperature profile, or by impulses entering the African area from further upstream. Further investigation is required to answer this question.

5. Oscillations with periods equal to or greater than 40 days (Table II; Figs 22 and 23) were found to propagate westwards with a wavelength of about 18 degrees of longitude or 2000 km. A comparison of these characteristics with those of known major tropical waves (Table VI) shows that the wavelength corresponds to that of the thermally forced easterly waves; the periods, however, correspond to none of the known wave disturbances.

Ramage (1971, p. 45) writes from studies by others that in July and August for the years 1929-1938, 37 monsoon depressions developed over the northern Bay of Bengal. From this information Murakami (1974, p. 344), derived the frequency of the development of monsoon depressions over the Bay of Bengal as about "1.8 per month. . . , corresponding to a period of about 17 days."

If, following this procedure, it is assumed that, in West Central Africa, in the long run, about 9 major systems, on the average, develop in the course of the year (or 3 in the course of our monsoon season as

to the south of the ITD. The period of 40 days suggests that about 9 such vortices would develop in the course of a year or 3 during the summer monsoon season (June through September), when the easterly jet stream is present in the upper troposphere. The depressions travel from east to west, concurrently with high-level easterly waves and bursts of speed in the easterly jet stream.

From the long range point of view, it is suggested that the dominant factors in the rainfall of this part of Africa are the position of the ITD and the easterly jet stream (TEJ) and its oscillations in speed. The former controls the depth and the stability of the monsoon air, while the latter offers a dynamically justifiable explanation for low-level convergence, tropospheric lifting, cyclogenesis and wave activity.

In view of the great importance of rainfall and its distribution to the economy of this area, these relations of the rainfall to the position of the ITD, and to the TEJ and its oscillations should be investigated further. Another extension of the present work would be an independent determination of the dynamical nature of the oscillations present in the rainfall records. The upcoming GARP Atlantic Tropical Experiment will provide an opportunity to obtain the requisite data toward the above goals.

REFERENCES

Adejokun, J. A., 1963: The three-dimensional structure of the Inter-tropical discontiniuty over Nigeria. Technical Note No. 39, Nigerian Meteor. Services. Lagos, Nigeria, 20 pp.

Altantawy, A. H., 1964: Tropical easterly jet stream over Africa Scientific Papers, No. 1, United Arab Republic, Meteor. Dept., Cairo, 20 pp.

Arnold, J., 1966: Easterly wave activity over Africa and the inter-tropical convergence zone during July, 1961. Satellite and Mesometeorology Research Report, SMRP Research Paper No. 65, University of Chicago.

Barrefors, B. B., 1966: Disturbances in West Africa as gravity waves in the inter-tropical discontiniuty surface. The Nigerian Meteor. Services, Tech. Note No. 29, Lagos, Nigeria, 10 pp.

Bates, J. R., 1970: Dynamics of disturbances on the intertropical convergence zone. Quart. J. Roy. Met. Soc., Vol. 96, 677-701.

Bendat, J. S., and Piersol, A. G., 1971: Random data: analysis and measurement procedures. John Wiley and Sons, Inc., N. Y., 407 pp.

Bernet, G., 1968: Recherche d'un mode de formation des lignes de grains en Afrique Centrale. Publications de la Direction de l'Exploitation Météorologique, No. 5, ASECNA, Dakar, Sénégal, 16 pp.

Berrit, G. R., 1961: Contribution à la connaissance des variations saisonnières dans de Golfe de Guinée: observations de surface le long des lignes de navigation, première partie, étude, régionale. Centre d'Océanographie de Pointe-Noire, Comité Central d'Océanographie et d'Etudes des Côtes, Cahiers Océanographiques, Vol. 13, No. 10, 715-727.

_____, 1962: ibid, part II. Vol. 14, No. 9, 633-643; No. 10, 719-729.

Bisseck, H., 1968: Etude des lignes de grains au Cameroun. Compte-rendus, Série B. Académie des Sciences, Vol. 266 No. 19, Paris, 1295-1296.

Blackman, R. B., and Tukey, J. W., 1958: The measurement of power spectra from the point of view of communications engineering. Dover Publications, Inc., N. Y., 190 pp.

Bryson, R. A., 1973: The Sahelian effect. (unpublished paper), 19 pp.

Burpee, R. W., 1972: The origin and structure of easterly waves in the lower troposphere of North Africa. J. Atmos. Sci., Vol. 29, 77-90.

_____, 1974: Characteristics of the North African easterly waves during the summers of 1968 and 1969. Submitted for publication to J. Atmos. Sci. 21 pp.

Carlson, T. N., 1969a: Some remarks on African disturbances and their progress over the tropical Atlantic. Mon. Wea. Rev., Vol. 97, No. 10, 716-726

_____, 1969b: Hurricane genesis from disturbances formed over Africa. Mariners Weather Log, Vol. 13, No. 5. 197-202

_____, 1971: A detailed analysis of some African disturbances, NOAA TM ERL NHRL - 90, National Hurricane Research Laboratory, Miami, Florida 58 pp.

Chang, Chih-Pie, 1973: A dynamical model of the intertropical convergence zone. J. Atmos. Sci., Vol. 30, No. 2, 190-212.

Charney, J. G., 1969: The intertropical convergence zone and the Hadley circulation of the atmosphere. Proc. WMO/IUGG Symposium on Numerical Weather Prediction in Tokyo, Meteor. Soc. Japan, Tokyo, 73-79.

_____, 1972: Tropical Cyclogenesis and the formation of the intertropical convergence zone. Lectures in Applied Mathematics, Vol. 13, Amer. Math. Soc., Providence, Rhode Island, 355-368.

_____and Stern, M. E., 1962: On the stability of internal baroclinic jets in a rotating atmosphere. J. Atmos. Sci., Vol. 19, 159-172.

Clackson, J. R., 1957: The seasonal movement of the boundary of northern air. Technical Note No. 5, Nigerian Meteor. Services, Lagos, Nigeria.

Cochemé, J., and Franquin, P., 1967: An Agroclimatological survey of a semiarid area in Africa south of the Sahara. WMO, technical Note No. 86, Geneva, Switzerland, 136 pp.

Derrick, J., 1973: The Great hunger. Africa, No. 23, 23-27.

_____, 1974: Famine at the gates. Africa, No. 33, May, 1974, 50-51.

Dhonneur, G., 1971: General circulation and types of weather over western and central Africa. Annexe IV, GARP Atlantic Tropical Experiment (GATE) Design, Extracts from the draft report of the Interim Scientific and Management Group, Joint GARP organizing committee, 22 pp.

Dobertiz, R., 1969: Cross spectrum and filter analysis of monthly rainfall and wind data in the tropical Atlantic. Bonner Meteorol. Abh. 11, 43 pp.

Eldridge, R. H., 1957: A synoptic study of West African disturbance lines. Quart. J. Roy. Meteor. Soc., Vol. 83, No. 357, 303-314.

Enochson, L. D., and Otnes, R. K., 1968: Programming and analysis for digital time series data. Shock and Vibration Information Center, Naval Research Laboratory, Washington, D.C., 277 pp.

Erickson, C. O., 1963: An incipient hurricane near the West African Coast. Mon. Wea. Rev., Vol. 91, No. 2, 61-69.

Flohn, H., 1960: Equatorial Westerlies over Africa, their extension and significance. Proceedings, Joint Symposium on Tropical Meteor. in Africa, Nairobi, Kenya, December, 1959.

_____, 1964: Intertropical convergence zone and meteorological equator. WMO Technical Note No. 64, Geneva, Switzerland, 21-29.

Garstang, M., 1966: Atmospheric scales of motion and rainfall distribution. Proceedings, 1966 Army Conf. on Tropical Meteor., Univ. of Miami, Report No. 12, 24-27.

Génieux, M., 1957: Climatologie du Cameroun in Atlas du Cameroun. Institut de Recherches Scientifigues du Cameroun, Yaoundé, 33 pp.

Germain, H., 1956: Synoptic analysis for West Africa and the southern part of the Atlantic Ocean. Final Report of the Carribean Hurricane Seminar, Ciudad Trujillo, February, 1956, 173-186.

Gicam, 1969: Examen de la conjoncture économigue au Cameroun. Bulletin de l'Afrique Noire, Ediafric, Dakar, Sénégal, 10245-10247.

Gleave, M. B., and H. P. White, 1969: The West African middle belt: environmental fact or geographer's fiction? Geographic al Review, N. Y., Vol. 59, No. 1, 123-139.

Hamilton, R. A. and J. W. Archibold, 1945: Meteorology of Nigeria and adjacent territory. Quart. J. Roy. Meteor. Soc., Vol. 71, 231-265.

Haudecoeur, B., 1965: Le front intertropical (FIT) et ses perturbations en Afrique de l'ouest. WMO, Technical Note No. 69, Geneva, Switzerland, 109-112.

Hubert, L. F., A. F. Krueger and J. S. Winston, 1969: The double intertropical convergence zone. Fact or fiction? J. Atmos. Sci., Vol. 26, No. 4, 771-773.

Ilesanmi, O. O., 1971: An Emperical Formulation of an ITD rainfall model for the tropics: A case study of Nigeria. J. Appl. Meteor. Vol. 10, 882-891.

Jeandidier G., and P. Rainteau, 1957: Prévision du temps sur le bassin du Congo. Monographies de la Météorologic Nationale, No. 9, 13 pp.

Johnson, D. H., 1964: Weather systems of West and Central Africa. Proceedings, Symposium on Tropical Meteor. Rotorua New Zealand, November, 1963, 339-346.

_____, 1965: African tropical meteorology. WMO, Technical Note No. 69, Geneva, Switzerland, 48-90.

Jones, R. H., 1971: Spectrum estimation and time series analysis--A review. Paper presented at the International Symposium on Probability and Statistics in the Atmospheric Sciences June 1-4.

Krishnamurti, T. N., 1972: Transient disturbances in the tropics. Part III: energy sources. In Dynamics of the Tropical Atmosphere, National Center for Atmospheric Research, Boulder, Colorado, U.S.A., 67-73.

_____, et al., 1973: Tibetan high and upper tropospheric tropical circulations during northern summer. Bull. Amer. Meteor. Soc., Vol. 54, 1234-1249.

Kuo, H. L., 1973: Nonlinear theory of the formation and structure of the intertropical convergence zone. J. Atmos. Sci., Vol. 30, No. 6, 969-983.

La Seur, N. E., 1971: A meteorological perspective for GATE. Annex II, draft report of the ISMG on the GATE Experiment Design, 14 pp.

Manabe, S., J. L. Holloway, Jr. and H. M. Stone, 1970: Tropical circulation in a time integration of a global model of the atmosphere. J. Atmos. Sci. Vol. 27, 580-613.

Mandengué, D., 1965: Les perturbations atmosphériques et les précipitations dans la région de Douala. Notes de l'Etablissement, d'Etudes et de Recherches Météorologigues, No. 209, Direction de la Météorologie Nationale, Paris, 30 pp.

Markovic, R. D., 1967: Discriminating the change in means of hydrologic variables. Proceedings, the International Hydrology Symposium, September 6-8, 1967, Fort Collins, Colorado, U.S.A. Vol. 7, Colorado State University, Fort Collins, Colorado, U.S.A. 581-588.

Mbele-Mbong, S., 1972: Some characteristics of the rainfall regime at Douala, Cameroun. Atmos. Sci. Paper No. 194, Colorado State University, Fort Collins, Colorado, 59 pp.

Mitchell, J. M., Jr., et al., 1966: The power spectrum and general principles of its application to the evaluation of non-randomness in climatological series. WMO Technical Note No. 79, WMO, Geneva, Switzerland.

Muller, F. B., 1966: Notes on the meteorological application of power spectrum analysis. Canada, Dept. of Transport, Meteor. Branch, Meteor. Memoirs, No. 24, Meso-Metor. and Short Range Forecasting Rept. No. 1, 84 pp.

Murakami, M., 1971: On the disturbances appearing in precipitation near the ITC Zone in the tropical Pacific J. Meteor. Soc. Japan, Vol. 49, No. 3, 184-189.

Murakami, T., 1974: Steady and transient waves excited by diabatic heat sources during the summer monsoon. J. Atmos. Sci., Vol. 31, 340-357.

Nevière, E., 1959a: Note sur la variation du front intertropical en Afrique équatoriale française. Monographies de la Météorologie Nationale, No. 14, Part I., 11 pp.

_____, 1959b: Relation entre les courants rapides et les types de temps en Afrique équatoriale. Monographies de la Météorologie Nationale, No. 14, Part II, 19 pp.

Nitta, Tsuyoshi, 1970: On the role of transient eddies in the tropical troposphere. J. Meteor. Soc. Japan, Vol. 48, 47-60.

Obasi, G. O. P., 1965: Atmospheric, synoptic and climatological features of the West African region. Technical Note No. 28, Nigerian Meteor. Services, Lagos, Nigeria, 45 pp.

_____, 1966: Some prominent meso-scale meteorological phenomena in West Africa. Proceedings 1966 Army Conf. on Tropical Meteor., Univ. of Miami, 75-84.

Okulaja, F. Ola., 1970: Synoptic flow perturbations over West Africa. Tellus, Vol. 22, No. 6, 664-668.

Palmén, E. and C. W. Newton, 1969: Atmospheric circulation systems--Their structure and physical interpretation. Academic Press, N. Y., 603 pp.

Panofski, H. A. and G. W. Brier, 1958: Some applications of statistics to meteorology. The Pennsylvania State Univ., Univ. Park, Pennsylvania, U.S.A., 224 pp.

Ramage, C. S., 1971: Monsoon meteorology. Academic Press, New York 296 pp.

Reiter, E. R., 1963: Jet-stream meteorology. The University of Chicago Press, Chicago. 515 pp.

Rosenthall, J. E., 1973a: Drought: the creeping catastrophy. Africa Report, Vol. 18, No. 4, 7-13.

_____, 1973b: The edge of catastrophy. War on Hunger, Vol. III, No. 8, 1-5, 11-21.

Sadler, J. C., 1967: On the origin of tropical vortices. Proceedings, Working Panel on Tropical Dynamic Meteor., Navy Weather Research Facility, Virginia, 39-75, 299-307.

_____. 1972: Global circulation patterns and their relation to tropical cyclone activity. In Dynamics of the Tropical Atmosphere, National Center for Atmospheric Research, Boulder, Colorado, U.S.A., 220-230

_____ and Harris, B. E., 1970: The mean tropospheric circulation and cloudiness over southeast Asia and neighboring areas. Rep. AFCRL - 70 - 0489, HIG - 70 - 26, Hawaii, Institute of Geophysics, Univ. of Hawaii, Honolulu, Hawaii, 38 pp.

Sansom, H. W., 1965: The structure and behavior of the inter-tropical convergence zone (ITCZ). WMO, Technical Note No. 69, Geneva, Switzerland. 91 pp.

Sawyer, J. S., 1971: The scientific objectives of the GARP Atlantic Tropical Experiment (GATE) GARP Atlantic Tropical Experiment (GATE) Experiment Design, Extracts from the draft report of the Interim Scientific and Management Group (ISMG), Joint organizing Committee, 4-7.

Schmidt, F. H., 1951: Streamline patterns in equatorial regions. J. Meteor., Vol. 8, 300-306.

Sikdar, D. N., J. A., Young and V. E. Suomi, 1972: Time-spectral characteristics of large-scale cloud systems in the tropical Pacific. J. Atmos. Sci., Vol. 29, No. 2, 229-239.

Skinner, E., 1973: Suffering in the Sudan-Sahel: a void to fill. IFCO News, Vol. IV, Issue V, 1, 4-5.

Soliman, K. H., 1960: On the intertropical front and intertropical convergence zone over Africa and adjacent oceans. Monsoons of the World, Indian Meteor. Dept, New Delhi, 135-142

Struning, J. O., and H. Flohn, 1969: Investigations on the atmospheric circulation above Africa. Bonner Meteorologishe Abhandlunger, No. 10, 55 pp.

Suraud, P., 1954: Le front intertropical en Afrique Occidentale. Annuaire Hydrologique de la France d'Outre Mer, 1952, 29-36.

Thompson, B. W., 1965: The Climate of Africa. N. Y., Oxford University Press, 132 pp.

Tucker, G. B., 1964: Zonal Winds over the equator. Quart. J. Roy. Met. Soc., Vol. 90, 405-423.

Tschirhart, G., 1958: Les conditions aérologiques à l'avant des lignes de grains. Monographies de la Météorologie Nationale, No. 11,

_____, 1959: Les perturbations atmosphériques intéressant l'AEF méridionale. Monographies de la Météorologie Nationale, No. 13, Paris, 32 pp.

Walker, H. O., 1960: The monsoon in West Africa. Monsoons of the world, India Meteor. Dept., 35-42.

Wallace, J. M., 1972: On the general circulation of the tropics. Part I: Monsoon and synoptic scale disturbances. In Dynamics of the Tropical Atmosphere, National Center for Atmospheric Research, Boulder, Colorado, U.S.A., 185-201.

_____, 1971: Spectral studies of tropospheric wave disturbances in the tropical western Pacific. Rev. of Geo. and Space Sci., Vol. 9, No. 3, 557-612.

Winstanley, D., 1973: Recent rainfall trends in Africa, the Middle East and India. Nature, Vol. 243, 464-465.

Yanai, Michio, 1971: A review of tropical meteorology relevant to the Planning of GATE. Annex I, draft report of the Interim Scientific and Management Group (ISMG) on GATE experimental design.

Yevjevich, V. M., 1963: Fluctuations of Wet and dry years. Part I, research data assembly and mathematical models. Hydrologic Paper No. 1, Colorado State University, Fort Collins, Colo. U.S.A.

_____, 1972: Stochastic processes in hydrology. Water Resources Publication, Fort Collins, Colorado, U.S.A., 276 pp.

Yin, M. T., 1949: A synoptic--aerologic study of the onset of the summer monsoon over India and Burma. Jour. Meteor. Vol. 6, 393-400.

APPENDIX I

DATA SOURCES

Rainfall

Rainfall data acquired through the Inter-Library Loan Service from the Atmospheric Sciences Libraries, NOAA, Springfield, Maryland, were found in the following official publications of the various meteorological services:

1. Cameroun: Résumé Mensuel du Temps, Direction de la Météorologie, Douala, Cameroun.

2. Central Africa: Résumé Mensuel du Temps, Service Météorologique, Gouvernement Général de l'A.E.F.; and since 1960, Résumé Mensuel du Temps dans les Territoires des Républiques: Centrafricaine, du Congo, Gabonaise et du Tchad, ASECNA, Dakar, Sénégal.

3. Francophone West Africa: Résumé Mensuel des Observations Climatologiques, Service Météorologique Fédéral de l'A.O.F., and since 1960, Résumé Mensuel des Observations Météorologiques dans les Territoires des Républiques de: Côte d'Ivoire, Dahomey, Haute-Volta, Mali, Mauritanie, Niger, Sénégal; ASECNA, Dakar, Sénégal.

APPENDIX II
RAINFALL STATIONS

No.	Name	Location in Central Africa Country	Latitude	Longitude	Elevation, m
01	ABECHE	Tchad	13.50N	20.83E	542
02	AM-TIMAN	Tchad	11.02N	20.28E	436
03	BAMBARI	C.A.R.	05.46N	20.67E	448
04	BANGASSOU	C.A.R.	04.44N	22.83E	500
05	BANGUI	C.A.R.	04.23N	18.57E	381
06	BATOURI	Cameroun	04.25N	14.40E	655
07	BERBERATI	C.A.R.	04.15N	15.47E	594
08	BIRAO	C.A.R.	10.17N	22.47E	465
10	BOUSSO	Tchad	10.29N	16.72E	336
11	BRAZZAVILLE	Congo	04.15S	15.25E	314
12	DJAMBALA	Congo	02.32S	14.46E	797
13	DOUALA	Cameroun	04.04N	09.68E	13
14	EDEA	Cameroun	03.46N	10.04E	32
15	FAYA-LARGEAU	Tchad	18.00N	19.10E	234
16	FRANCEVILLE	Gabon	01.38S	13.34E	426
17	FORT ARCHAMBAULT	Tchad	01.08N	18.23E	365
18	FORT LAMY	Tchad	12.08N	15.03E	295
19	GAROUA	Cameroun	09.20N	13.23E	249
20	IMPFONDO	Congo	01.37N	18.07E	326
21	KOUNDJA	Cameroun	05.37N	10.45E	1217

No.	Name	Country	Latitude	Longitude	Elevation, m
22	KRIBI	Cameroun	02.56N	09.54E	19
23	LAMBARENE	GABON	00.43S	10.13E	82
24	LIBREVILLE	Gabon	00.27S	09.42E	12
25	LOMIE	Cameroun	03.09N	13.37E	640
26	MAKOKOU	Gabon	00.34N	12.87E	516
27	MAROUA	Cameroun	10.28N	14.27E	405
28	MAYUMBA	Gabon	03.25S	10.65E	40
29	MEIGANGA	Cameroun	06.32N	14.22E	1000
30	MOUILA	Gabon	01.52S	11.01E	--
31	MOUNDOU	Tchad	08.37N	16.04E	422
32	N'DELE	C.A.R.	08.24N	20.39E	510
33	NGAOUNDERE	Cameroun	07.17N	13.19E	1119
34	NKONGSAMBA	Cameroun	04.56N	09.55E	877
35	OUESSO	Congo	01.37N	16.05E	340
36	POINTE-MOIRE	Congo	04.49S	11.54E	17
37	PORT-GENTIL	Gabon	00.42S	08.75E	6
38	SANGMELIMA	Cameroun	02.56N	11.57E	713
39	SIBITI	Congo	03.41S	13.35E	--
40	YAOUNDE	Cameroun	03.52N	11.53E	760
41	YOKO	Cameroun	05.33N	12.22E	1031

Station				Periods (in days) corresponding to significant spectral peaks
No.	Name	Latitude	Longitude	
1	Abecher	13.8	20.8	2.84, 3.76, 6.45
5	Bangui	4.4	18.6	2.31, 2.42, 3.67, 5.19
6	Batouri	4.4	14.4	2.90, 3.25, 3.51
11	Brazzaville	-4.2	15.2	2.90, 3.88, 5.1, 7.1
13	Douala	4.1	9.7	3.8, 4.0, 4.4
15	Faya-Largeau	18.0	19.2	
16	Franceville	-1.6	13.6	2.6, 3.22, 5.0
18	Fort Lamy	12.1	15.0	2.04, 2.90, 3.03, 3.2, 4.2, 5.6
21	Koundja	5.6	10.8	2.63, 2.74, 3.33, 3.67
22	Kribi	2.9	9.9	2.68
24	Libreville	-0.5	9.4	3.33, 4.21
25	Lomie	3.2	13.6	2.03, 2.61, 2.92
27	Maroua	10.5	14.3	2.27, 3.05, 3.28, 3.54, 3.77, 4.35
28	Mayumba	-3.4	10.6	2.76, 2.98, 3.30, 3.74, 5.31
31	Moundou	8.6	16.1	2.03, 3.64, 10.25
32	N'Dele	8.4	20.6	2.35, 2.65, 3.01, 3.54
33	Ngaoundere	7.3	13.3	2.96, 3.12, 3.36, 4.54, 6.25
35	Ouesso	1.6	16.0	2.56, 7.14
40	Yaounde	3.9	11.5	2.52, 2.96, 3.39
41	Yoko	5.6	12.4	2.04, 3.08, 3.22, 3.63, 4.49

Table I: Periods corresponding to significant peaks in the spectrum of each station assuming a second order Markov model for the true spectrum. Underlined quantities correspond to maximum spectral values.

	Longitudinal difference		Phase difference, $\Delta\theta$ (deg) for periods (days)		Coherence square for periods (days)	
	$\Delta\lambda$ (deg)	$\lvert\Delta\lambda\rvert$* (km)	2.58 to 4.21	$\geq$ 40.0	2.58 to 4.21	$\geq$ 40.0
2,10	-3.56	395		-0.26,-0.52		.57, .48
2,18	-5.25	583		0.14,0.45		.67, .57
2,27	-6.01	667		-0.0.4,-0.027		.65, .52
10,18	-1.69	188	-16.8	2.4,3.3	.15	.72, .59
10,27	-2.45	272	-11.4	-0.3,-1.4,-2.1	.17	.71, .61, .16
18,27	-0.76	84	-2.0,-14.6	-0.73,0.67	.16, .13	.73, .61
4,5	-4.26	473		-1.2,-0.74		.48, .33
4,6	-8.43	974		-1.2,-0.1		.39, .23
4,40	-11.30	1254		-1.1,0.76		.24, .16
4,13	-13.15	1460		-1.8,-2.3		.33, .20
5,6	-4.70	522		-9.1,-14.1		.33, .22
4,40	-7.04	781		-14,-12.0		.18, .14
5,13	-8.89	987		-8.4,-12.3		.49, .38
5,6	-4.70	522		-9.1,-14.1		.33, .22
4,40	-7.04	781		-14,-12.0		.18, .14
5,13	-8.89	987		-8.4,-12.3		.49, .38
6.40	-2.87	319		0.77,3.3		.49, .35
6,13	-4.72	524		-10.1		.13
40,13	-1.85	205		--		--
24,37	-0.67	74		2.1,4.9		.51, .40
24,26	+3.45	383		8.3,11.4		.34, .24
37,26	+4.12	457		8.3,10.1		.30, .24
26,20	+5.20	577		5.4		.15
20,35	-2.02	224		5.5,-7.6		.26, .17
28,29	+3.57			6.2,8.9		.50, .38
28,39	+2.70	300		--		--
28,11	+4.60	511		3.8,4.5		.34, .26
39,11	+1.90	211	+37.5	-1.2,-1.7	.122	.64, .48

* One degree longitude $\simeq$ 111 km.

Table II: Coherence square, longitudinal difference, phase difference for station pairs with coherence square equal to or greater that $\beta = 0.122$.

		J	F	M	A	M	J	J	A	S	O	N	D	Year
With and without thunder-storms	Average rainfall	61.3	79.9	216.8	245.1	338.1	496.3	721.6	724.5	595.0	411.1	152.2	54.4	4096.5
	Number of rainy days	7	9	16	18	22	24	29	29	27	26	16	8	231
With thunder-storms	Average rainfall	22.8	53.7	135.0	161.0	250.0	244.4	142.4	122.7	245.0	207.5	77.0	40.0	1407
	Number of days with rain	4	5	10	10	14	12	5	3	11	14	9	4	98
Mean number of squall lines		1	2	5	5	6	3	1	1	2	3	4	1	34

Table III: Role of "thundery" disturbances in the rainfall at Douala for the years 1930-1963 (Adapted from Mandengué, 1965, p. 28).

		Number	Frequency (in days)	Period (days)
Rainy days with thunder activity	Year (365 days)	98	3.72	3.72
	Monsoon season (122 days)	31	3.94	3.94
Rainy days without thunder activity	Year (365 days)	133	2.74	2.74
	Monsoon season (122 days)	78	1.56	1.56
Rainy days with thunder activity and squall line	Year (365 days)	34	10.74	10.74
	Monsoon season (122 days)	7	17.43	17.43

Table IV: Average periods estimated from Table III

Scale	Wavelength Range		Name
	From (km)	To (km)	
A	10^3	10^4	Wave scale
B	10^2	10^3	Cloud cluster scale
C	10	10^2	Meso scale
D	1	10	Cumulus scale

Table V: Scales of tropical phenomena

Period (days)	Wavelength (10^3 km)	Propagation (degree/day)	Maximum amplitude			Wave Type	Wave Name	Remarks
			Wind Component (m/sec)	at Layer	at Latitude (degree)			
4-5	2-4	Westwards	v (3)	T	5-15	Thermally Forced	"Easterly wave" Riehl	c-core = L.T. w-core = U.T. vert. tilt = none or easterly
4-5	8-10	Westwards ~20	v (2-3)	LS	0	Mixed Rossby-Gravity	Yanai-Narujama	vert. tilt = T = easterly S = westerly
10-20	~40	Eastwards ~30	u (8)	S	0	"Kelvin"	Wallace and Kousky	u- component only

T = troposphere
S = stratosphere
L.T. = lower troposphere
U.T. = upper troposphere
c = cold
w = warm

Table VI: Characteristics of major waves

		YEAR	RAINY OR MONSOON SEASON	REST OF YEAR	% OF YEAR	
					RAINY SEASON	REST OF YEAR
Rainfall amount (mm)	Total	4096.5	2537.4	1559.1	62.0	38.0
	With thunder activity	1407.0	754.5	652.5	54.0	46.0
	Without thunder activity	2689.5	1782.9	906.6	66.0	34.0
% of Total	With thunder activity	34.0	30.0	42.0		
	Without thunder activity	66.0	70.0	58.0		

Table VII: Rainfall per centages for Douala derived from Table III (1930-1963).

Year \ Station	Douala, Cameroun (4.07N, 9.68E)			Garoua, Cameroun (9.33N, 13.38E)		
	Total (mm)	June-Sept (mm)	%	Total (mm)	June-Sept.	%
1936	3958.4	1880.0	47.5			
1937	3237.9	1931.7	59.7			
1938	4145.1	2564.6	61.9			
1939	3237.6	1729.8	53.2			
1940	4087.9	2474.1	60.5			
1941	3377.6	1699.5	50.3	832.9	536.7	64.4
1942	4794.4	3051.2	63.6	746.8	534.1	71.5
1943	4243.1	2337.4	55.1	927.1	601.2	64.8
1944	3287.9	1956.8	59.5	875.1	675.4	77.2
1945	3943.1	2647.8	67.2	1228.4	930.3	75.7
1946	4355.4	2780.7	63.8	921.7	709.6	77.0
1947	3460.4	2214.9	64.0	853.7	732.6	85.8
1948	3766.4	2287.8	60.7	1098.4	891.9	81.2
1949	3853.5	2422.0	62.9	911.8	652.1	71.5
1950	4526.0	2862.5	63.2	537.2	342.8	63.8
1951	4097.4	2877.9	70.2	1300.9	1005.5	77.3
1952	4590.7	2939.8	64.0	961.8	676.5	70.3
1953	4496.9	30.86.3	68.6	980.5	711.9	72.6
1954	4321.9	2535.0	58.7	1004.3	635.8	63.3
1955	3601.2	2161.7	60.0	1076.5	826.0	76.7
1956	5327.2	3174.9	59.6	715.1	616.2	86.2
1957	4631.3	2908.6	62.8	1190.3	875.2	73.5
1958	4215.3	2728.5	64.7	1027.4	842.1	82.0
1959	4651.6	2958.1	63.6	1203.0	899.5	74.8
1960	4336.1	3148.0	72.6	1343.7	952.8	70.9
1961	4245.5	2863.7	67.5	926.9	843.9	91.0
1962	4662.2	2849.4	61.1	866.7	788.5	91.0
1963	3415.5	2238.3	65.5	1427.3	1075.8	75.4
1964	4870.7	3458.8	71.0	1058.1	718.3	67.9
1965	4436.8	2931.0	66.1	911.5	778.3	85.4
1966	4384.1	2952.0	67.3	1019.7	664.1	65.1
1967	4340.3	2980.6	68.7	1002.7	833.9	83.2
1968	3275.3	2069.6	63.2	1179.3	980.2	83.1
1969	4271.7	2927.1	68.5	1291.5	1093.0	84.6
1970	4307.2	2971.1	69.0	809.8	595.3	73.5
1971	4597.0	3070.9	66.8	1691.6	946.8	56.0
Total	149,352.6	94,667.0	63.4	25,536.0	19,246.4	75.4
Mean	4,148.7	2,629.6	63.4	823.7	620.9	75.4

Table VIII: Monsoon components of annual rainfall at Douala and Garoua, Cameroun .

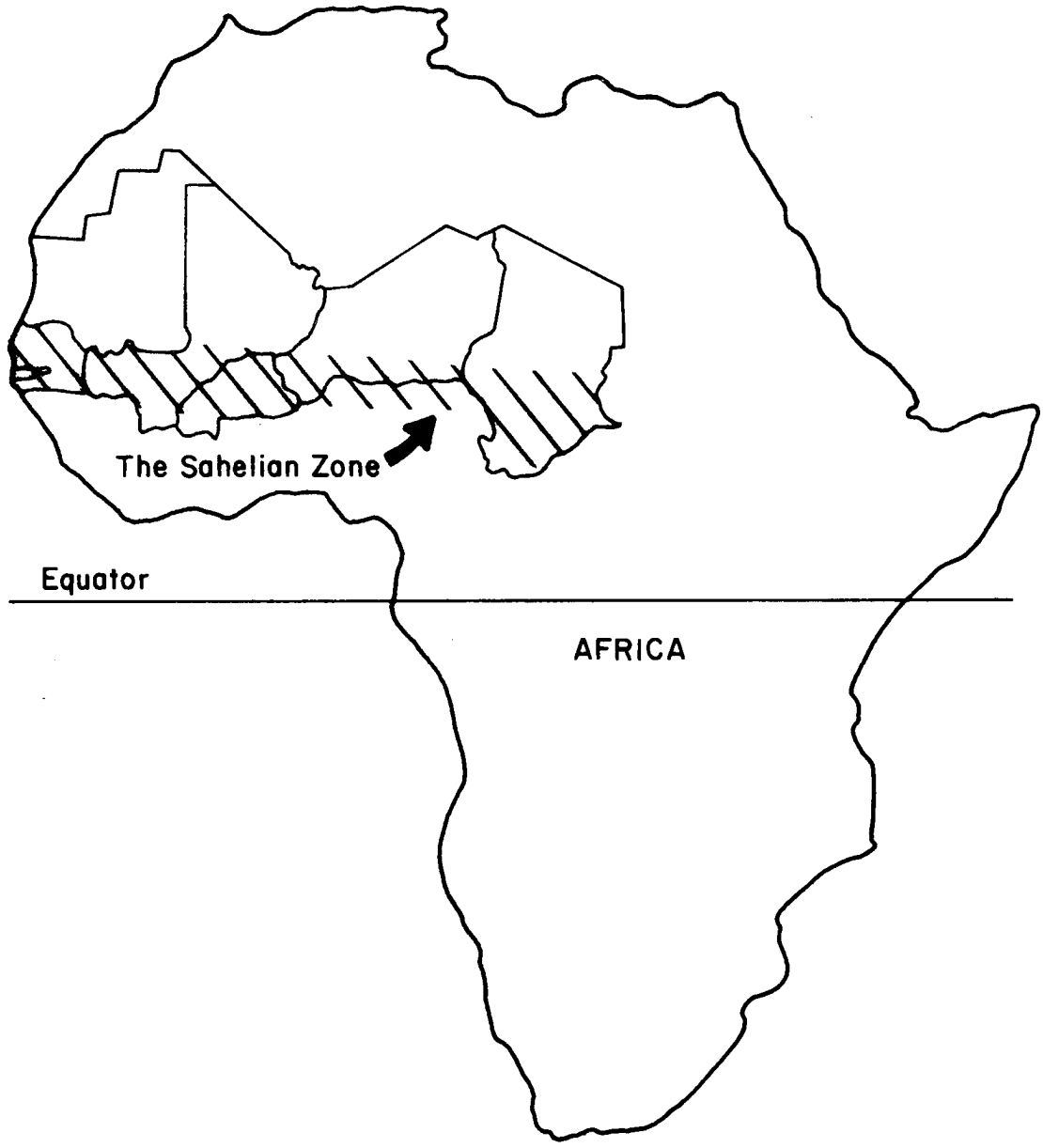

Fig. 1: The Sahelian Zone (Bryson, 1973)

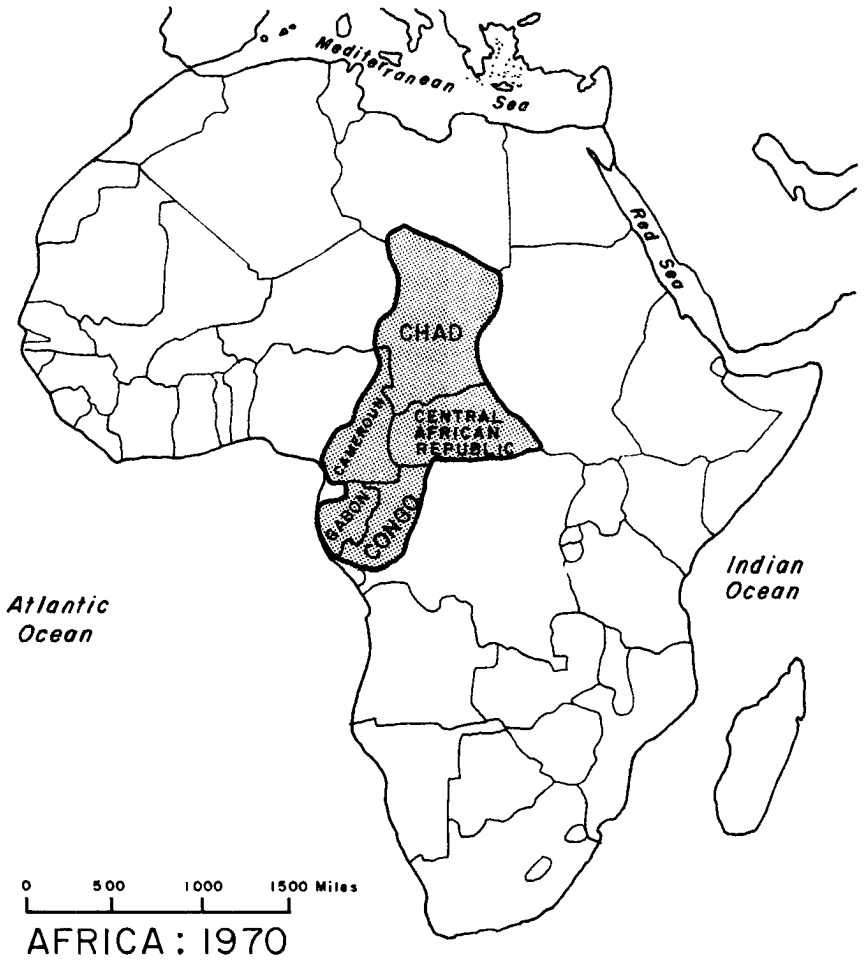

Fig. 2: Location of the study area.

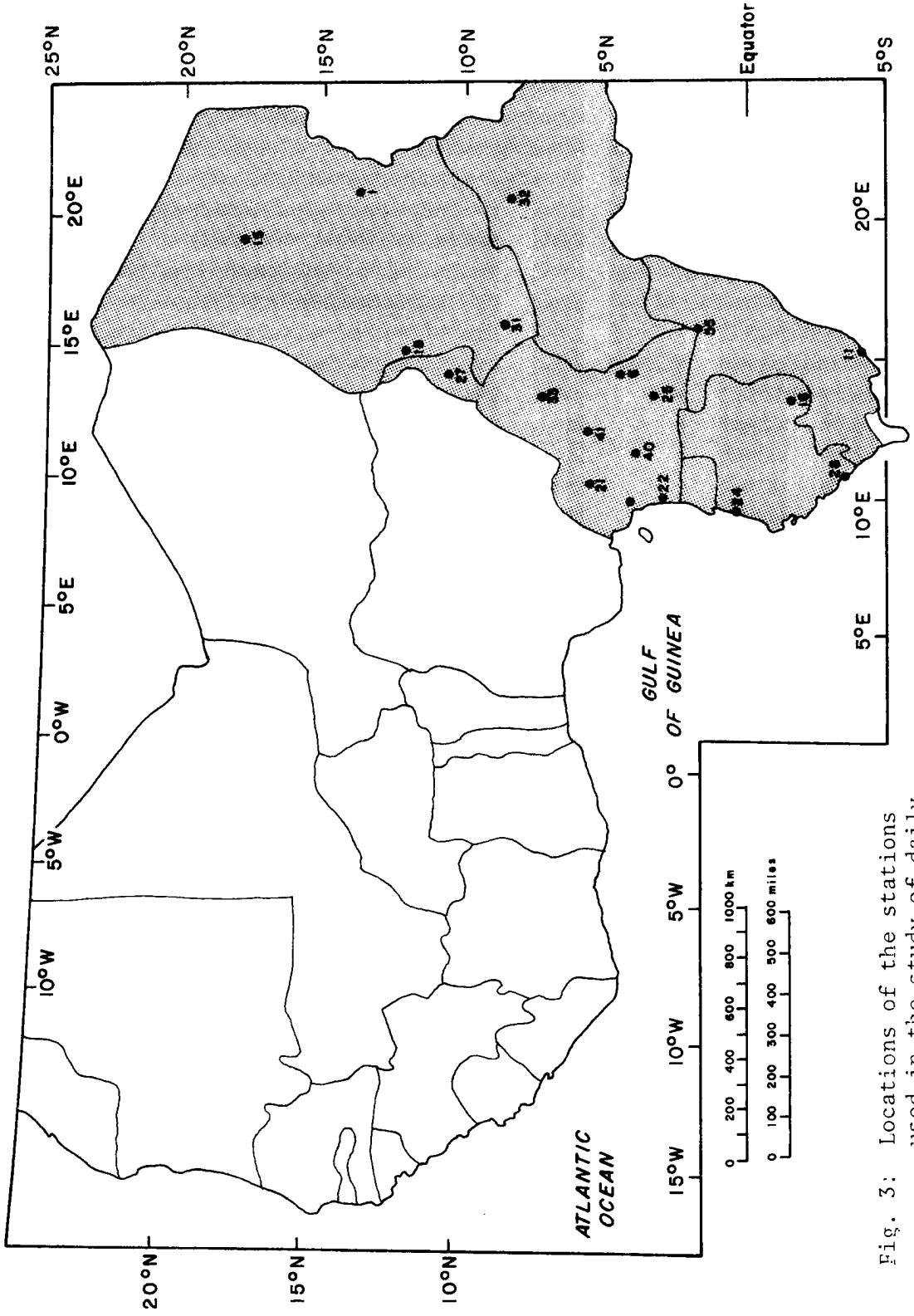

Fig. 3: Locations of the stations used in the study of daily rainfall amounts.

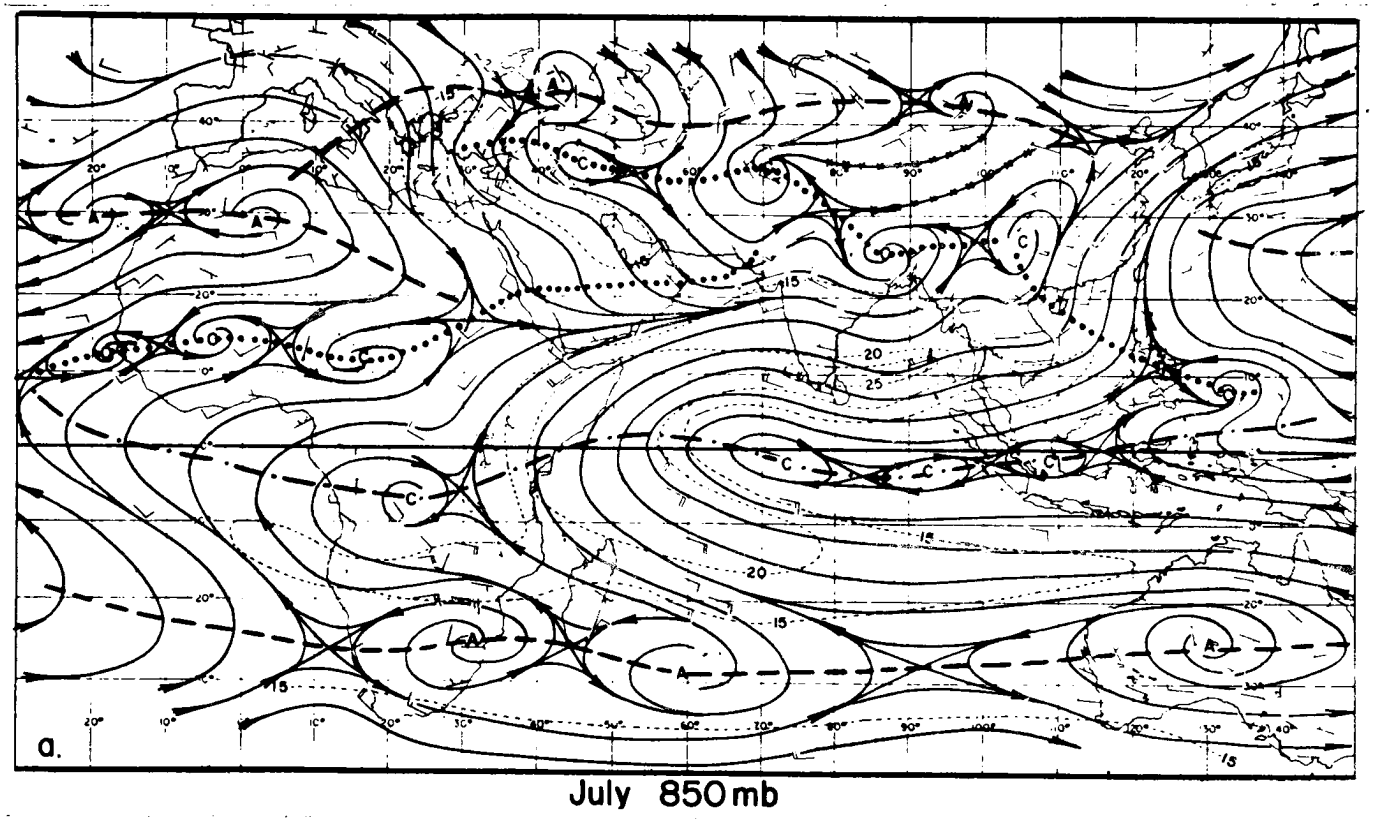

Fig. 4a: Mean resultant winds. Solid lines are streamlines, dashed lines are isotachs labeled in knots. July, 850 mb (Sadler and Harris, 1970).

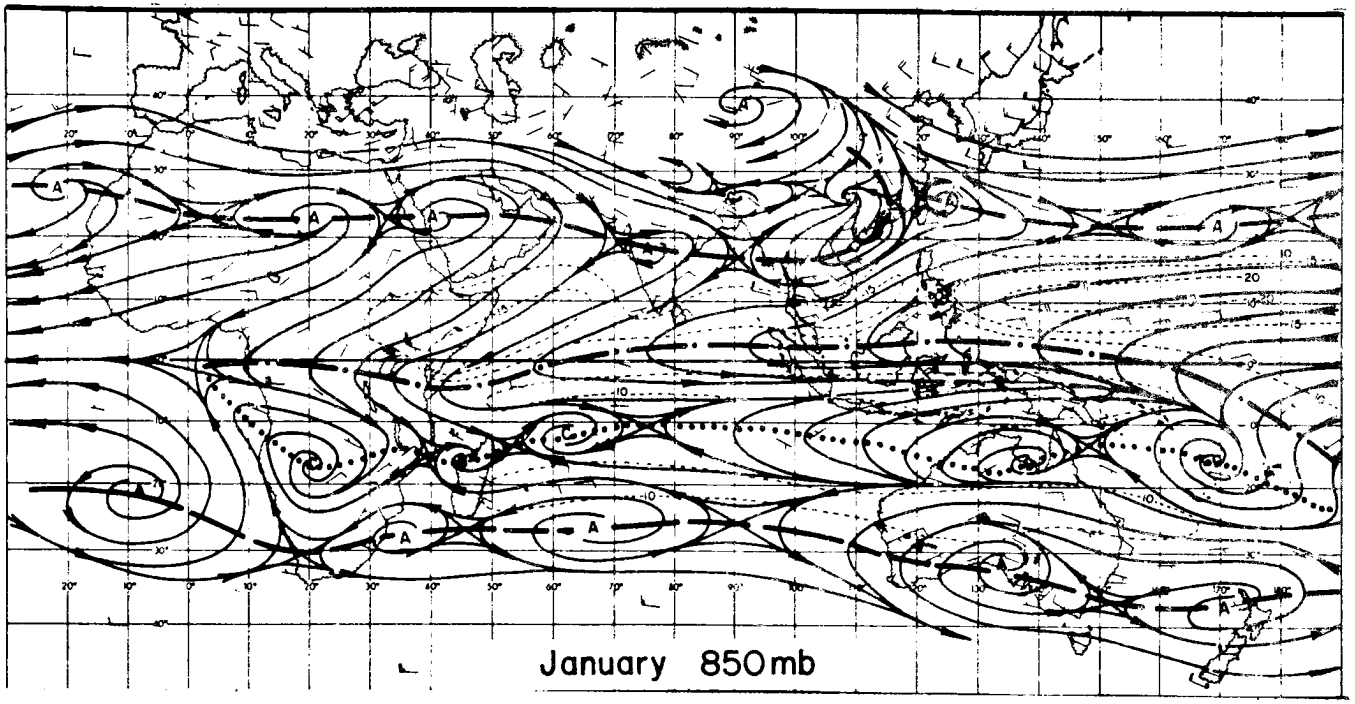

Fig. 4b: Mean resultant winds. Solid lines are streamlines, dashed lines are isotachs labeled in knots. January, 850 mb (Sadler and Harris, 1970).

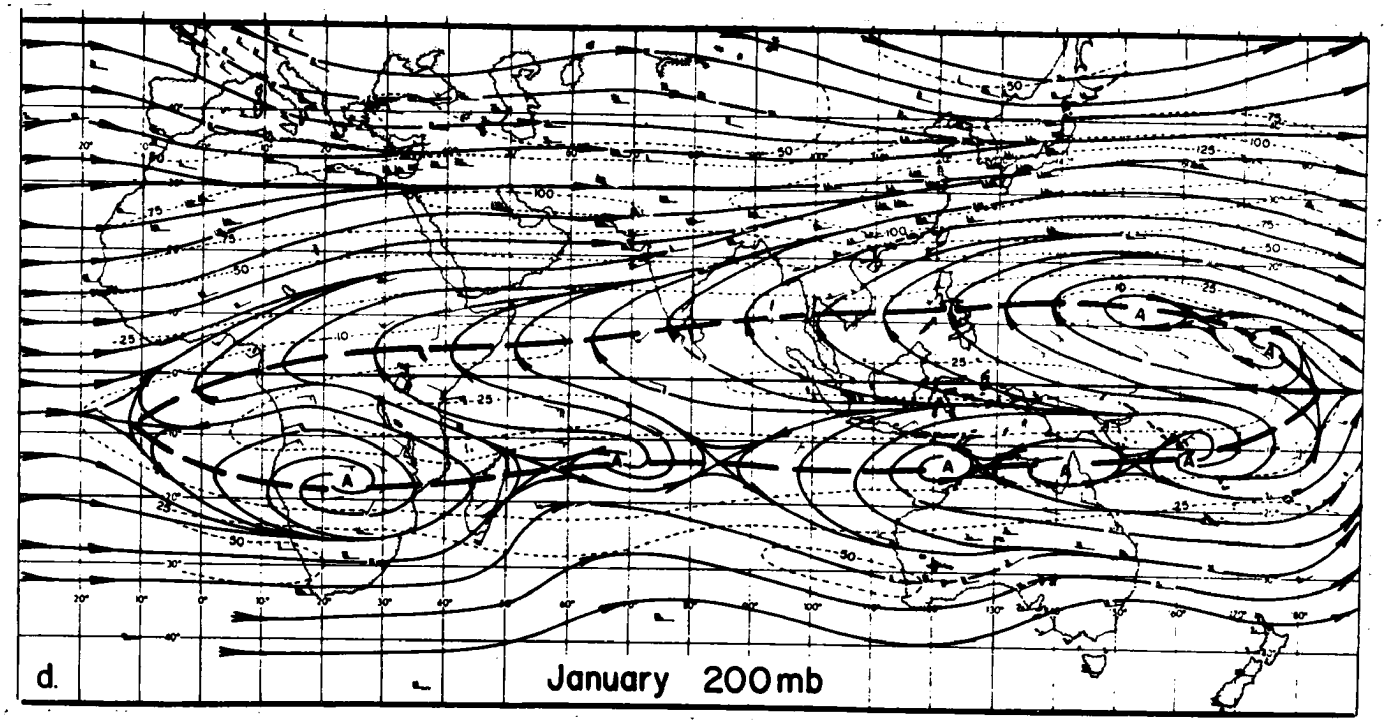

Fig. 4c: Mean resultant winds. Solid lines are streamlines, dashed lines are isotachs labeled in knots. January, 200 mb (Sadler and Harris, 1970).

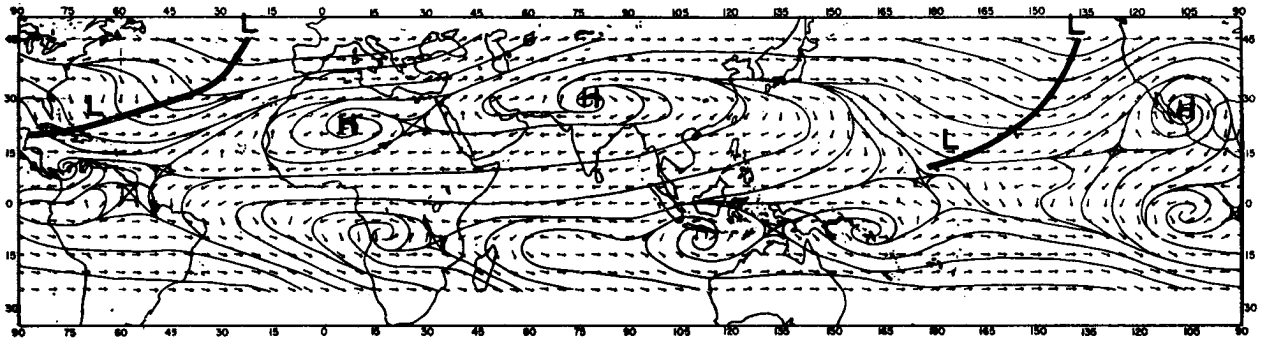

Fig. 4d: Observed time averaged streamlines (June, July and August 1967) at 200 mb (Krishnamurti, et al., 1973).

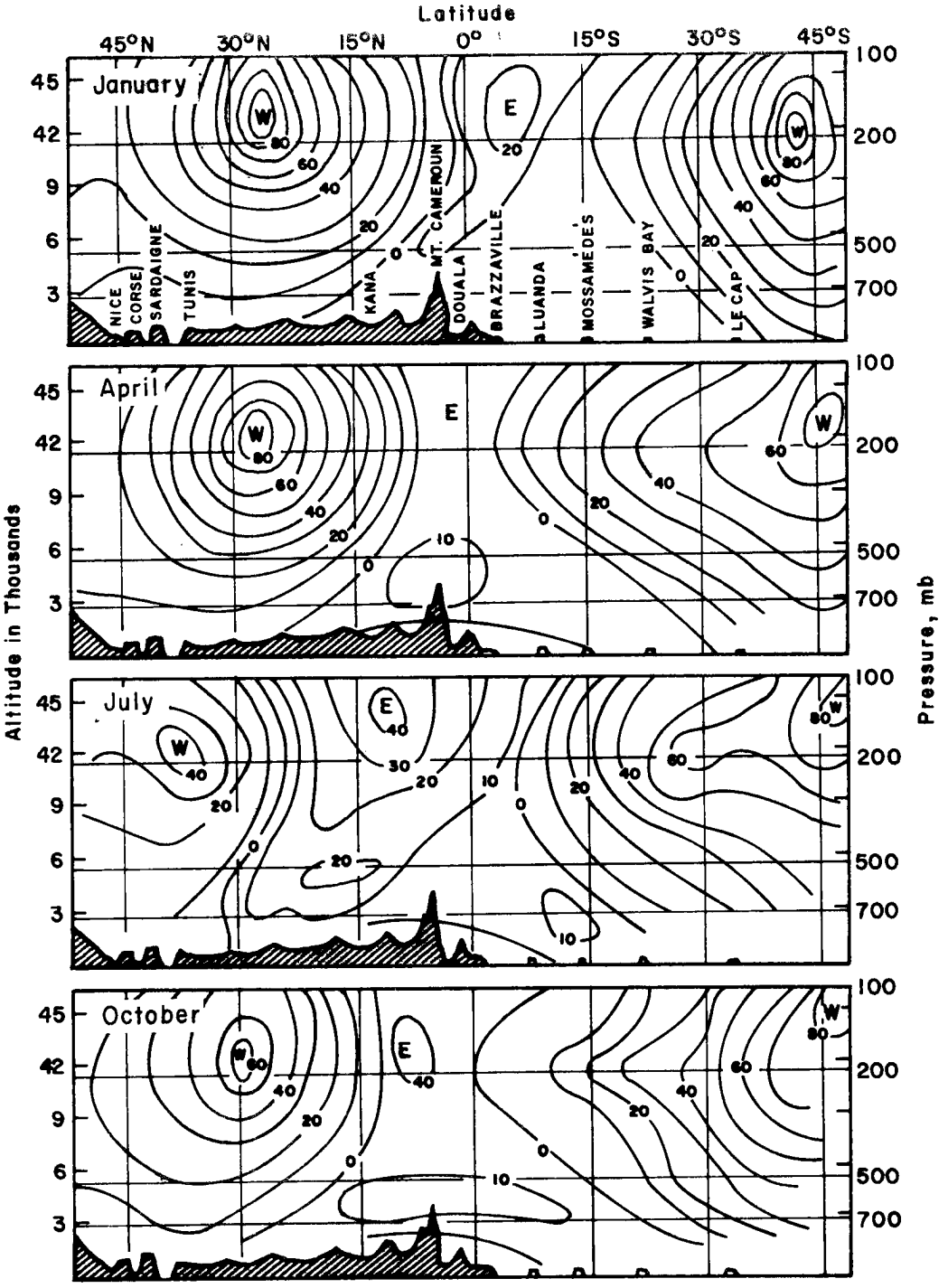

Fig. 5: Meridional cross sections of zonal wind near 10°E. Solid lines are isotachs labeled in knots (Mandengue, 1965).

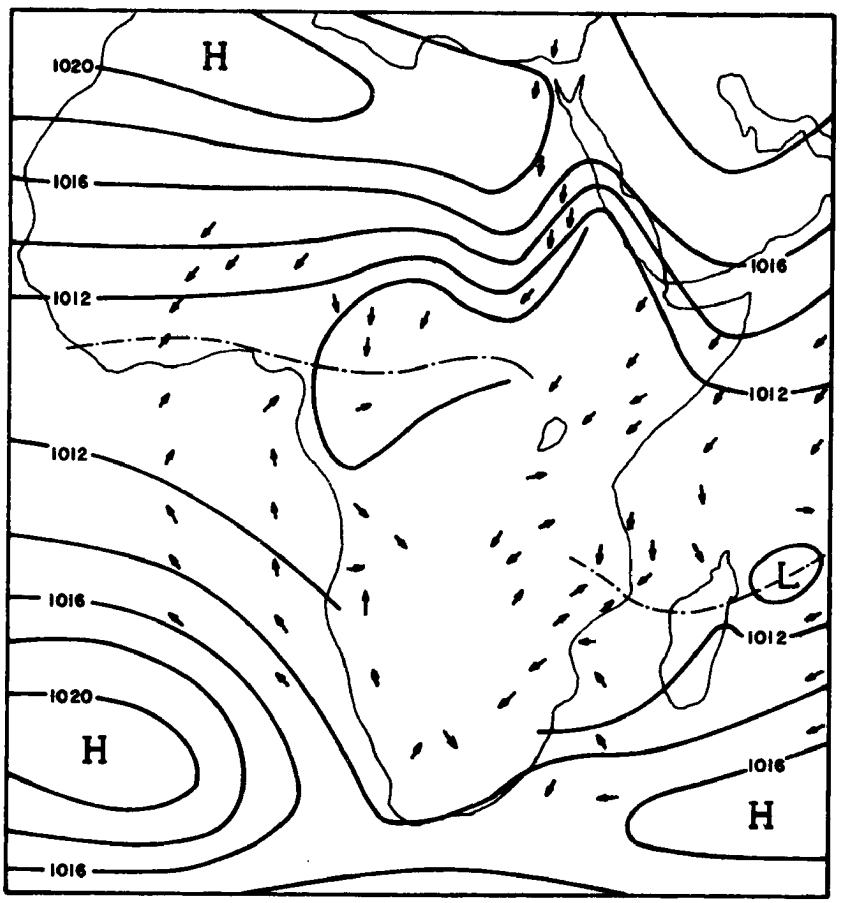

Fig. 6a: Mean sea-level pressure patterns and prevailing air currents. Solid lines are isobars in millibars. The dotted-dashed line represents the ITD. January (Sansom, 1965)

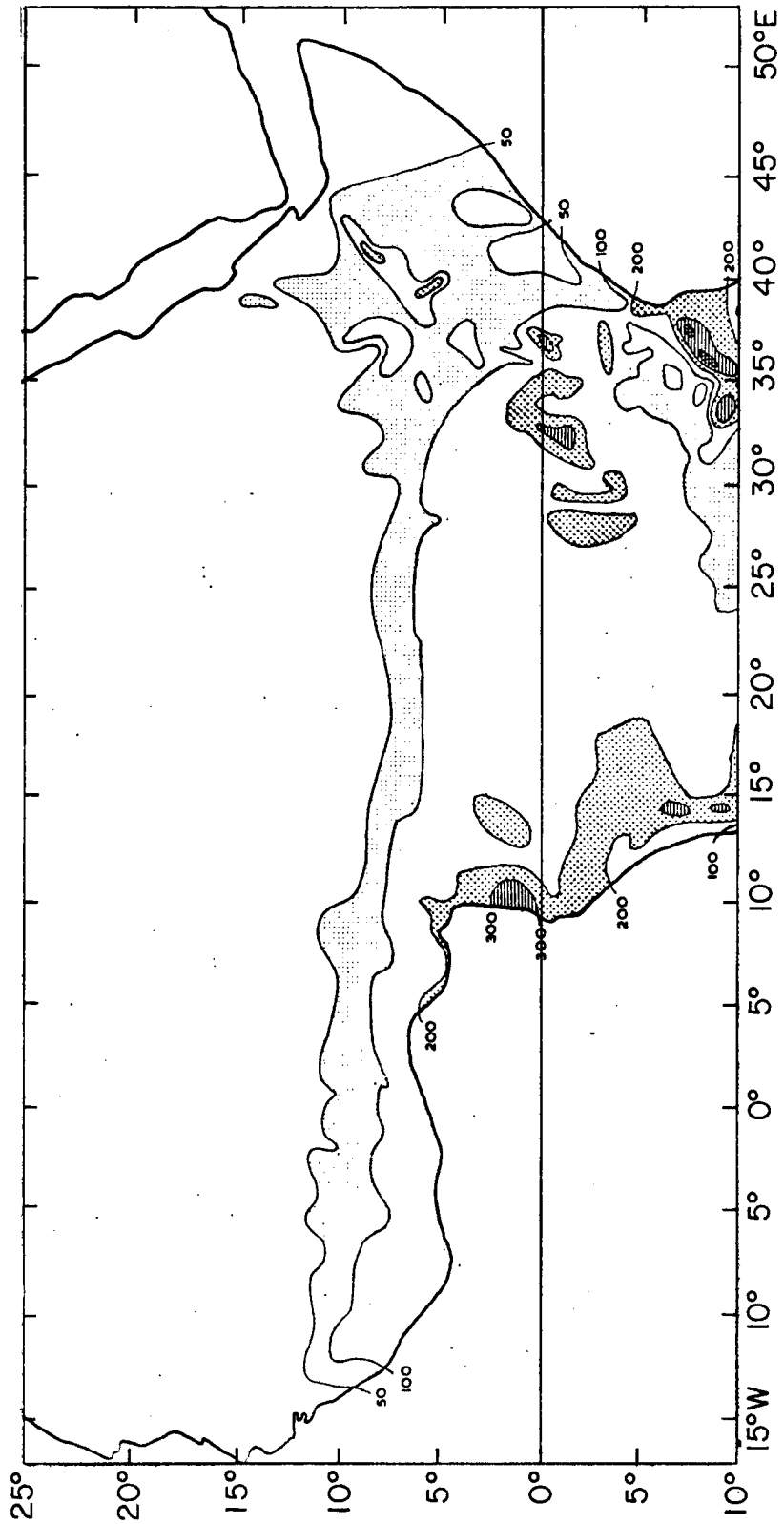

Fig. 7b: Mean rainfall amounts. April (Thompson, 1965).

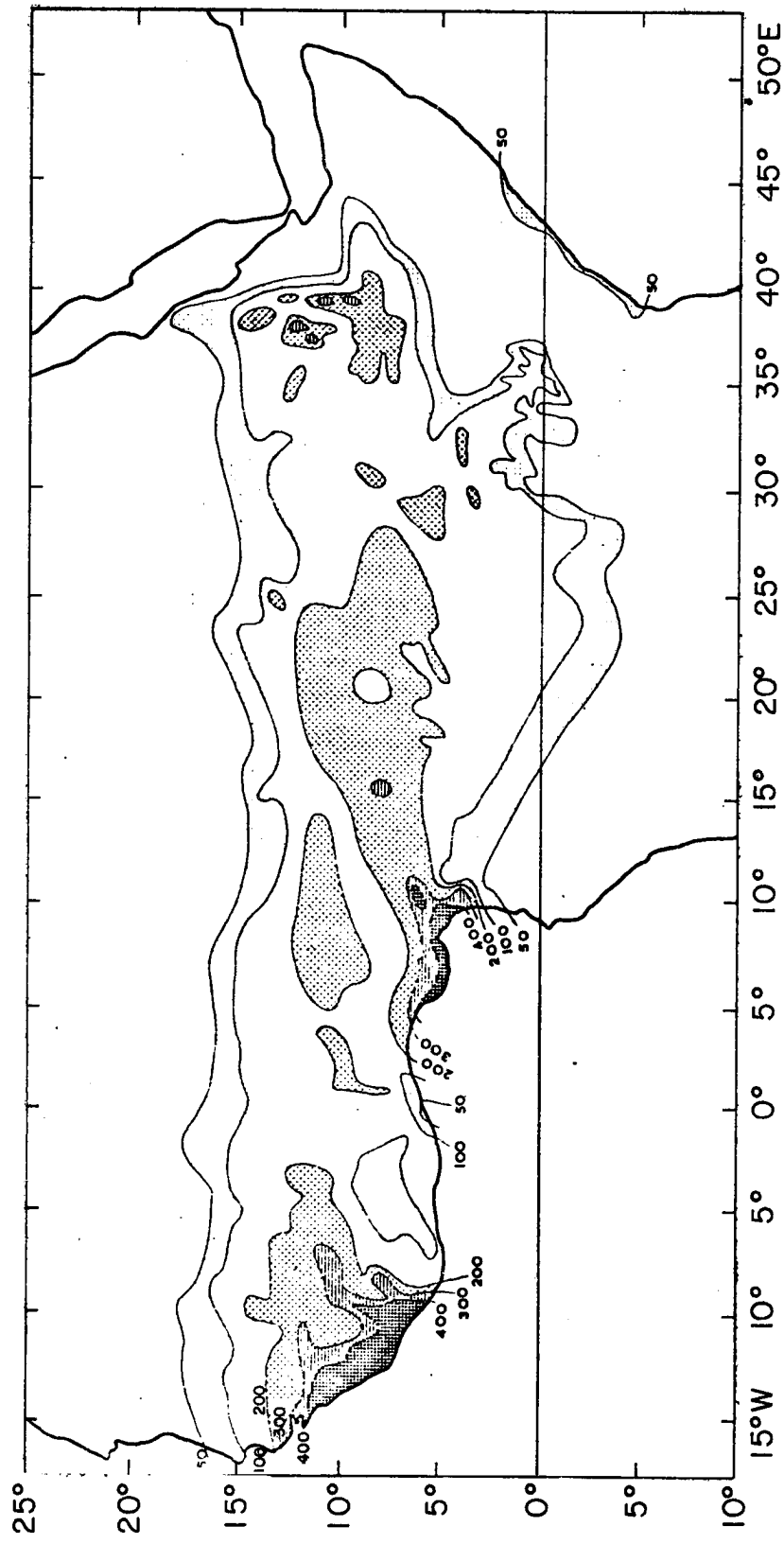

Fig. 7c: Mean rainfall amounts. July (Thompson, 1965).

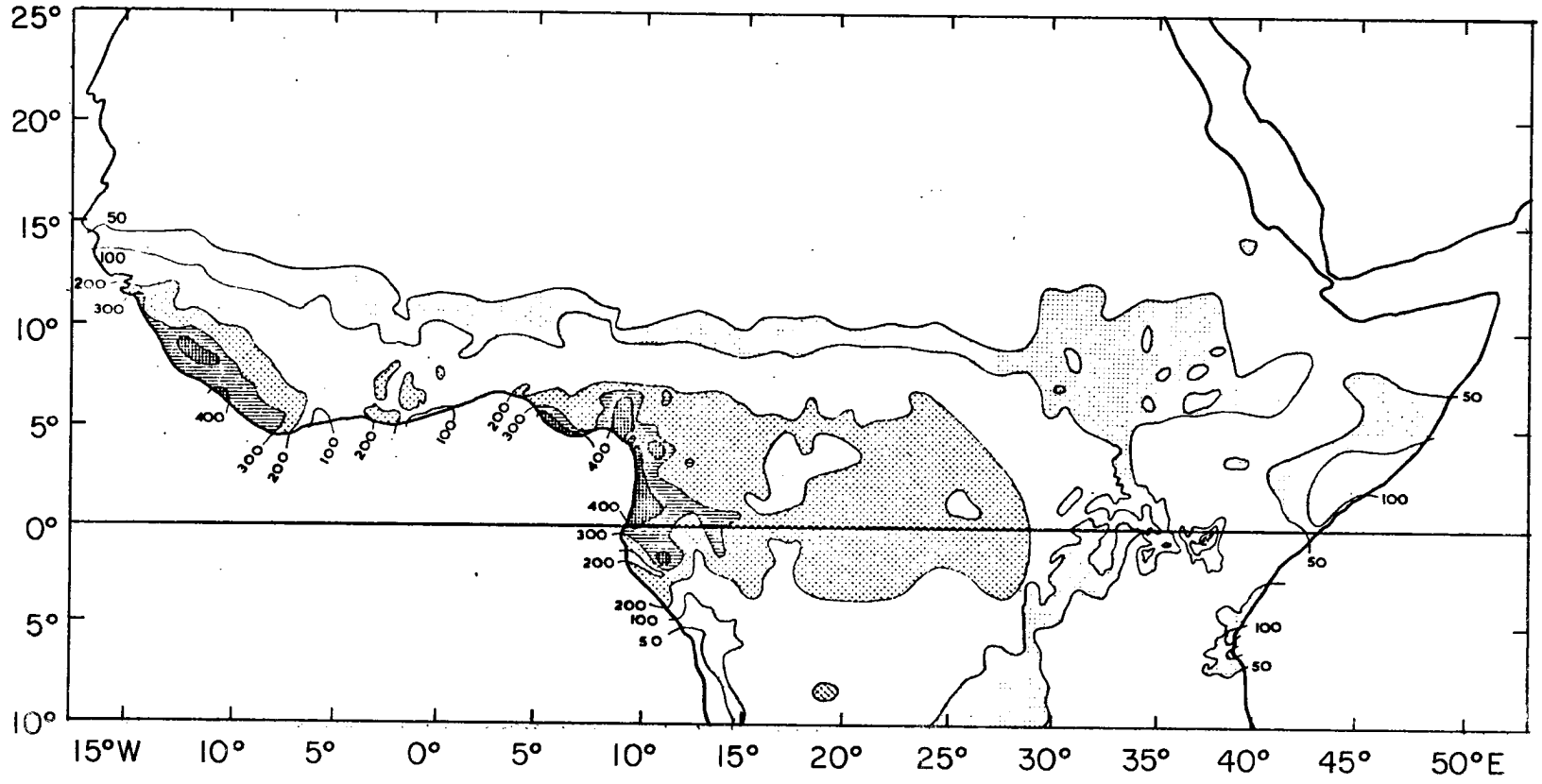

Fig. 7d: Mean rainfall amounts. October (Thompson, 1965).

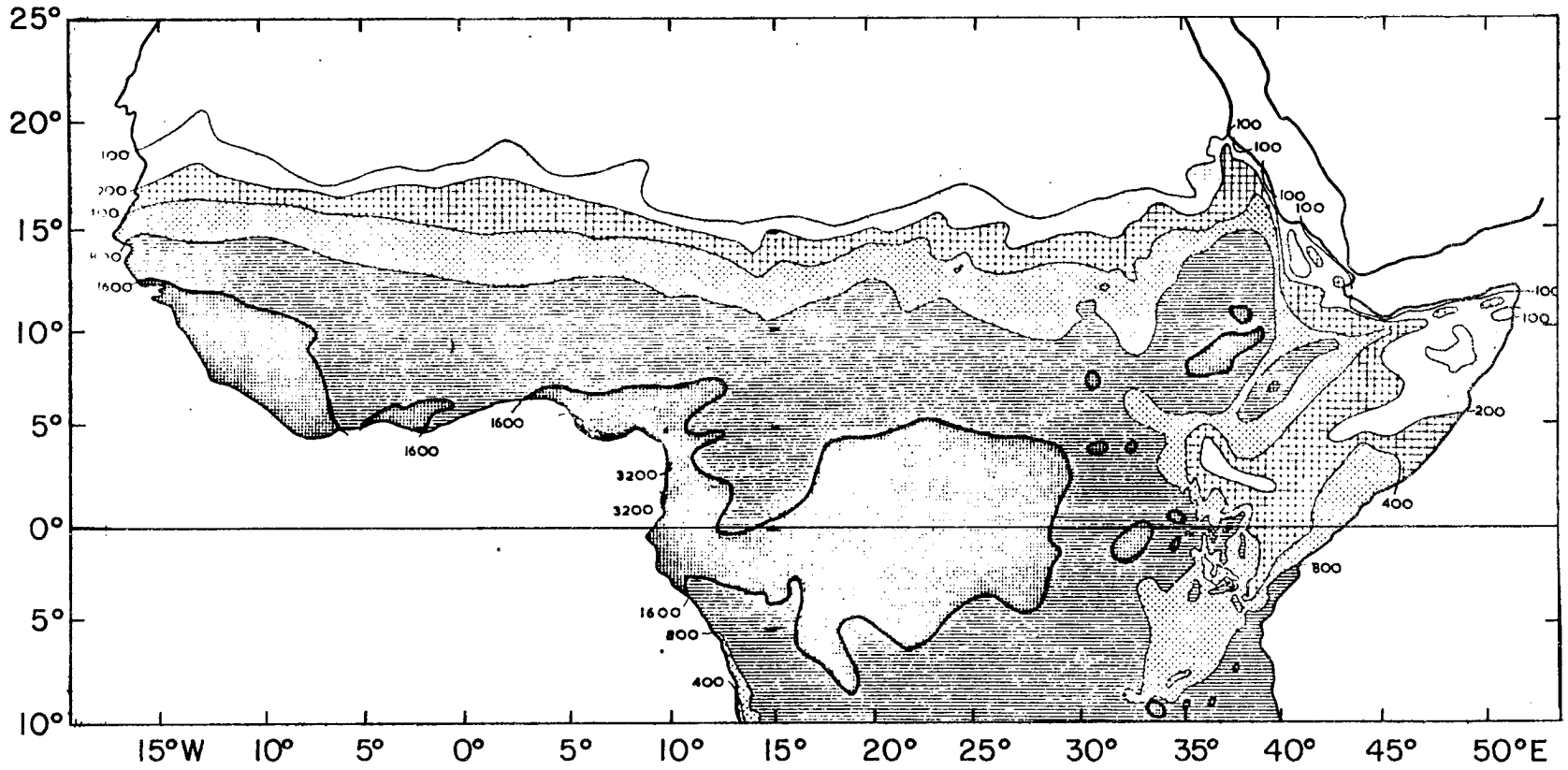

Fig. 7e: Mean rainfall amounts. Annual (Thompson, 1965).

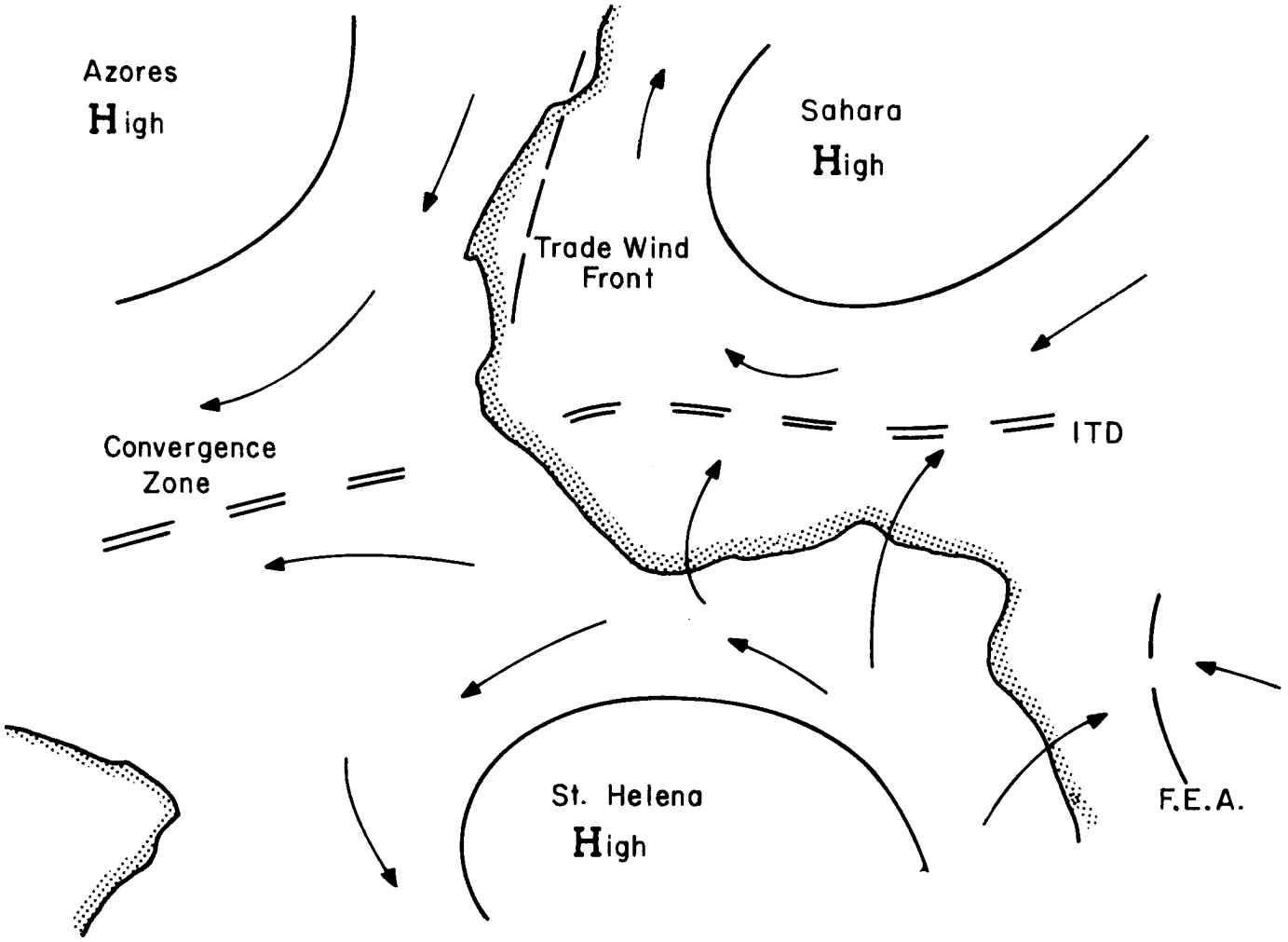

Fig. 8: Idealized average surface positions of the subtropical high pressure centers (Dhonneur, 1971).

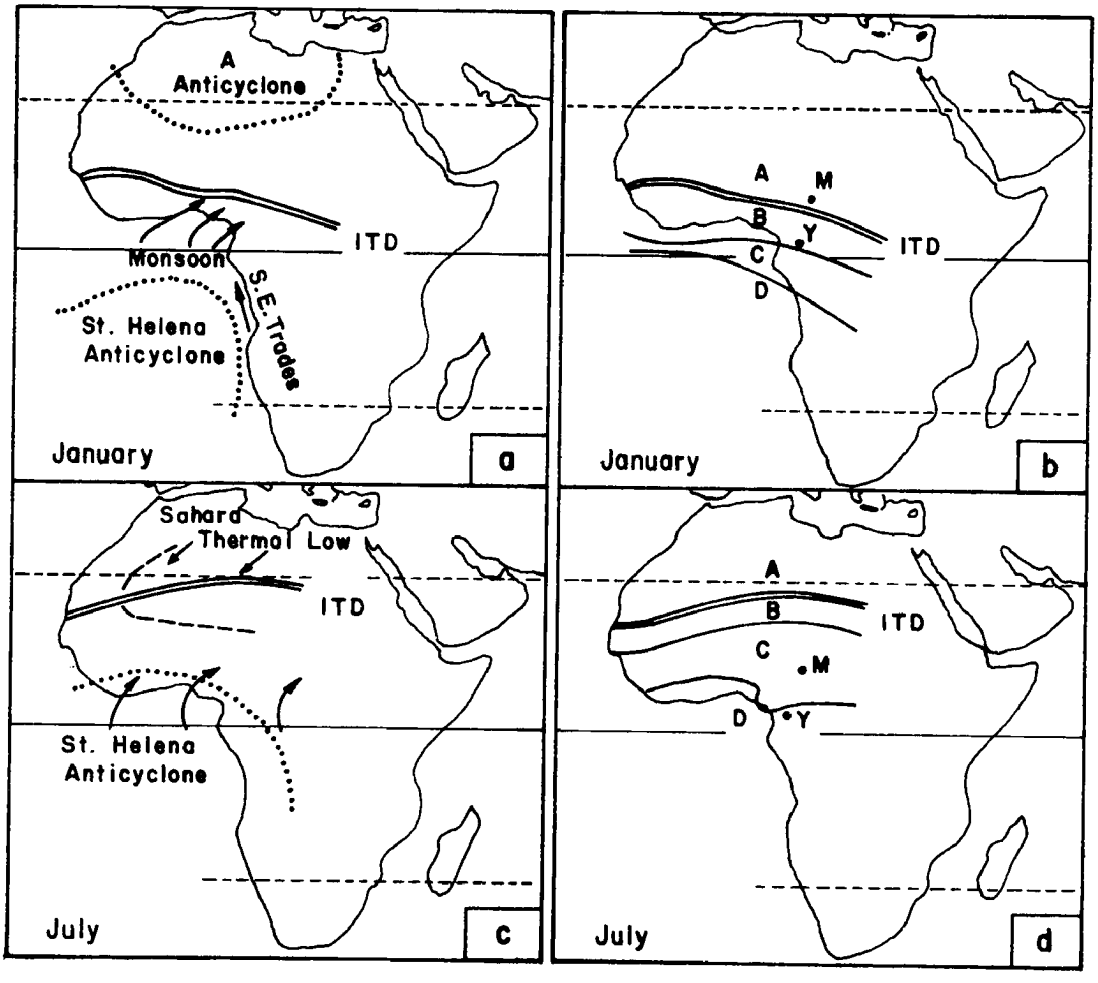

Fig. 9: Idealized average surface positions of the subtropical anticyclones and the ITD, together with prevailing air currents. The corresponding rainfall zones, A, B, C, D, are shown on the right (For explanation, see text. Genieux, 1957).

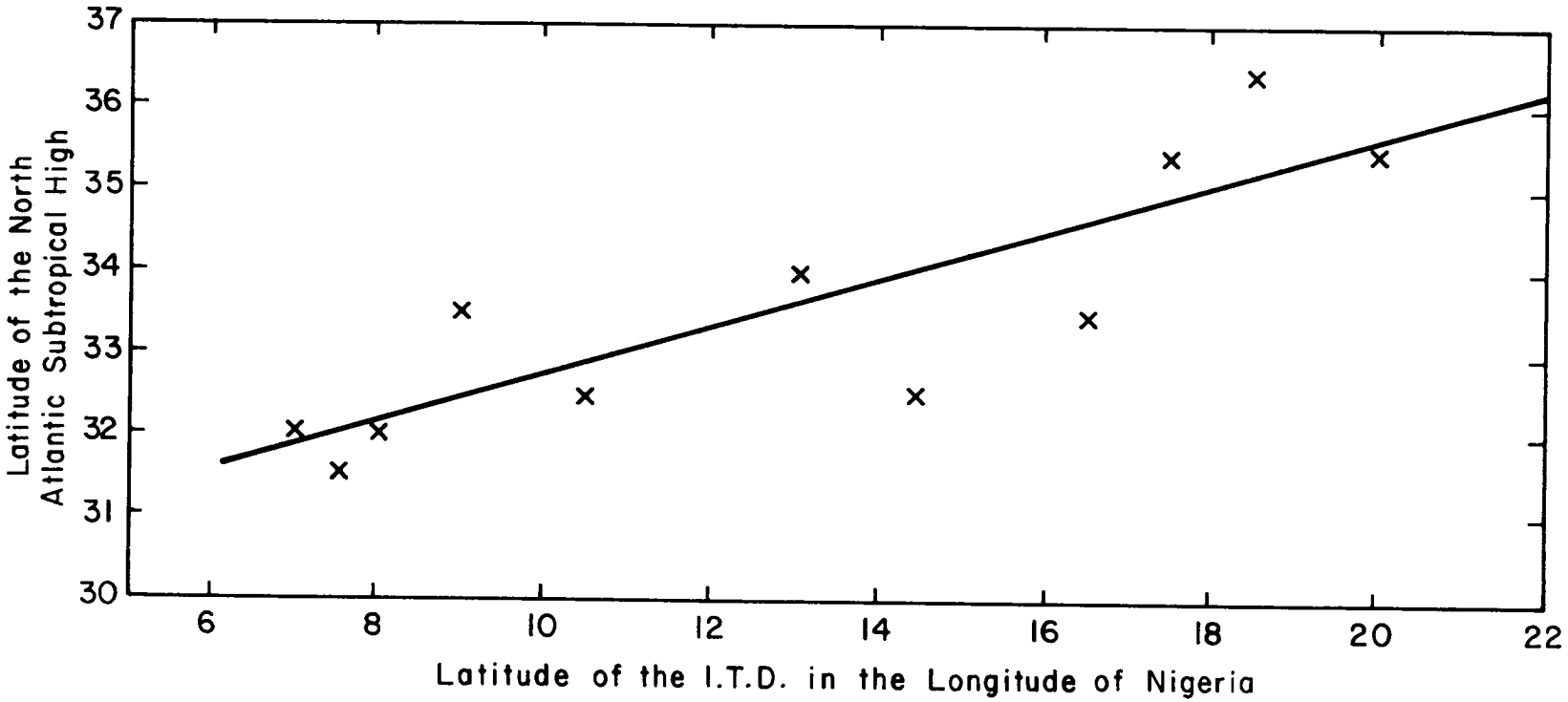

Fig. 10: The latitude of the subtropical anticyclone in the North Atlantic versus the latitude of the ITD in the longitudes of Nigeria (Bryson, 1973).

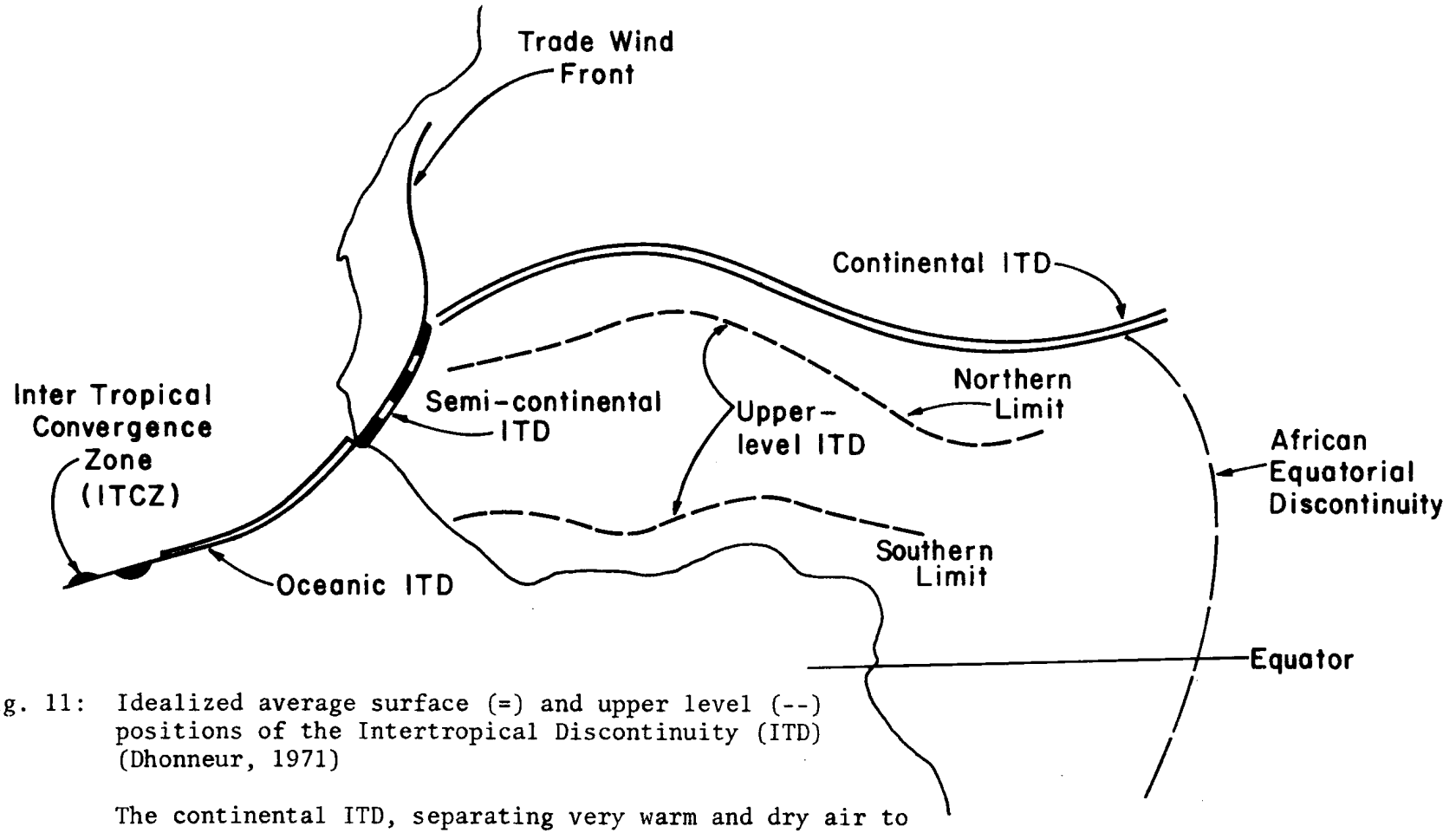

Fig. 11: Idealized average surface (=) and upper level (--) positions of the Intertropical Discontinuity (ITD) (Dhonneur, 1971)

The continental ITD, separating very warm and dry air to the north from warm and moist air to the south is drawn on synoptic charts with the aid of temperatures, dew points, and wind direction.

The semi-continental ITD separates the warm or cool and humid air associated with the Azores anticyclone from the warm and humid air of southern hemisphere origin. It is outlined on the basis of wind directions, the northerly component being associated with the trade winds, the southerly component with the monsoon.

The oceanic ITD connects the semi-continental ITD to the ITCZ over the Atlantic Ocean.

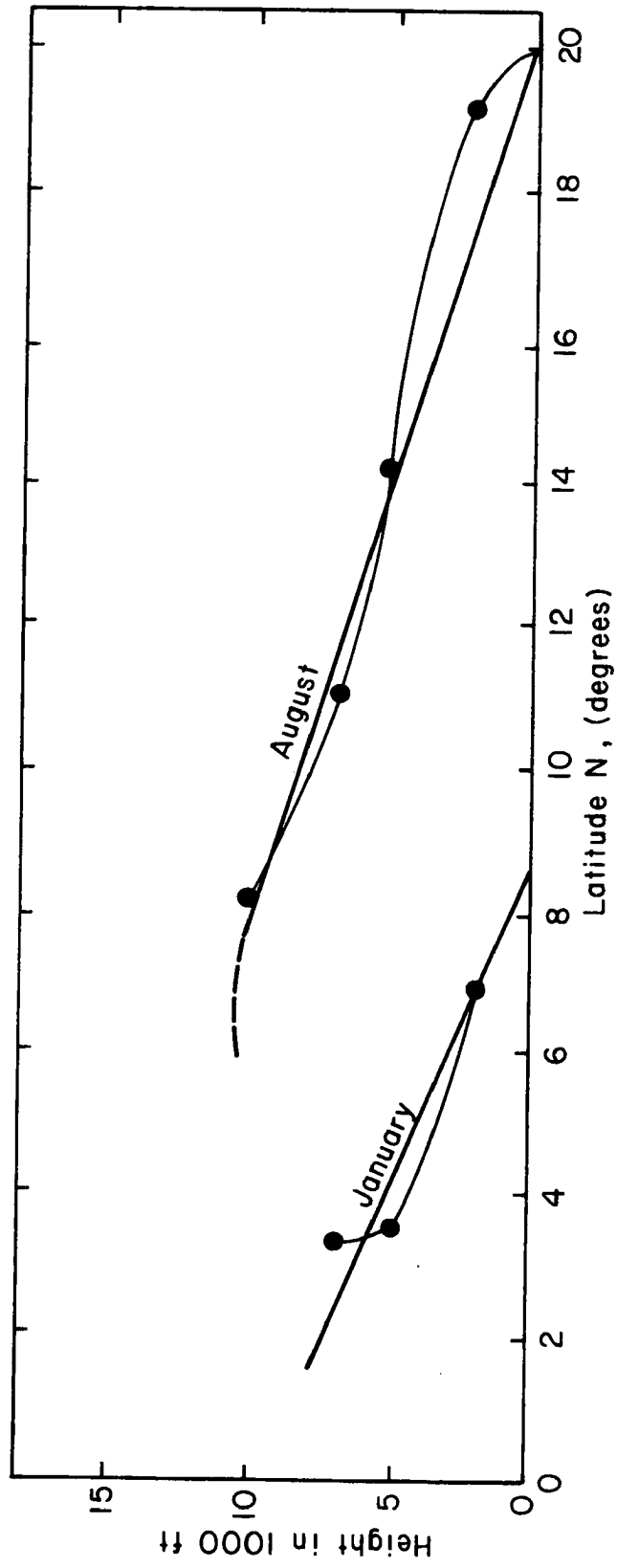

Fig. 12a: Mean slope of the Intertropical Discontimuity (ITD) near the longitudes of Nigeria during January and August (Obasi, 1965).

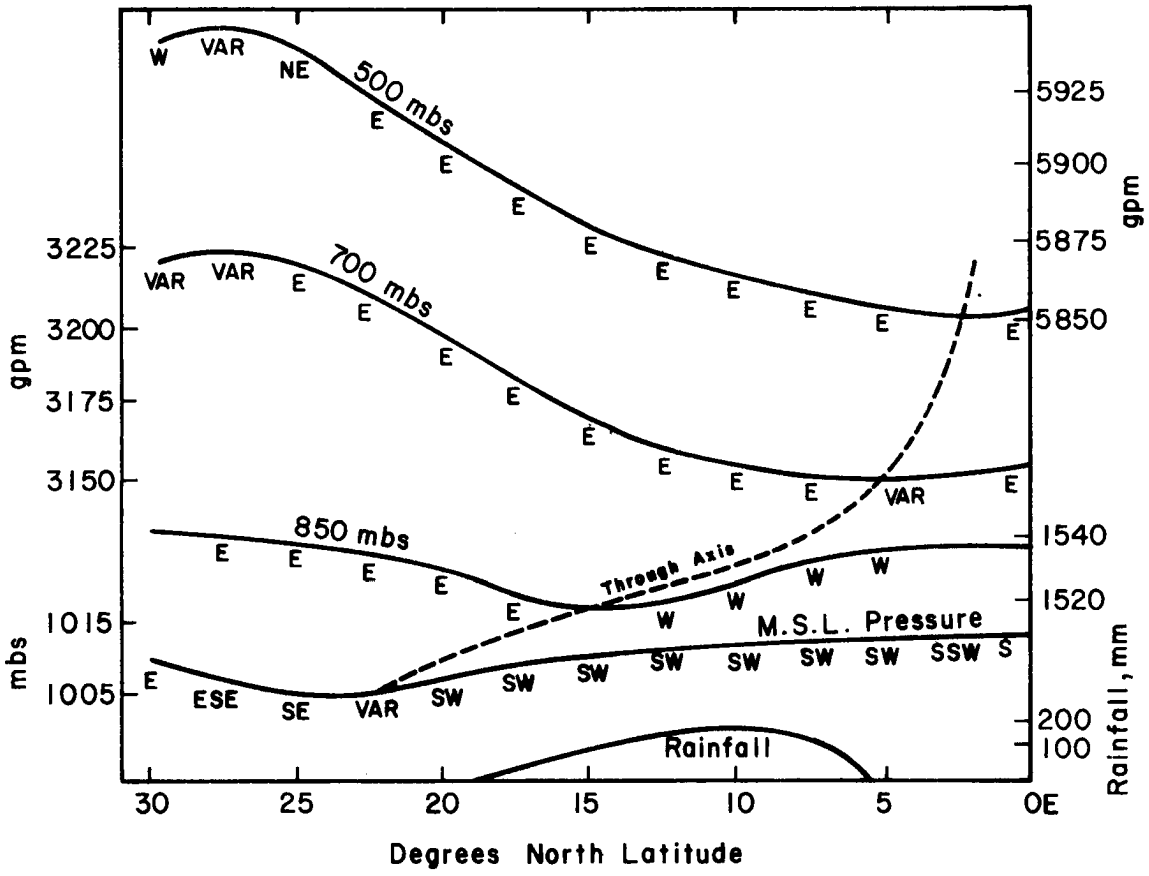

Fig. 12b: Mean slope of the Intertropical Discontinuity (ITD). Between the equator and 30°N, near the Greenwich meridian during July (Thompson, 1965).

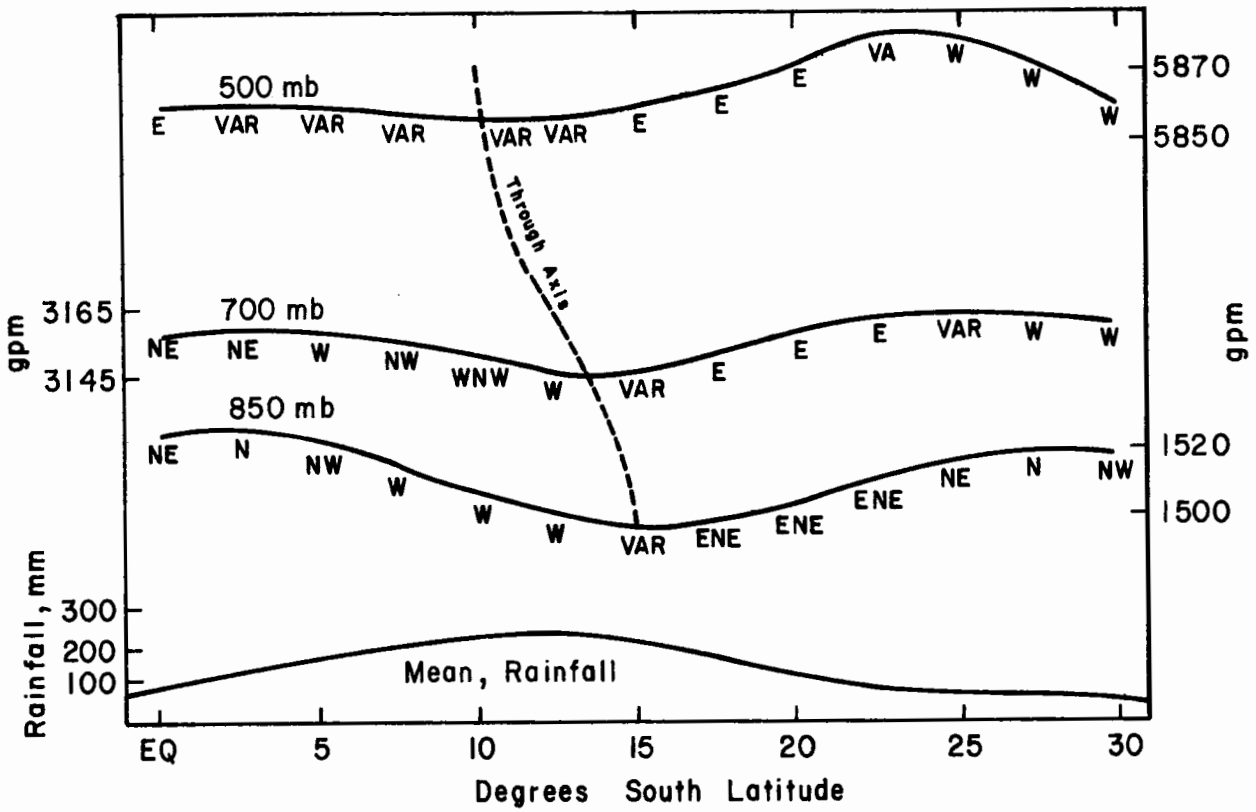

Fig. 12c: Mean slope of the Intertropical Discontinuity (ITD). Between the equator and 30°N, near longitude 25°E during January (Sansom, 1965).

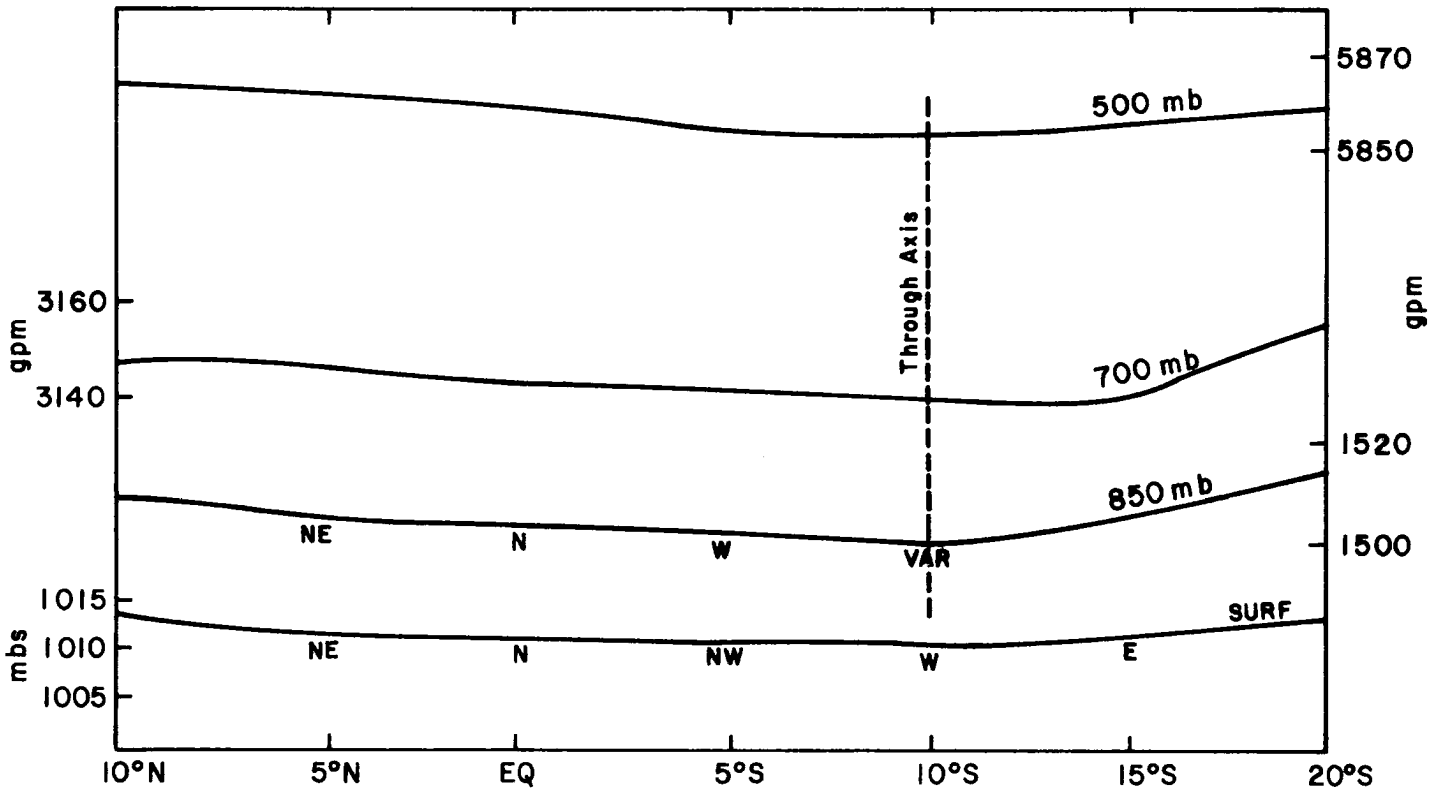

Fig. 12d: Mean slope of the Intertropical Discontinuity (ITD). Between the equator and 30°N, near longitude 60°E during January (Sansom, 1965).

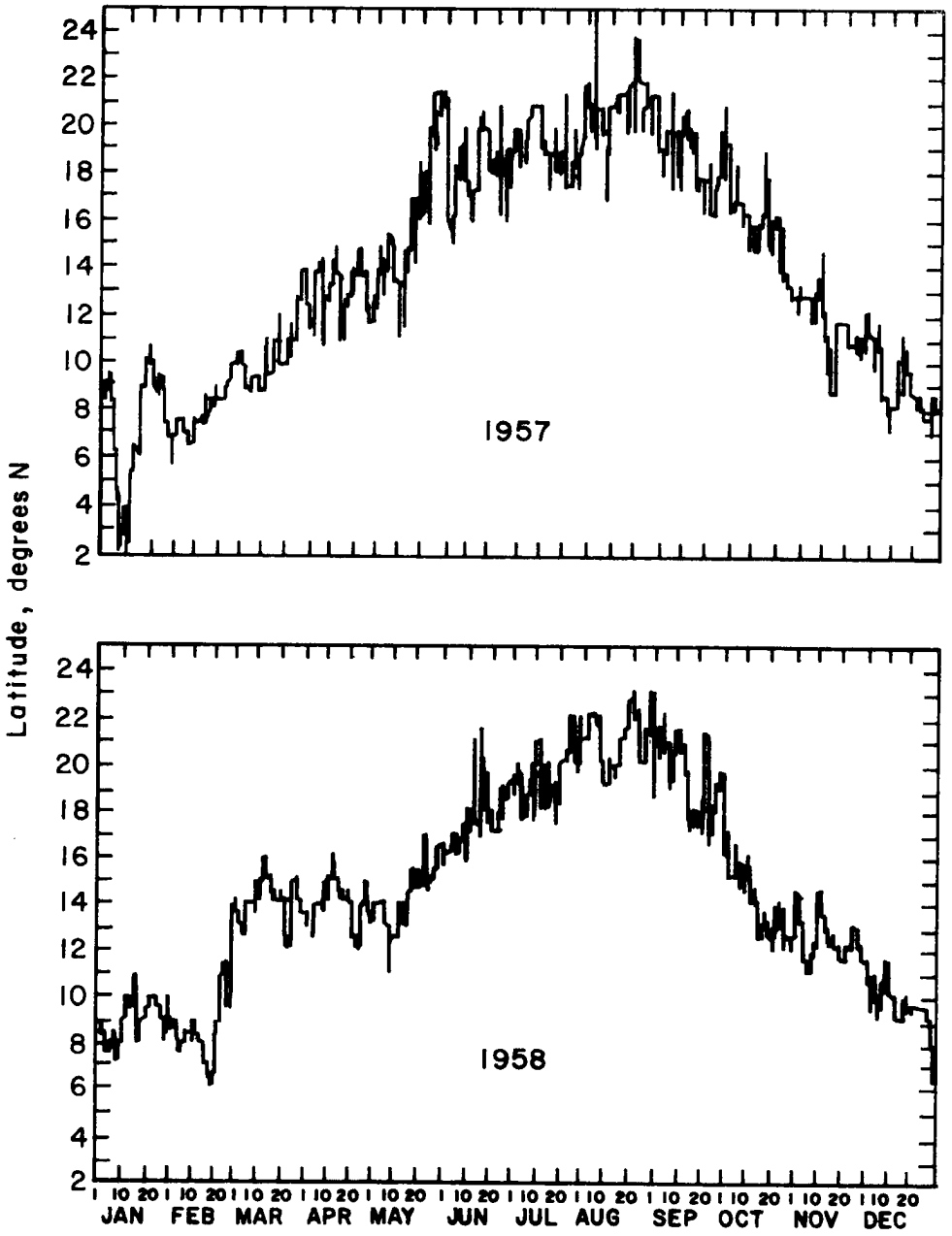

Fig. 13a: Range of the day-to-day and seasonal migrations of the surface ITD. Latitude of southern boundary at the surface of air of northern origin at longitude 3°E, at 0600 GMT each day (Johnson, 1964).

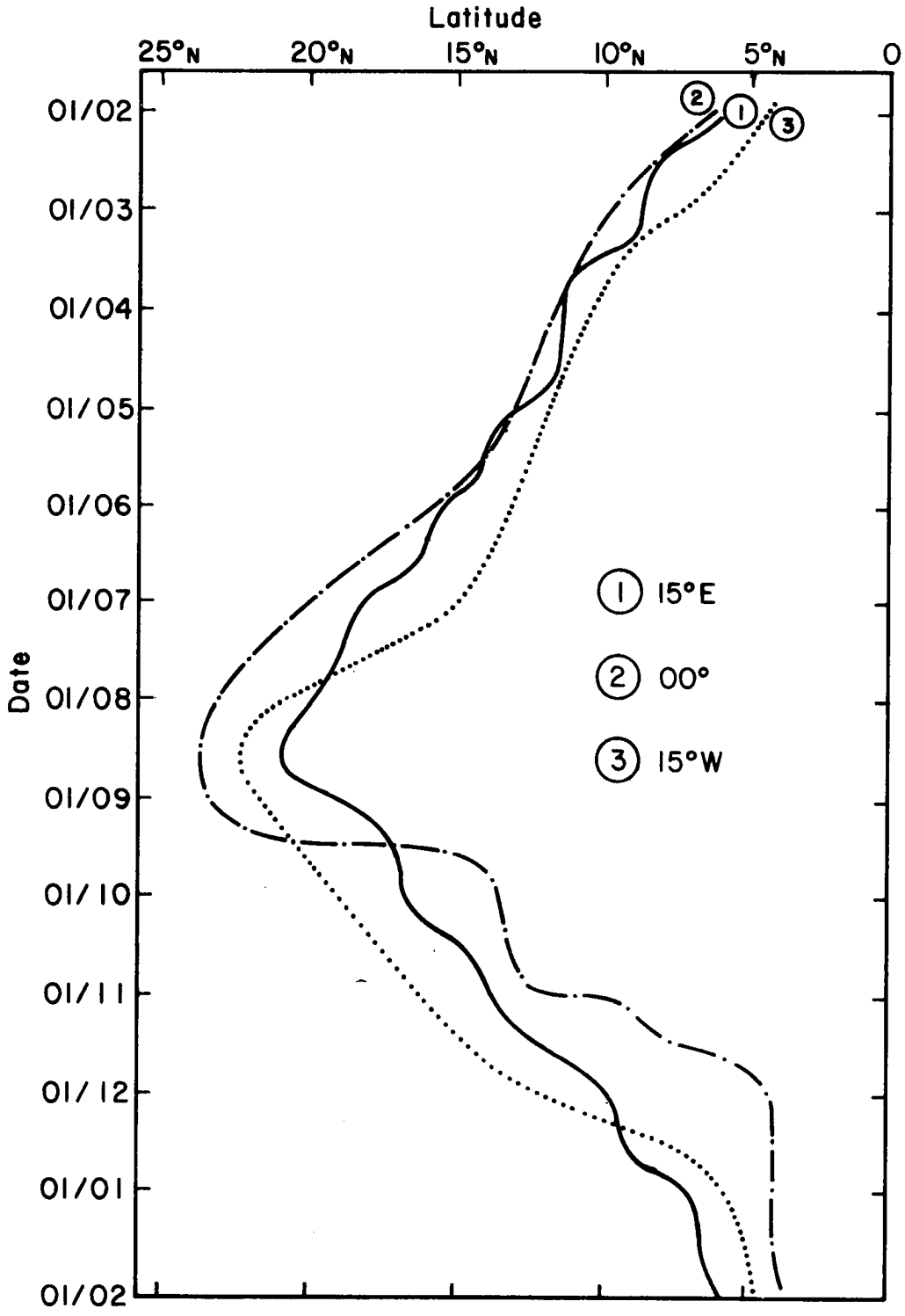

Fig. 13b: Range of the day-to-day and seasonal migrations of the surface ITD. Along 15°E, 00°, 15°W (Dhonneur, 1971).

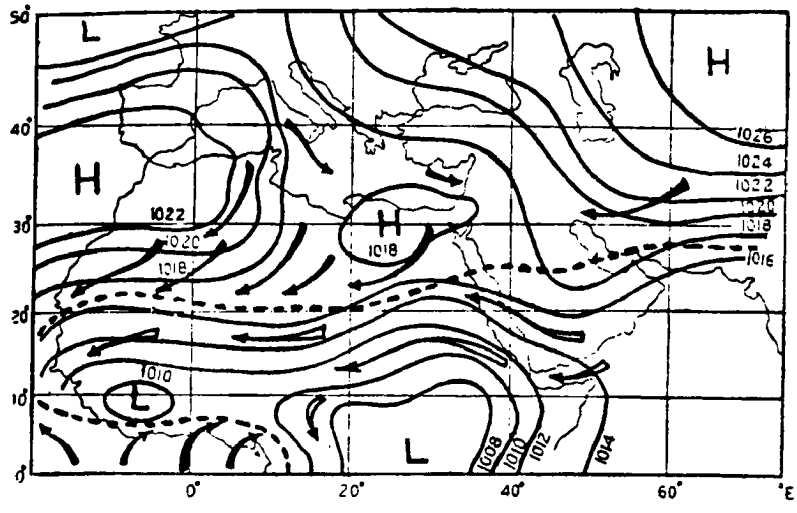

Fig. 14a: Seasonal evolution of the Intertropical Convergence Zone (ITC), the Intertropical Discontinuity (ITD), and the Subtropical Discontinuity (STD). Winter. (Soliman, 1960).

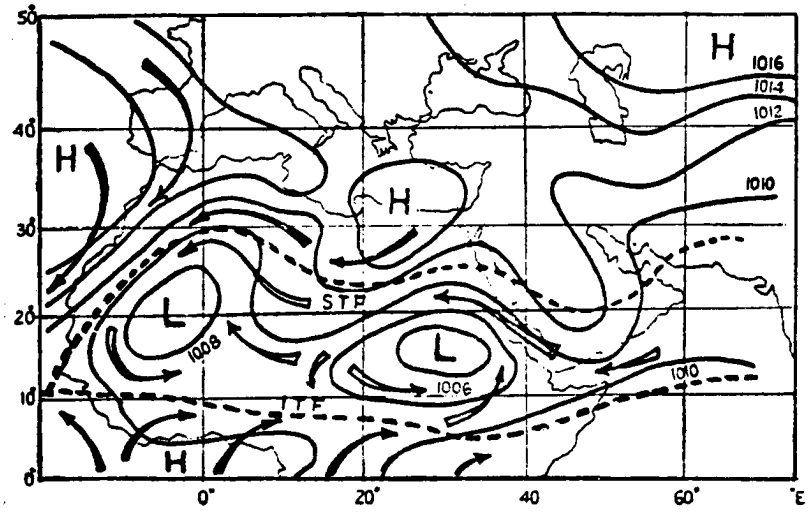

Fig. 14b: Seasonal evolution of the Intertropical Convergence Zone (ITC), the Intertropical Discontinuity (ITD), and the Subtropical Discontinuity (STD). Spring (Soliman, 1960).

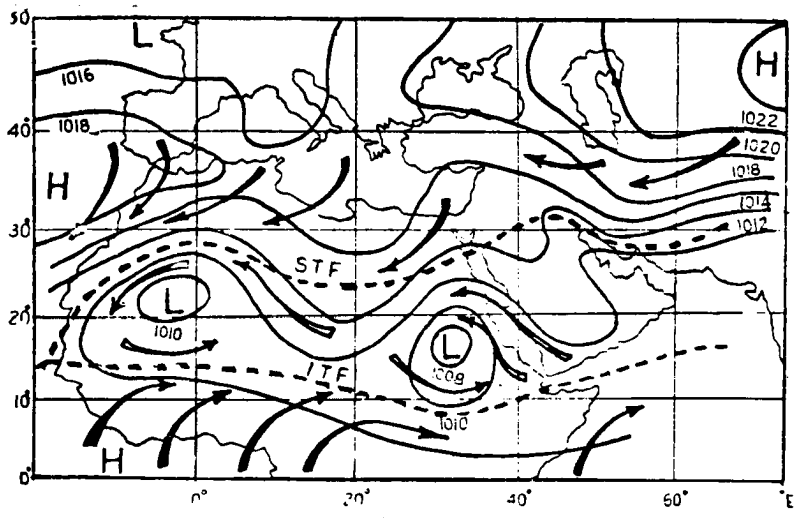

Fig. 14c: Seasonal evolution of the Intertropical Convergence Zone (ITC), the Intertropical Discontinuity (ITD, and the Subtropical Discontinuity (STD). Summer (Soliman, 1960).

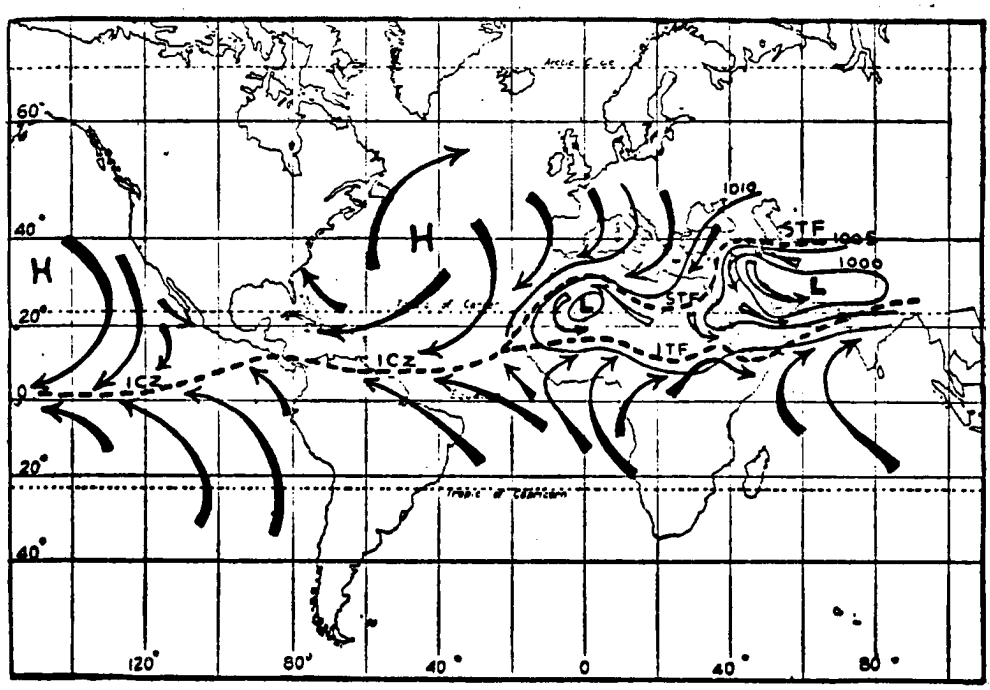

Fig. 14d: Seasonal evolution of the Intertropical Convergence Zone (ITC), the Intertropical Discontinuity (ITD), and the Subtropical Discontinuity (STD). Summer (Soliman, 1960).

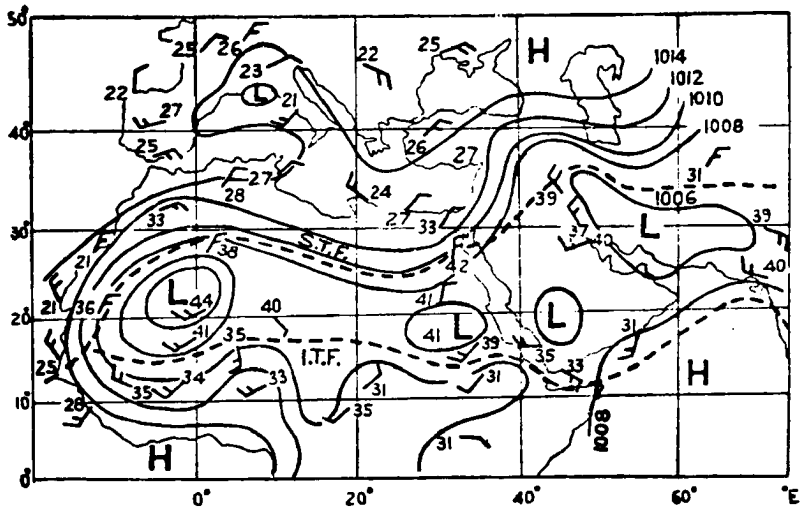

Fig. 14e: Seasonal evolution of the Intertropical Convergence Zone (ITC), the Intertropical Discontinuity (ITD), and the Subtropical Discontinuity (STD). Autumn (Soliman, 1960).

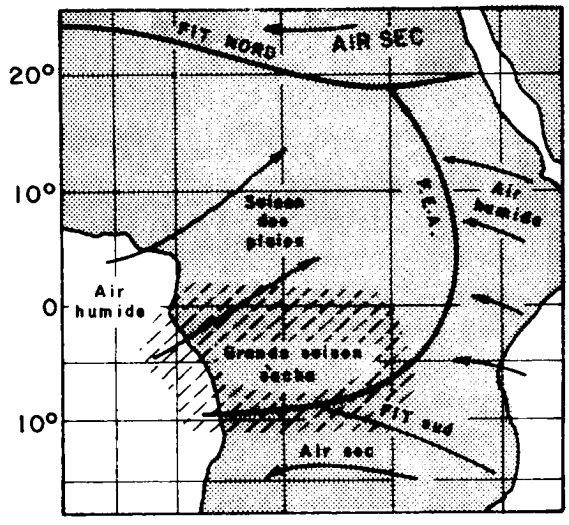

Southern winter - The Northern and Southern FIT are very far to the North; the Southern FIT is very marked during this period. The "front equatorial africain" oscillates around a longitude far to the East. The Atlantic air masses flowing, in the lower layers, over Gabon and Middle Congo are very stable (radiative type). These territories have a major dry season.

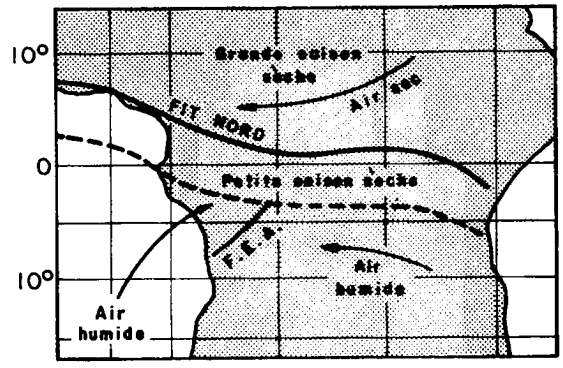

Southern summer - the Northern FIT is at its most southerly position in the year. The Southern FIT is indistinct. The "front equatorial africain" oscillates around longitudes far to the West.

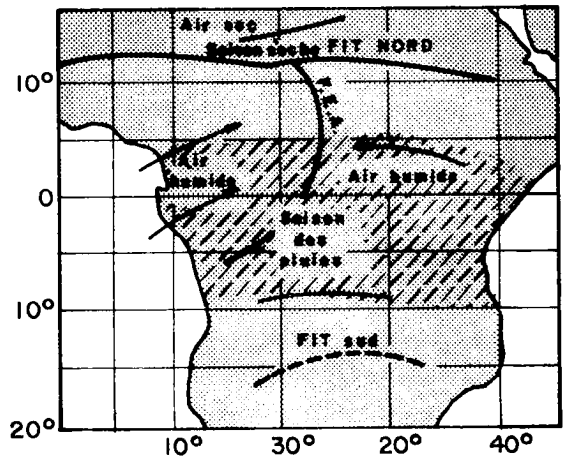

The FIT occupy intermediate positions, slowly shifting southwards from September to December, and northwards from February to July. The "front equatorial africain" oscillates very widely in the centre of Equatorial Africa, which has a rainy season.

Fig. 15: Tschirhart's scheme of three African Fronts (Discontinuities) (Johnson, 1964).

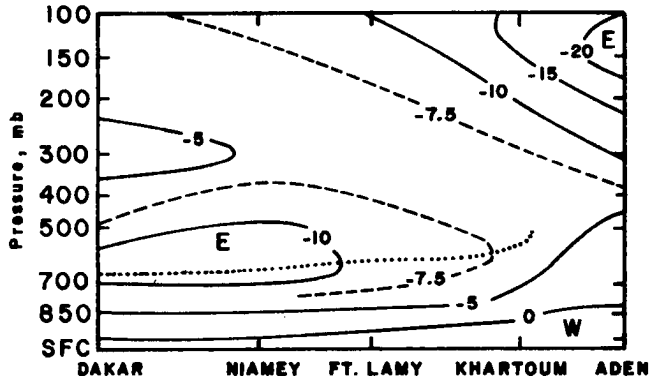

Fig. 16: Cross-section of monthly mean zonal wind (m sec^{-1}) for August near $13^{o}N$. The dotted line indicates the position of the easterly wind maximum in the middle trososphere (Burpee, 1972).

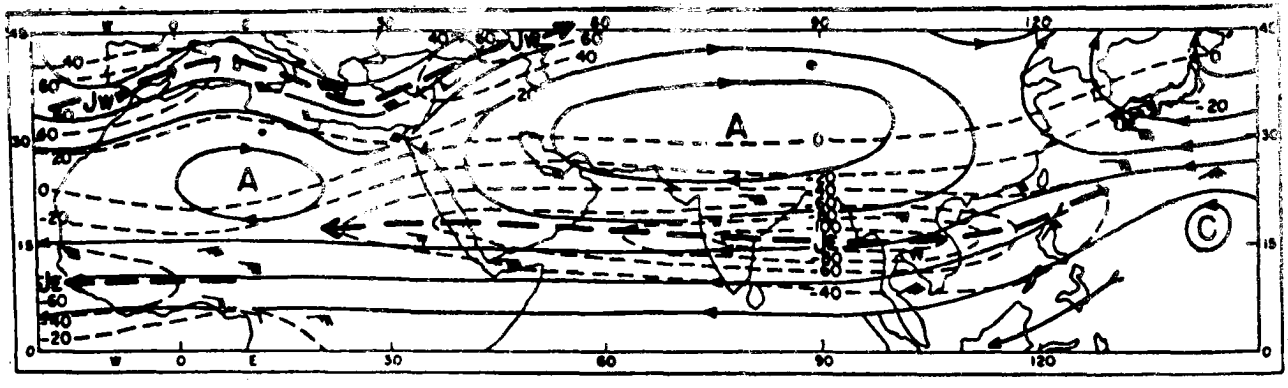

Fig. 17: Streamlines and isotachs at the 100 millibar level, 25 July 1955, 0300 GCT. Heavy dashed lines with arrows indicate position of jet axes.

JW = Westerly jet maximum
JE = Easterly jet maximum
A = Anticyclones
C = Cyclones

(From Koteswaram, See Reiter, 1961).

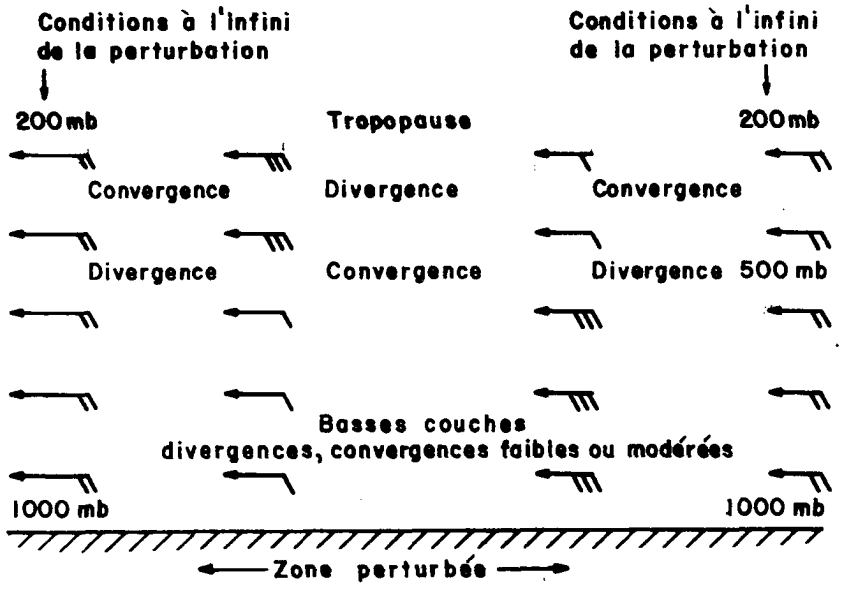

Fig. 18: Idealized representation of the wind field in a disturbance line (Tschirhart, 1958).

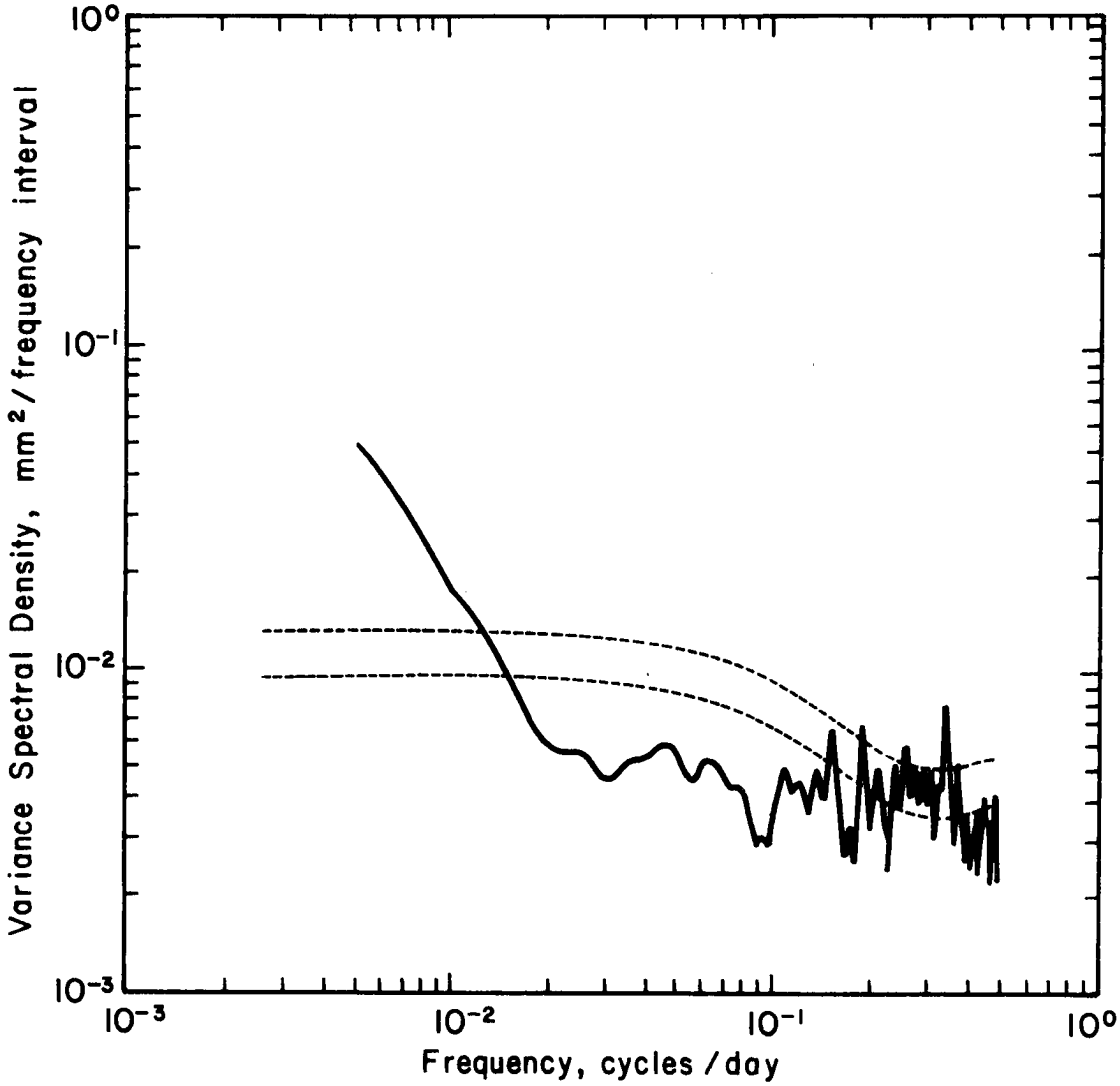

Fig. 19a: Rainfall variance spectral density for Station 1 (ABECHER, TCHAD).

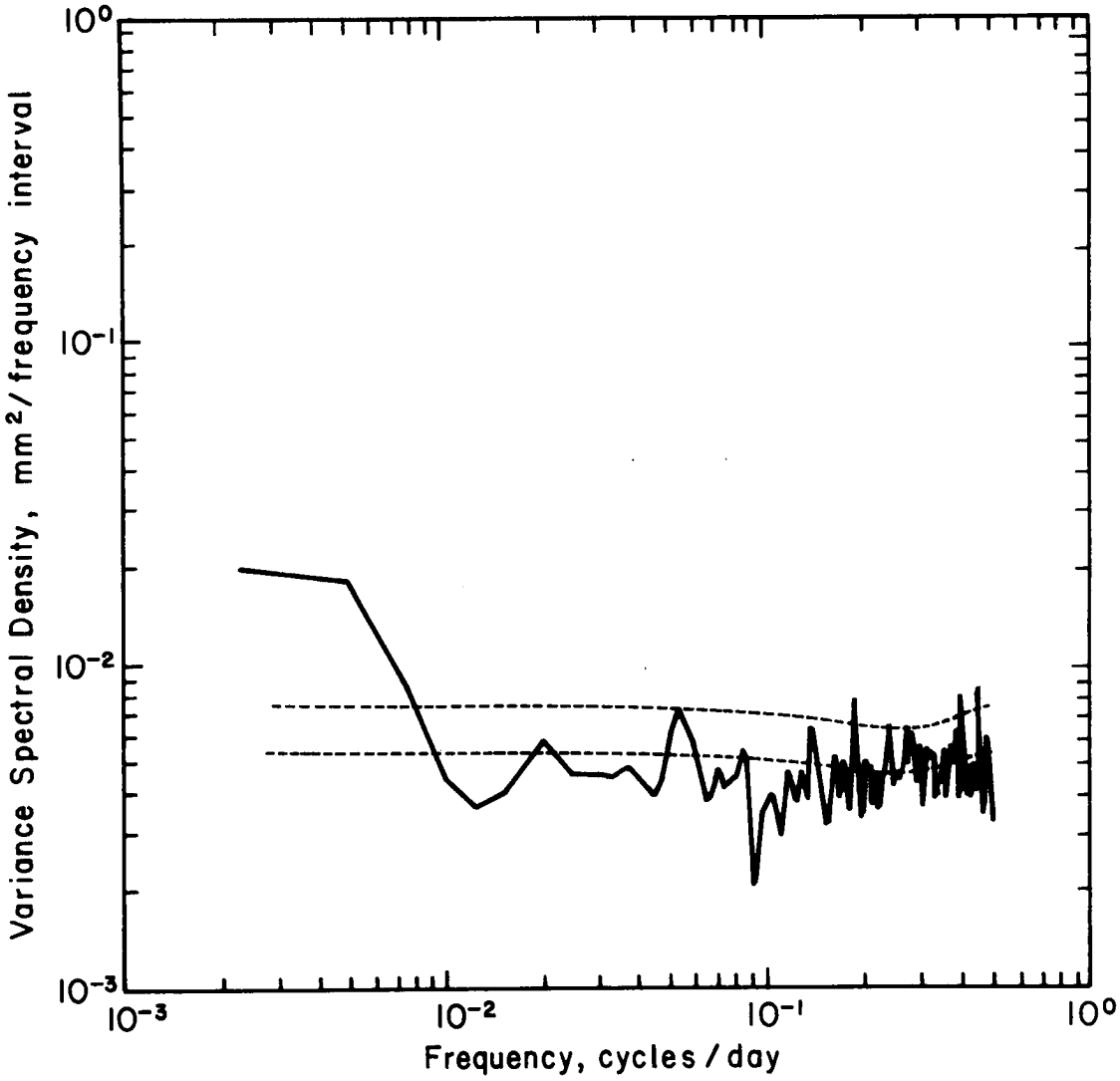

Fig. 19b: Rainfall variance spectral density for Station 5 (BANGUI, C.A.R.).

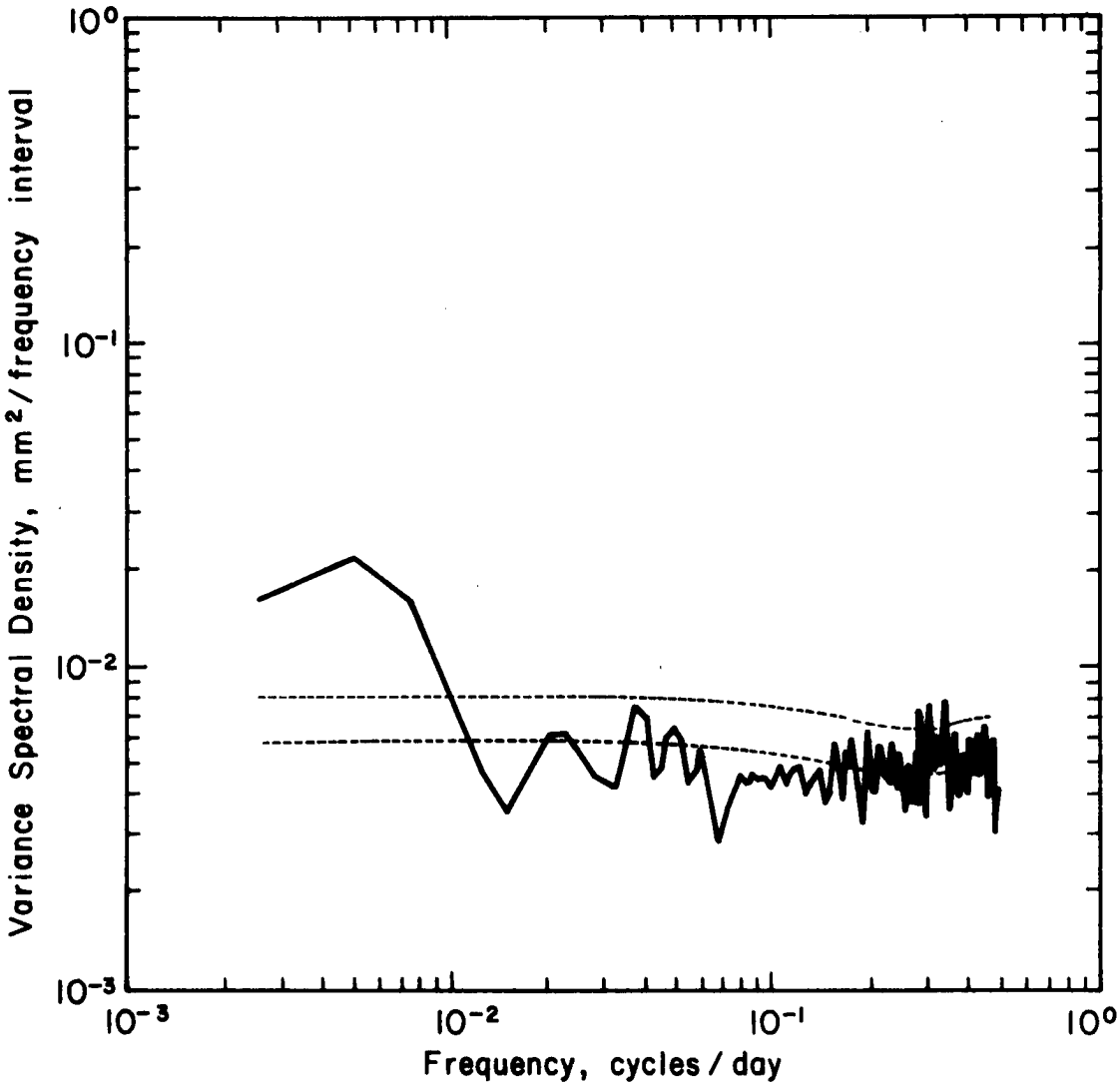

Fig. 19c: Rainfall variance spectral density for Station 6 (BATOURI, CAMEROUN).

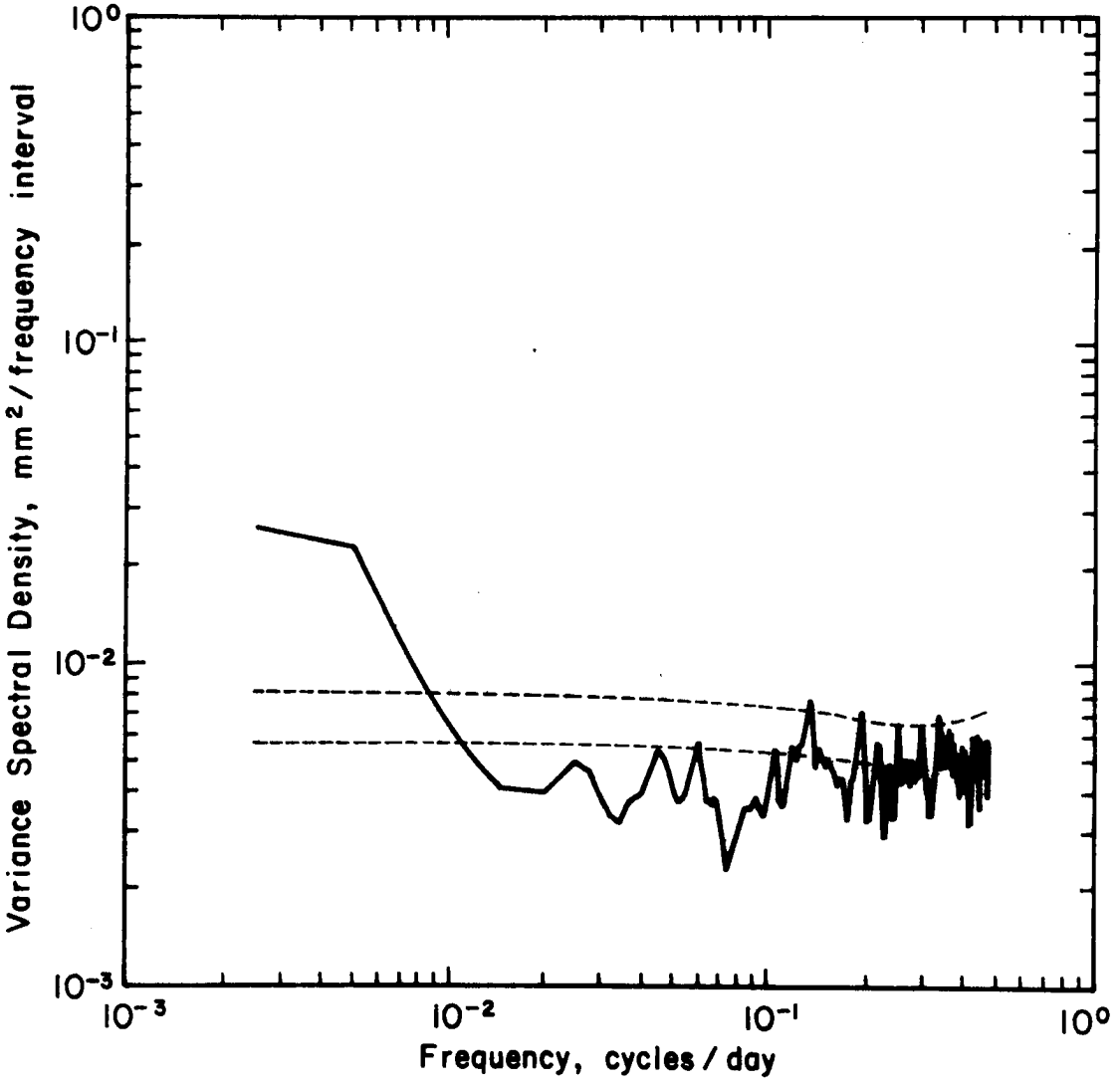

Fig. 19d: Rainfall variance spectral density for Station 11 (BRAZZAVILLE, CONGO).

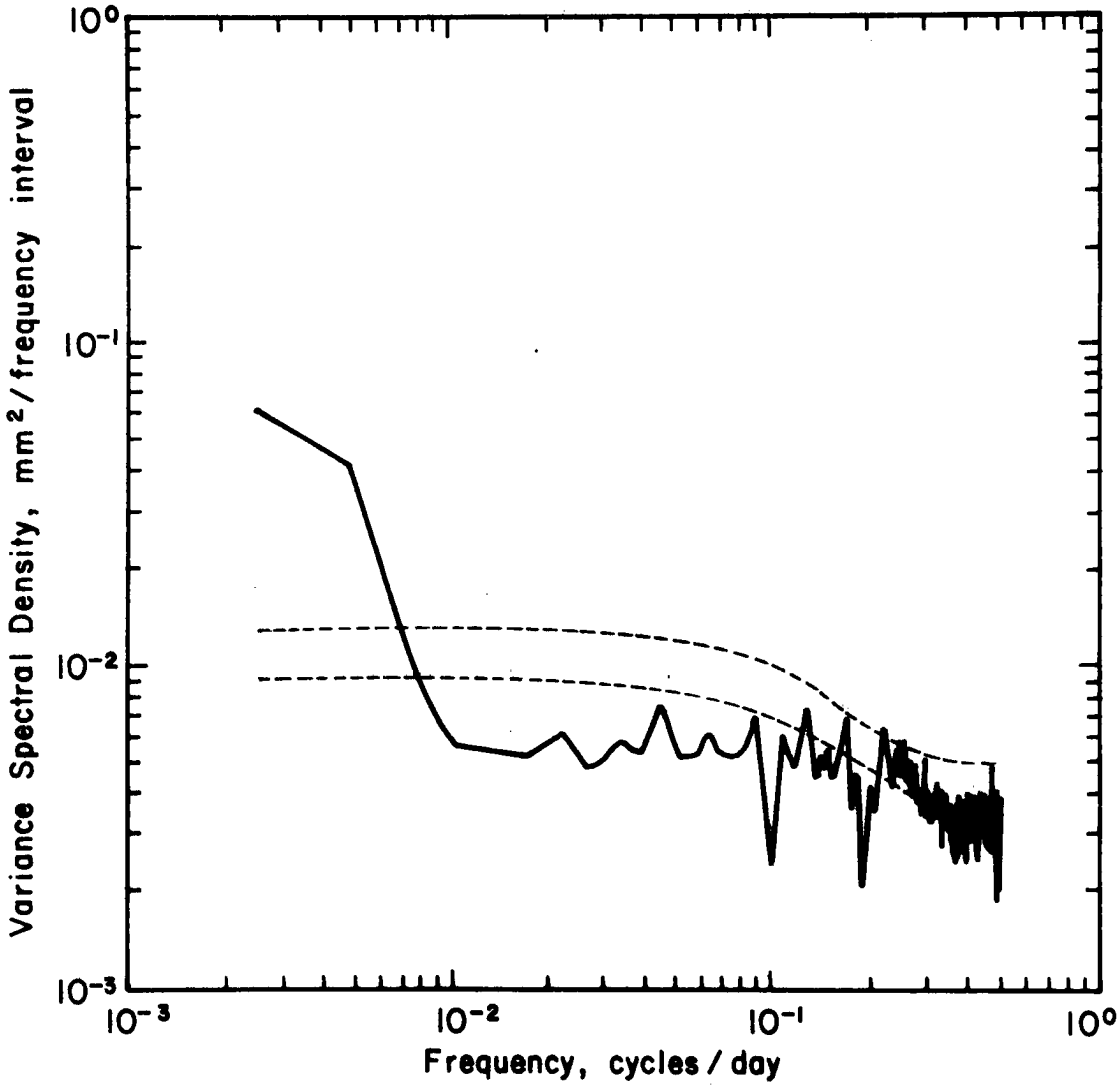

Fig. 19e: Rainfall variance spectral density for Station 13 (DOUALA, CAMEROUN).

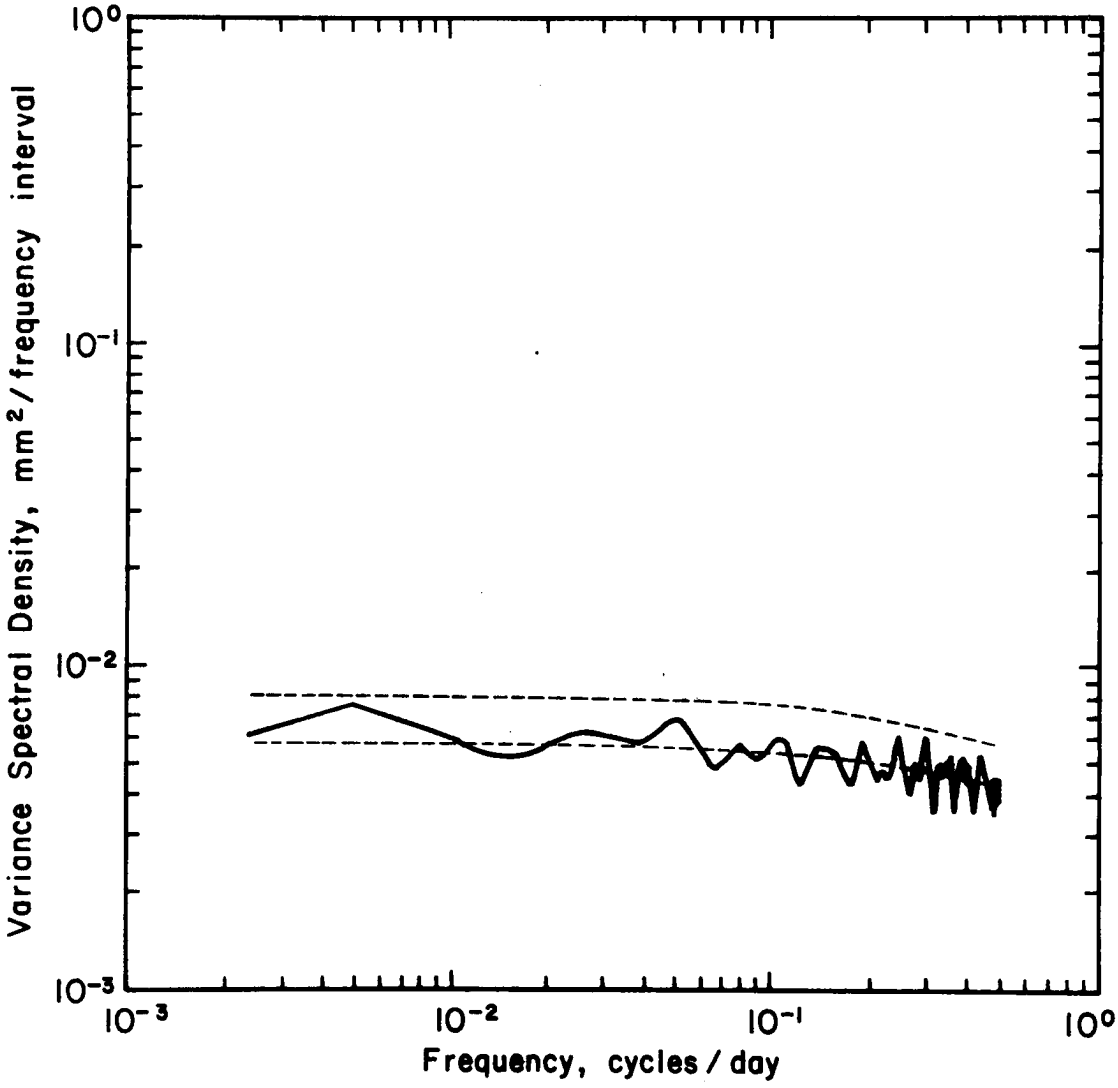

Fig. 19f: Rainfall variance spectral density for Station 15 (FAYA-LARGEAU, TCHAD).

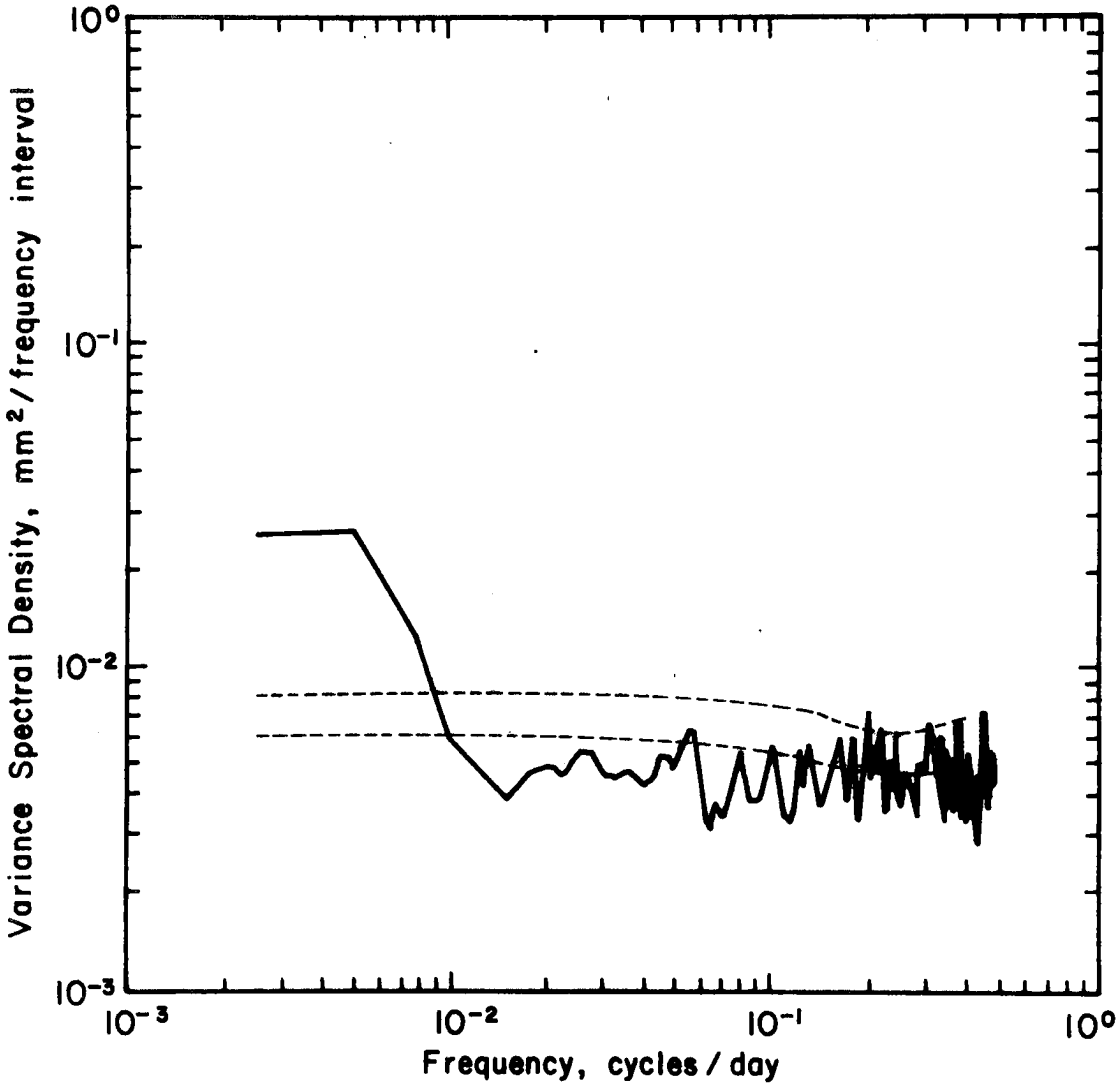

Fig. 19g: Rainfall variance spectral density for Station 16 (FRANCEVILLE, GABON).

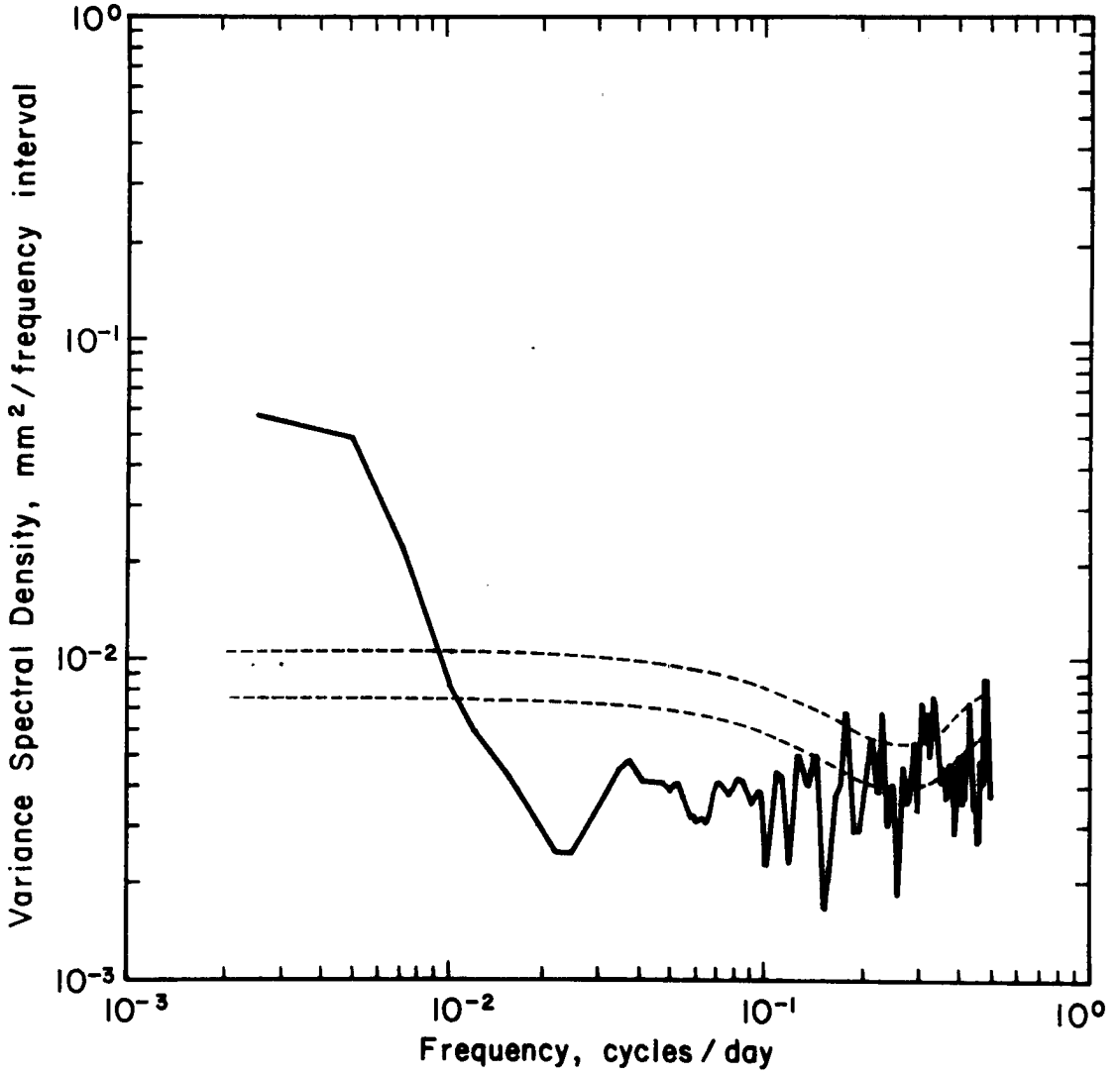

Fig. 19h: Rainfall variance spectral density for Station 18 (FORT LAMY, TCHAD).

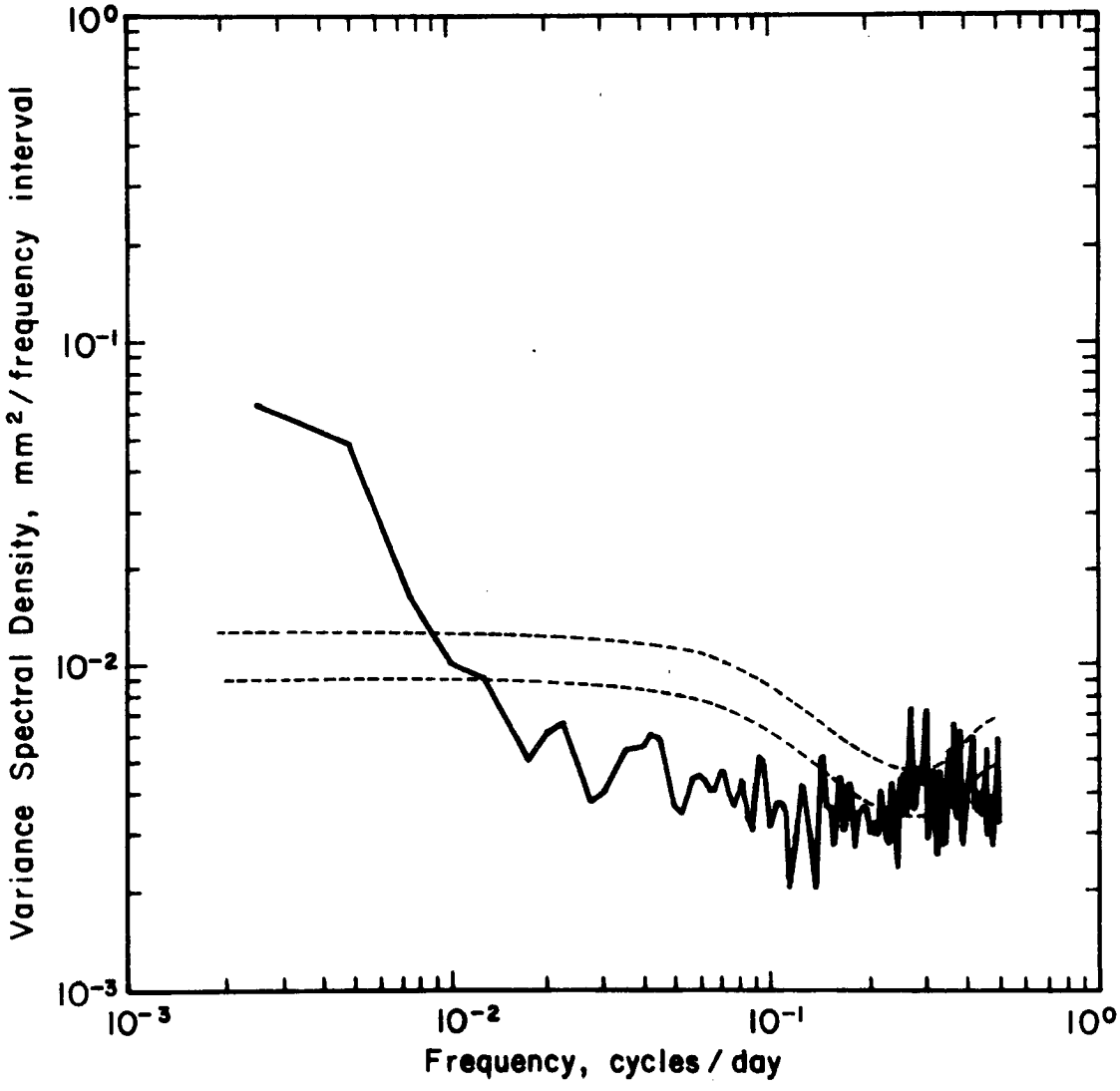

Fig. 19i: Rainfall variance spectral density for Station 21 (KOUNDJA, CAMEROUN).

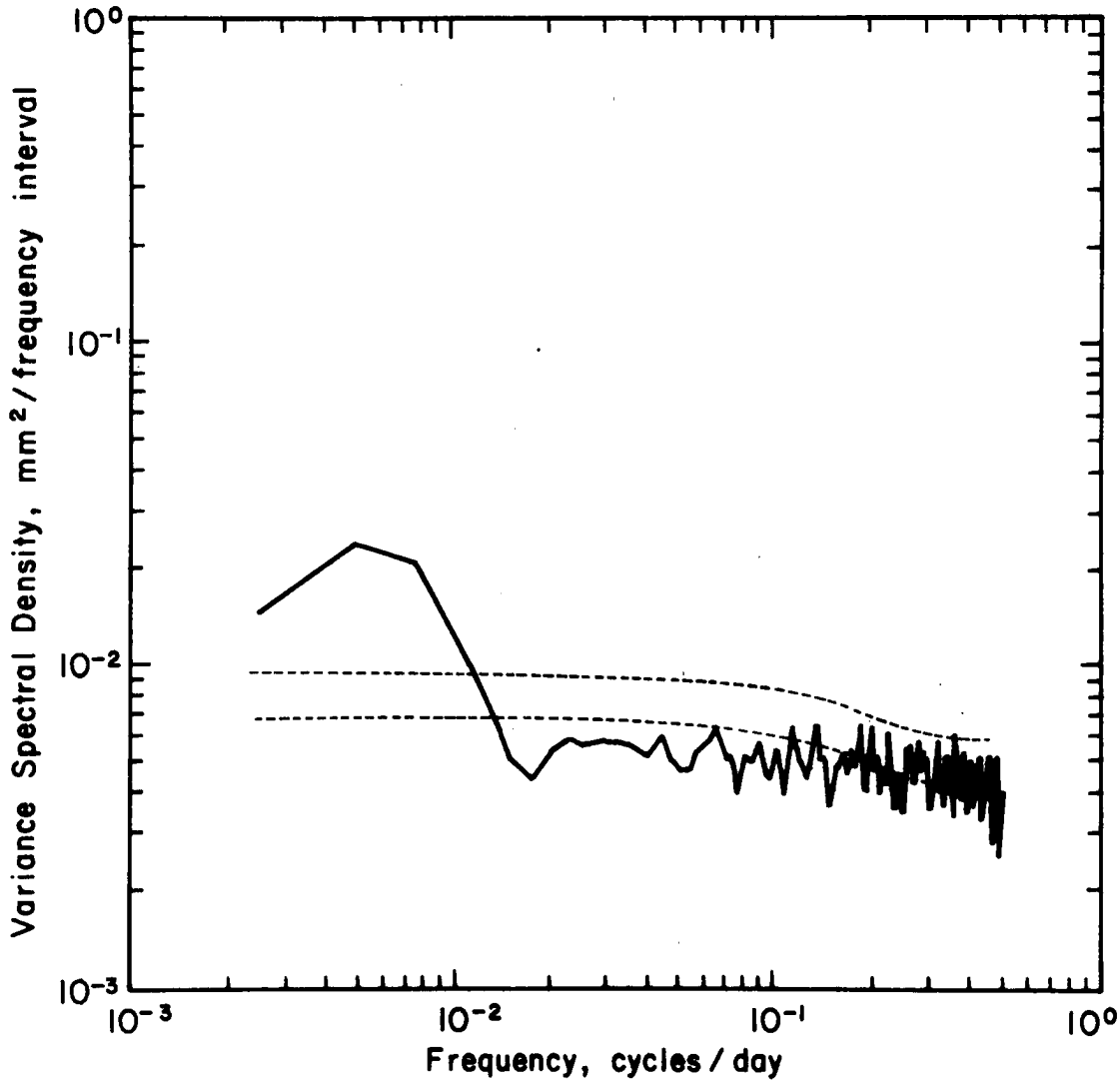

Fig. 19j: Rainfall variance spectral density for Station 22 (KRIBI, CAMEROUN).

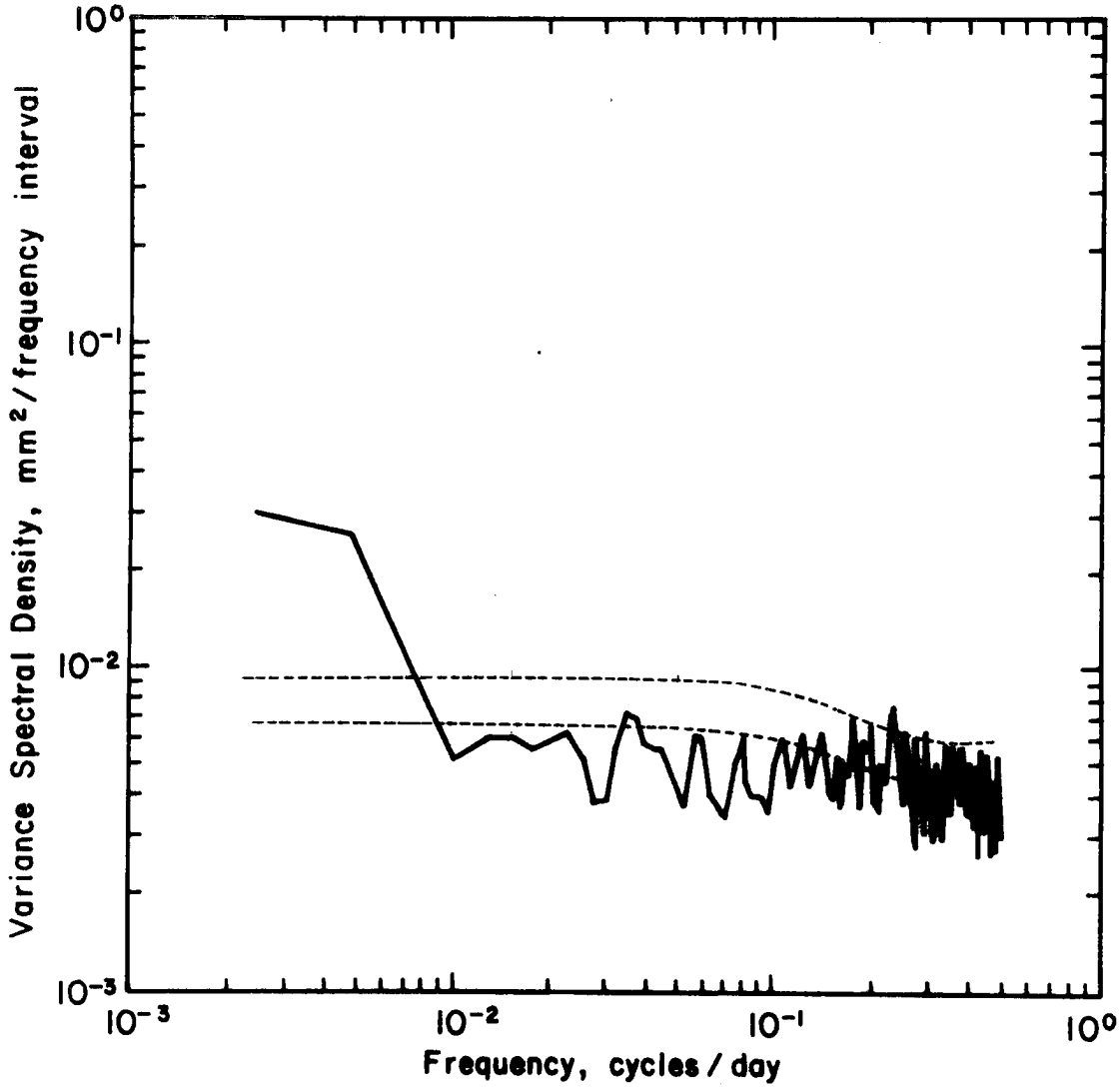

Fig. 19k: Rainfall variance spectral density for Station 24 (LIBREVILLE, GABON).

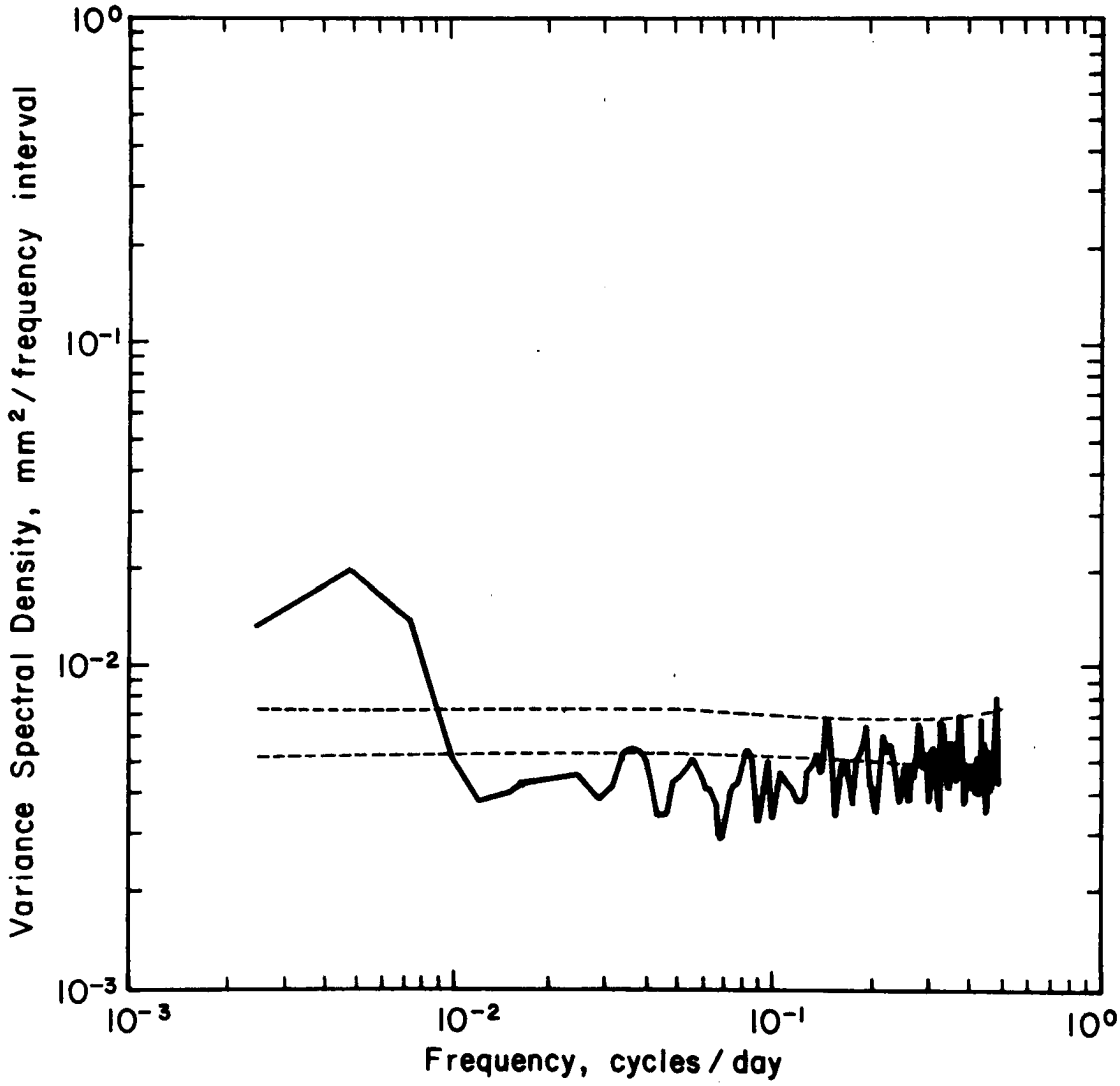

Fig. 19 1: Rainfall variance spectral density for Station 25 (LOMIE, CAMEROUN).

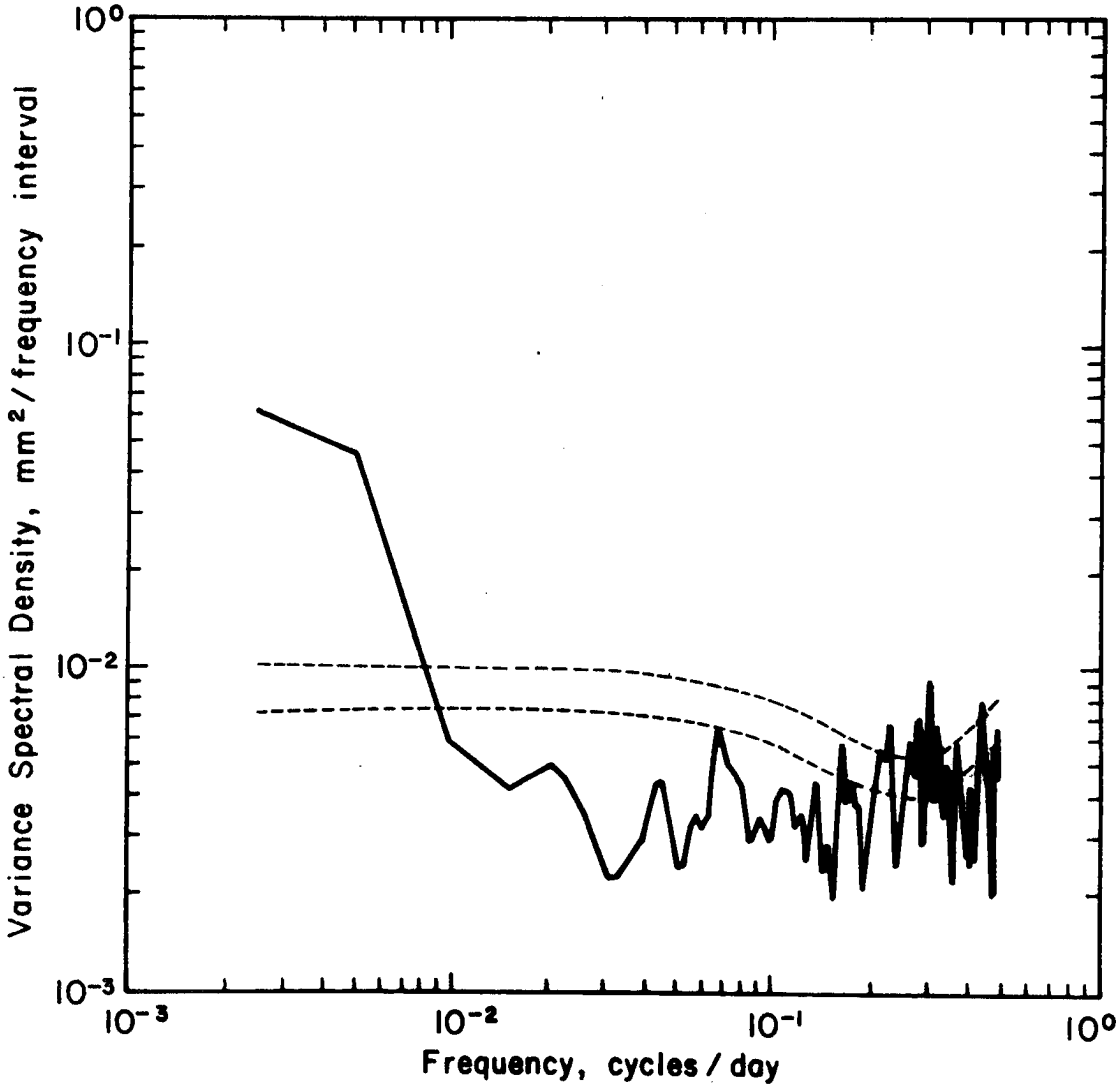

Fig. 19m: Rainfall variance spectral density for Station 27 (MAROUA, CAMEROUN).

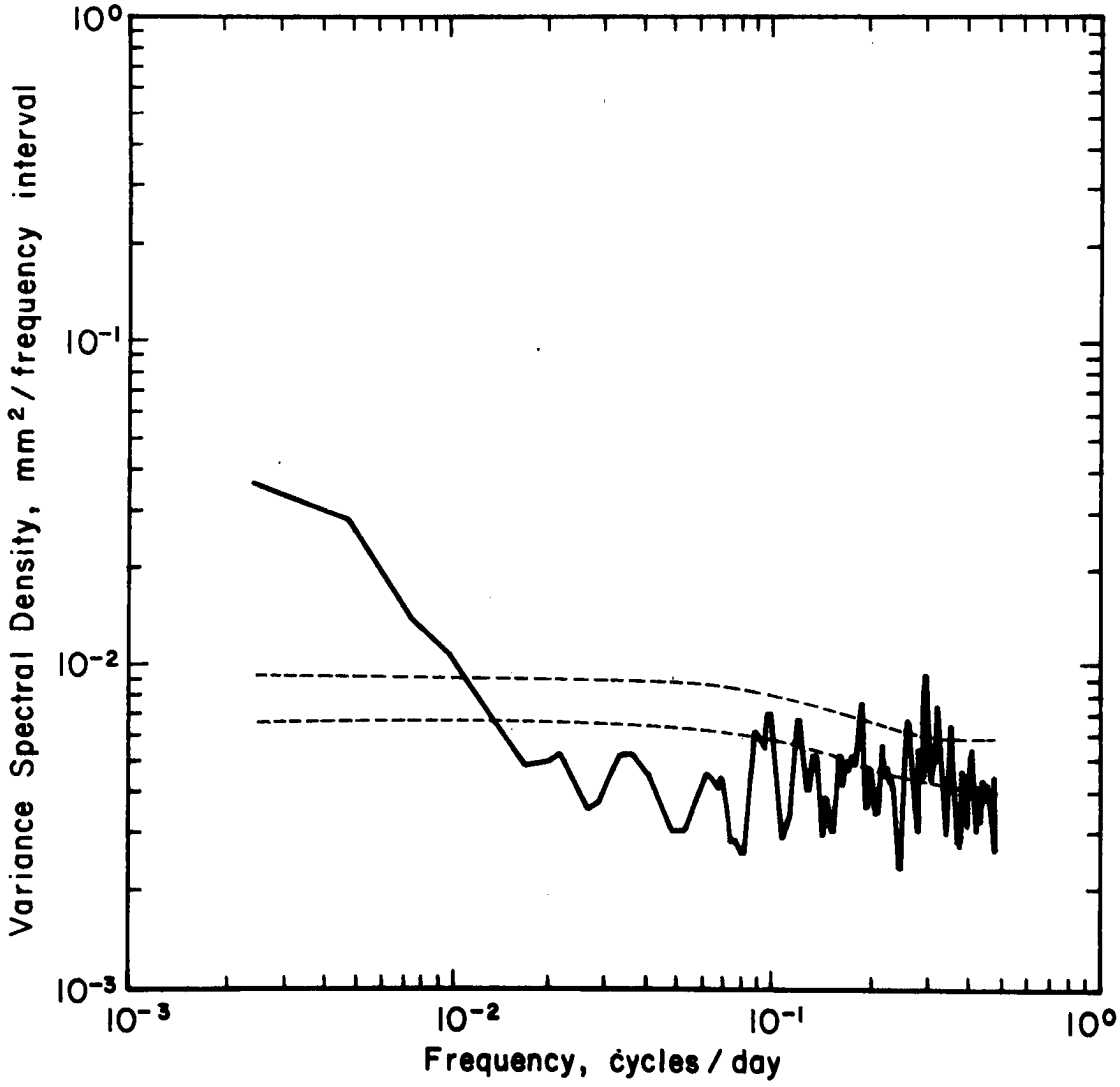

Fig. 19n: Rainfall variance spectral density for Station 28 (MAYUMBA, GABON).

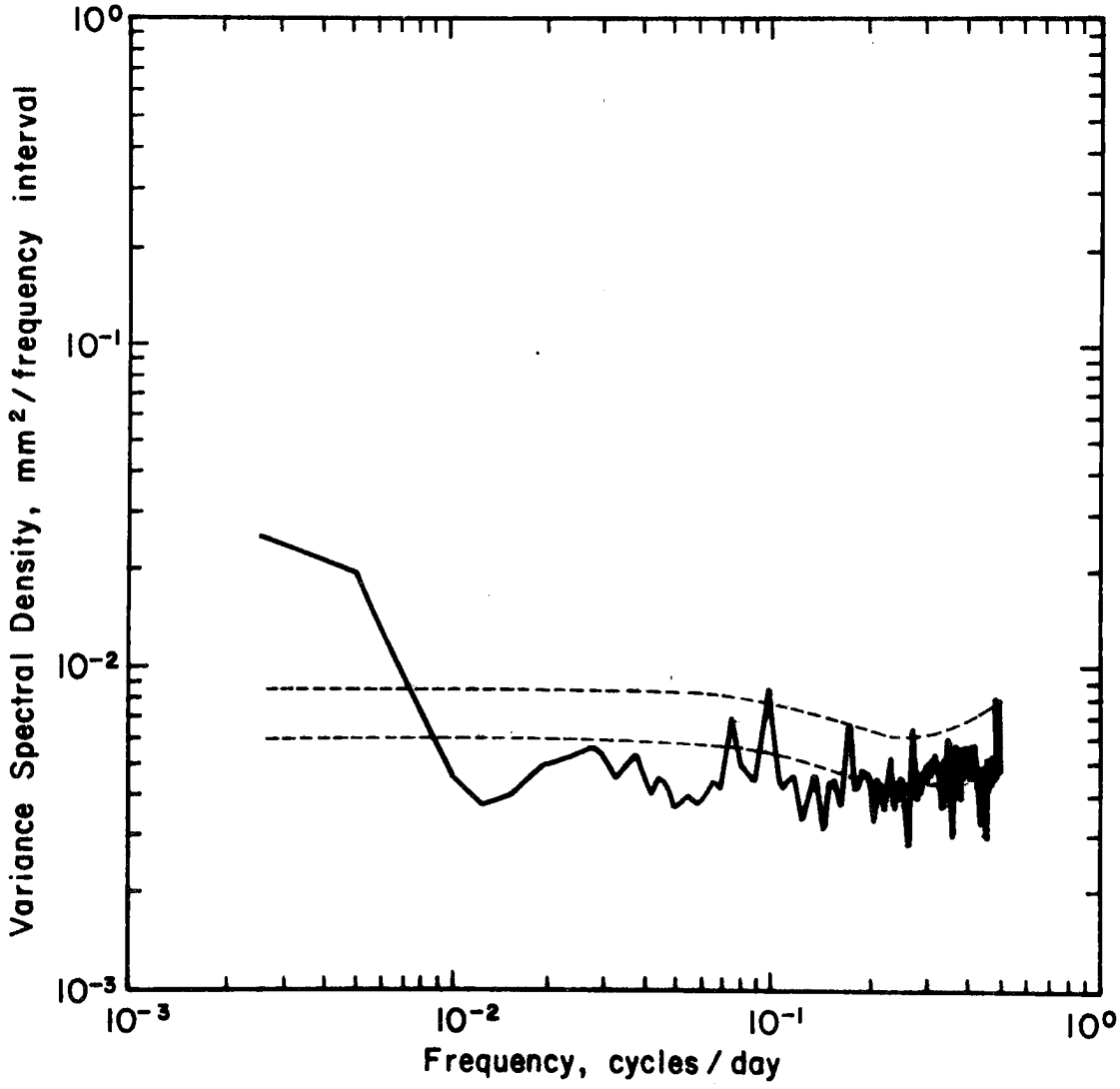

Fig. 19p: Rainfall variance spectral density for Station 31 (MOUNDOU, TCHAD).

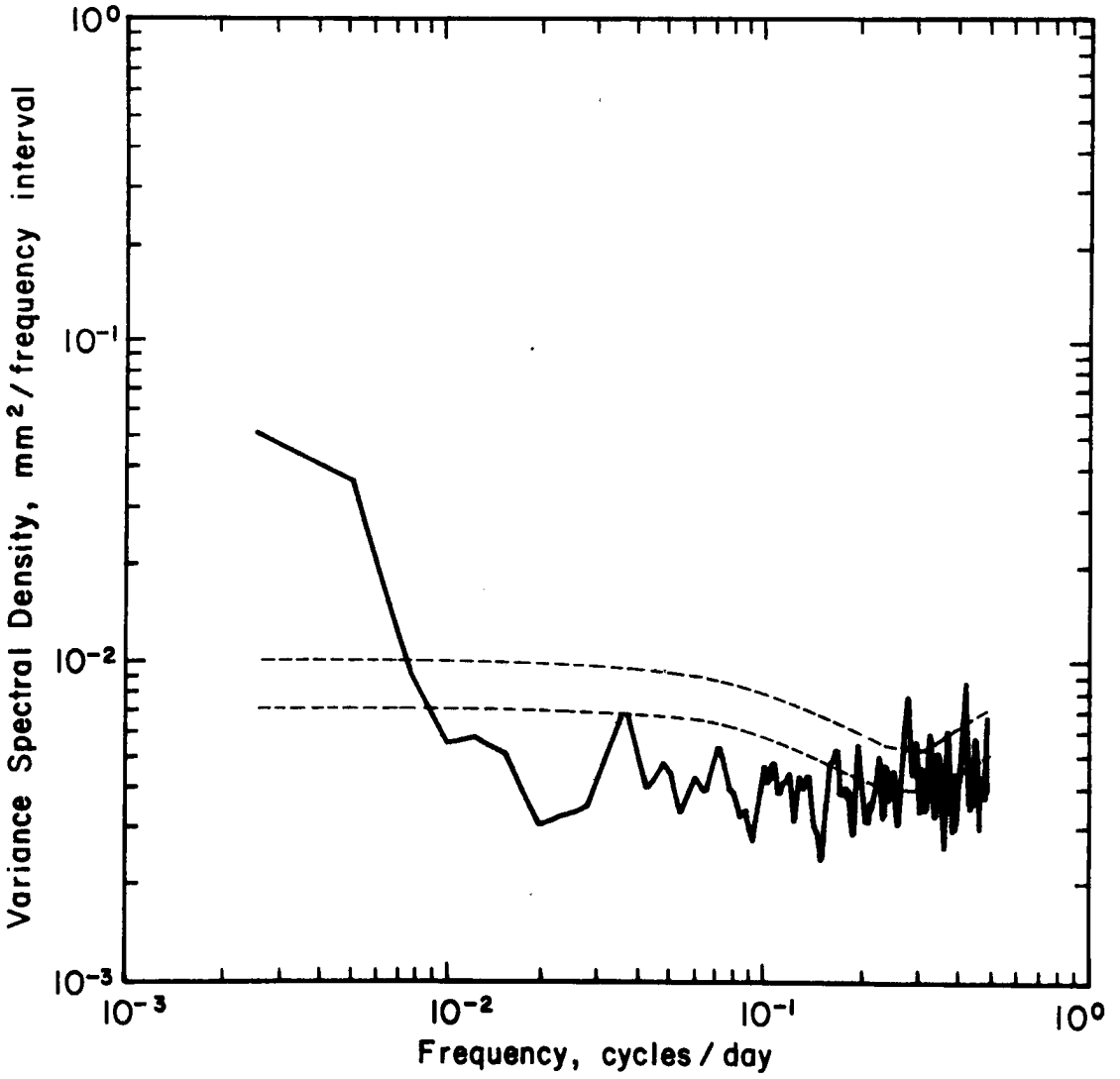

Fig. 19q: Rainfall variance spectral density for Station 32 (N'DELE, C.A.R.).

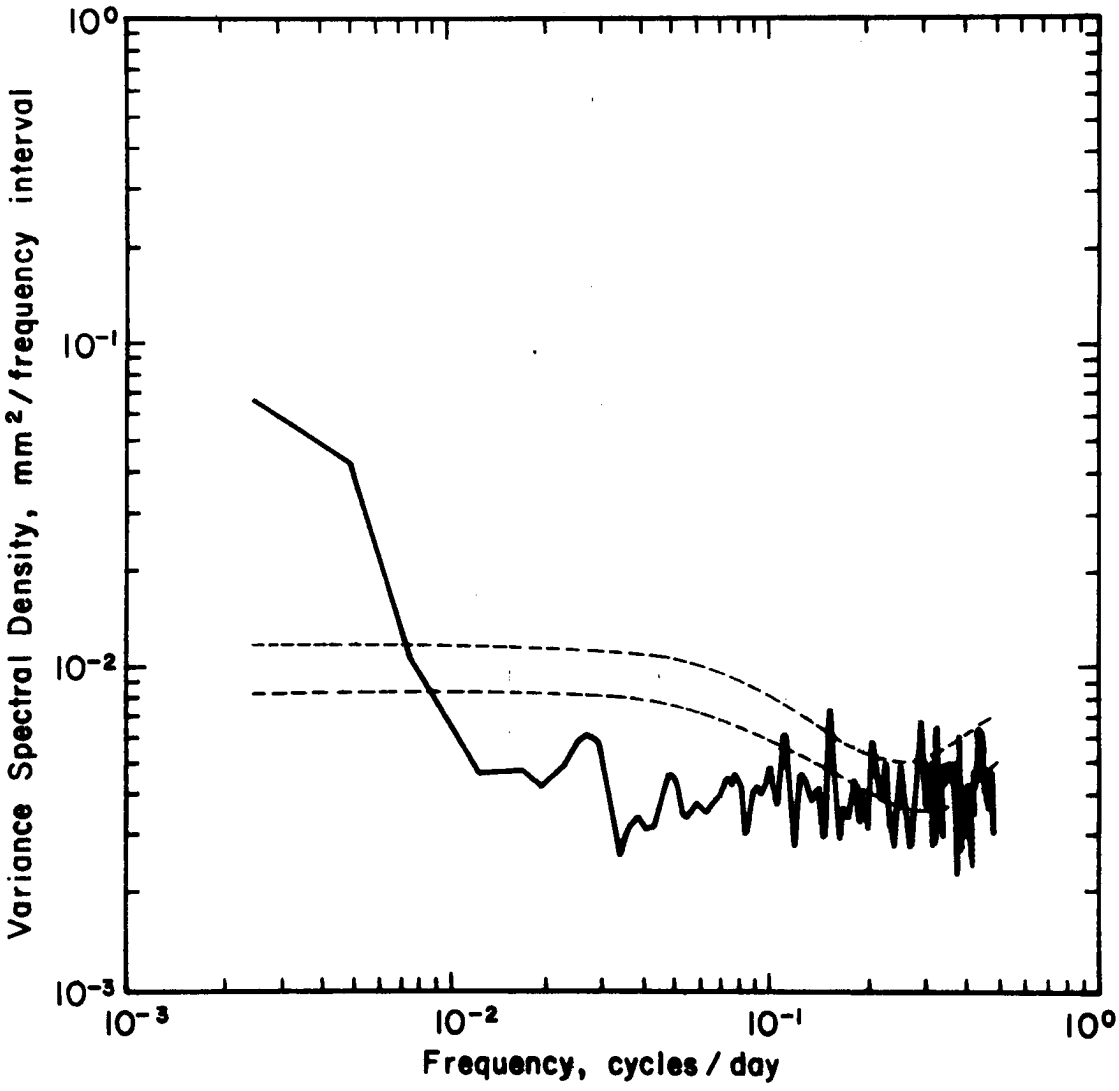

Fig. 19r: Rainfall variance spectral density for Station 33 (NGAOUNDERE, CAMEROUN).

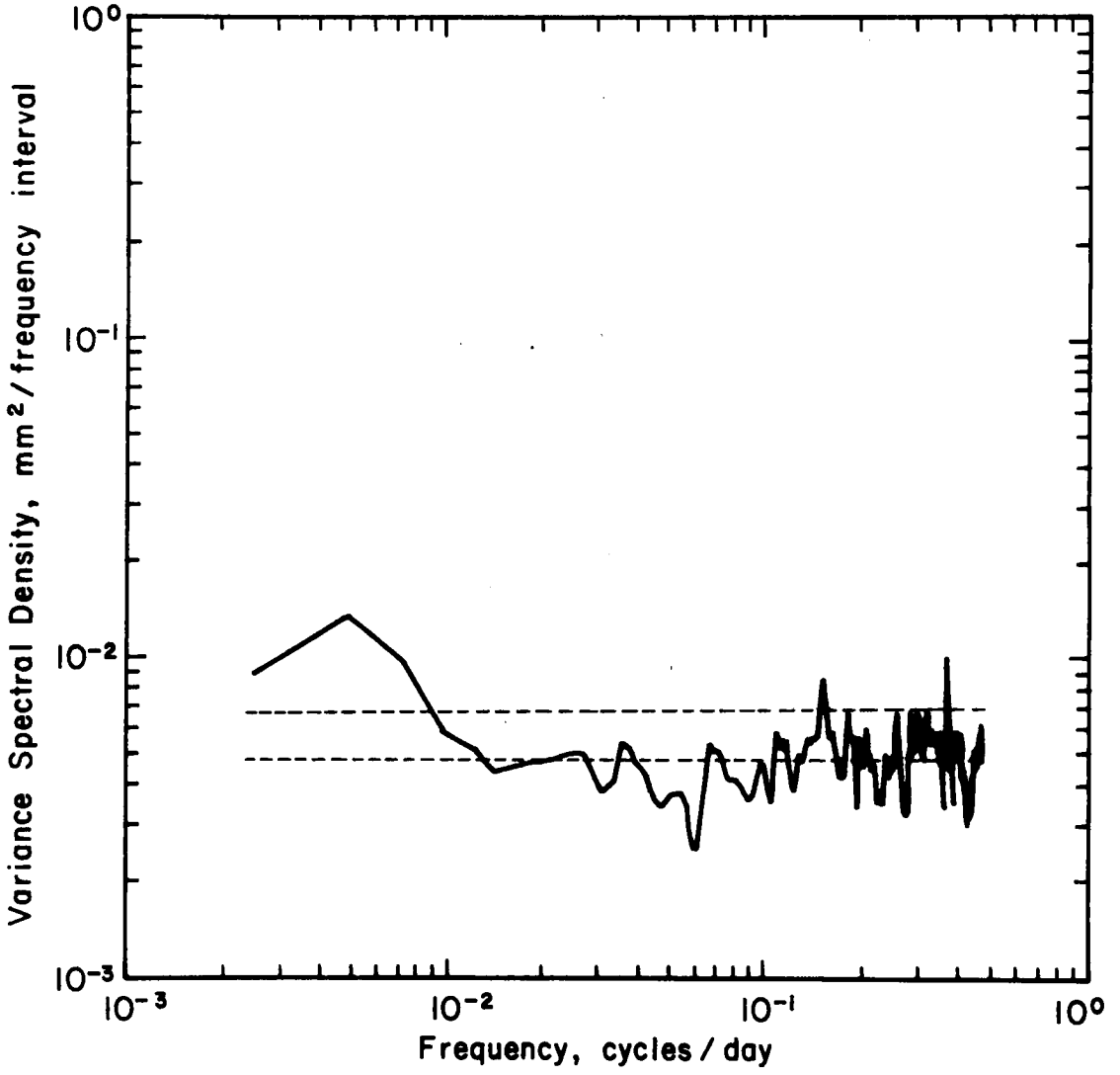

Fig. 19s: Rainfall variance spectral density for Station 35 (OUESSO, CONGO).

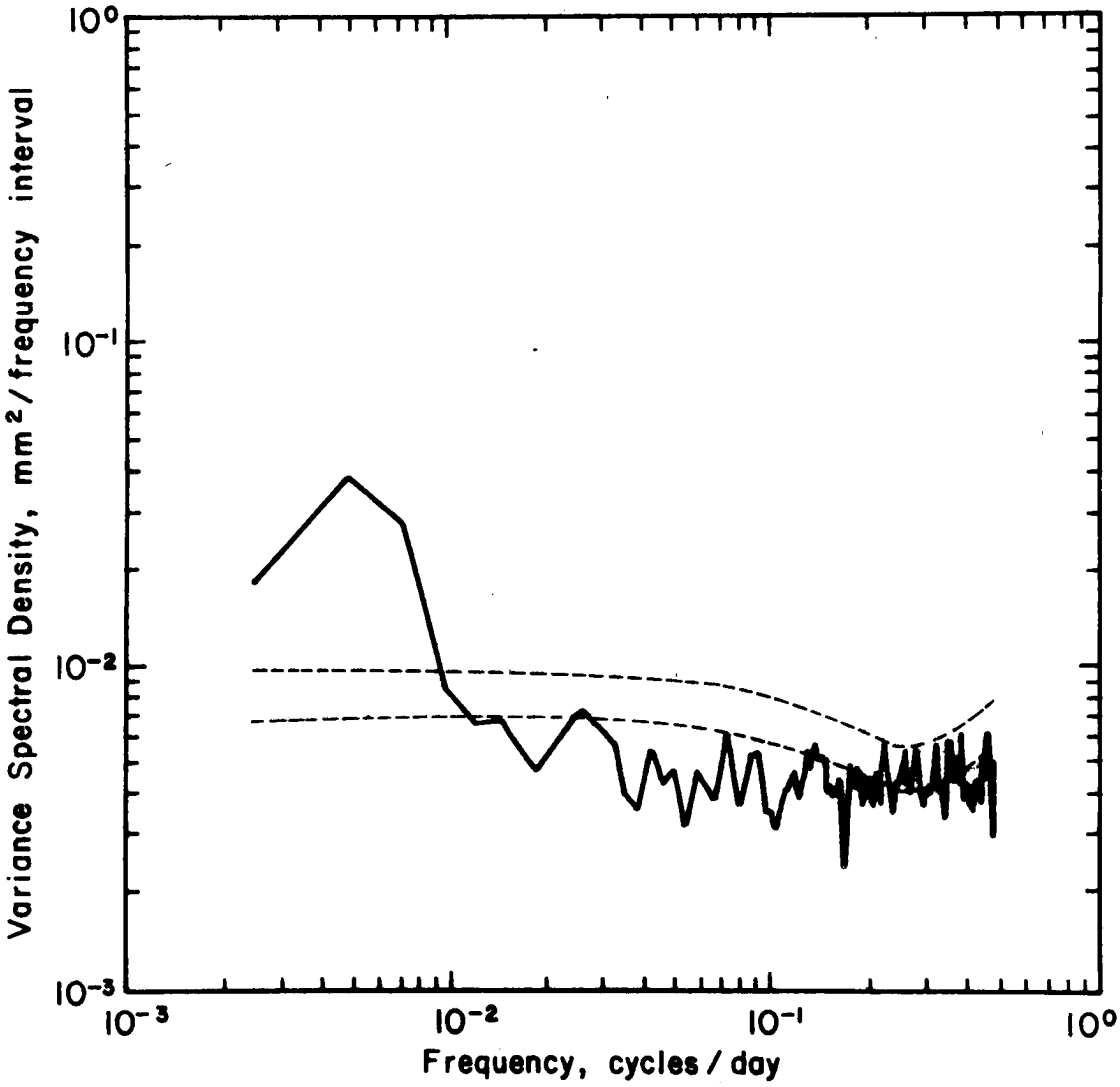

Fig. 19t: Rainfall variance spectral density for Station 40 (YAOUNDE, CAMEROUN).

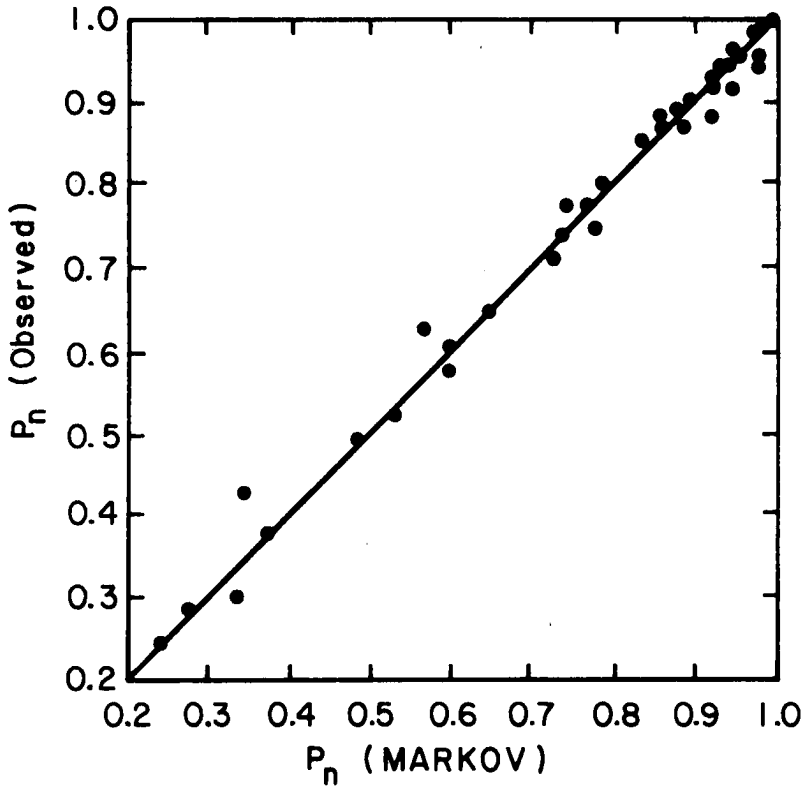

Fig. 21: Relation between observed and theoretical simple Markov chain model probabilities of rainfall occurrence (1.0 mm or more) in an interval of n days, n = 2, 3, . . . , 30 (Mbele-Mbong, 1972).

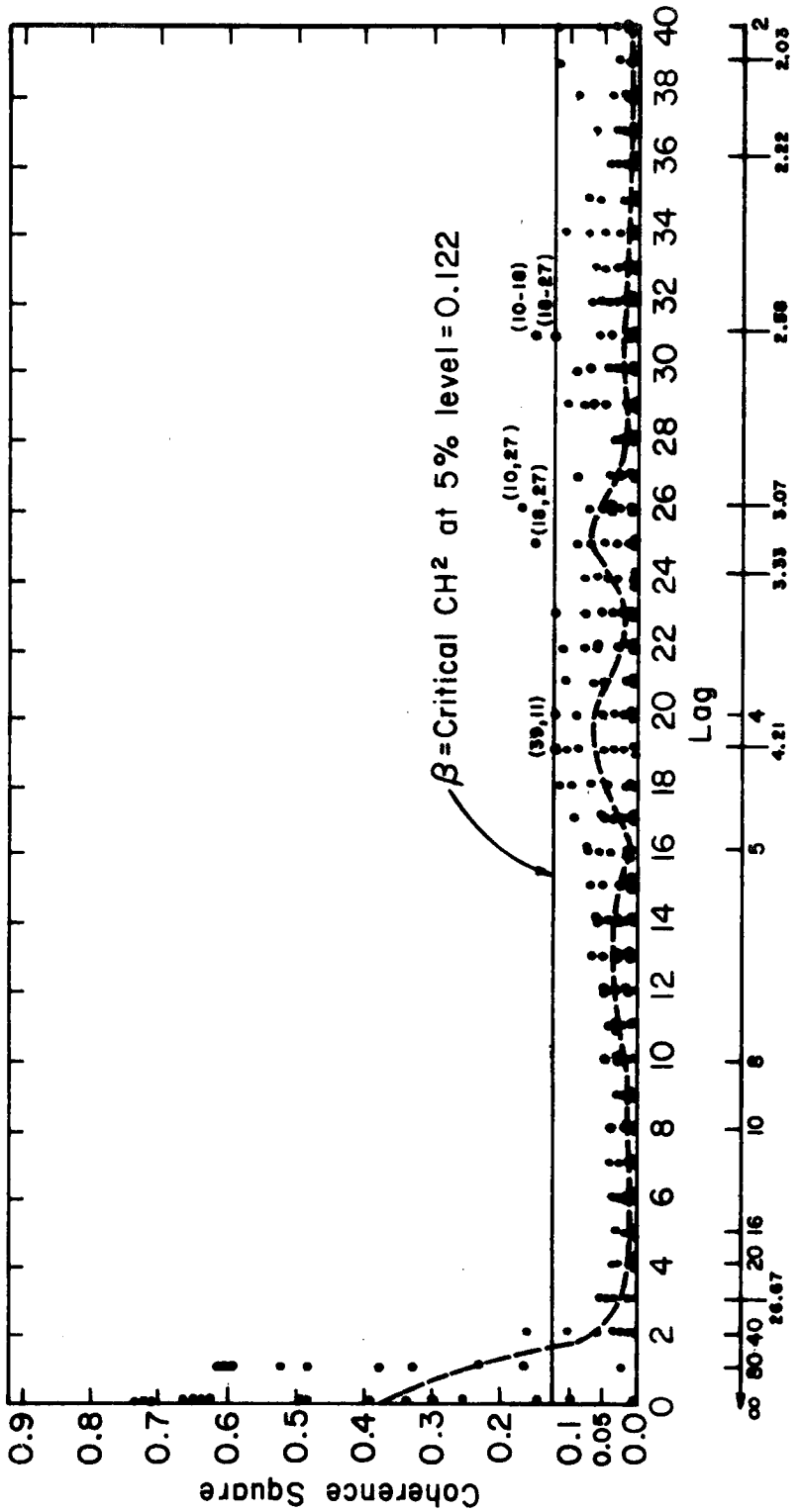

Fig. 22: Coherence square for daily rainfall amounts at all pairs of stations for the years 1954-1964.

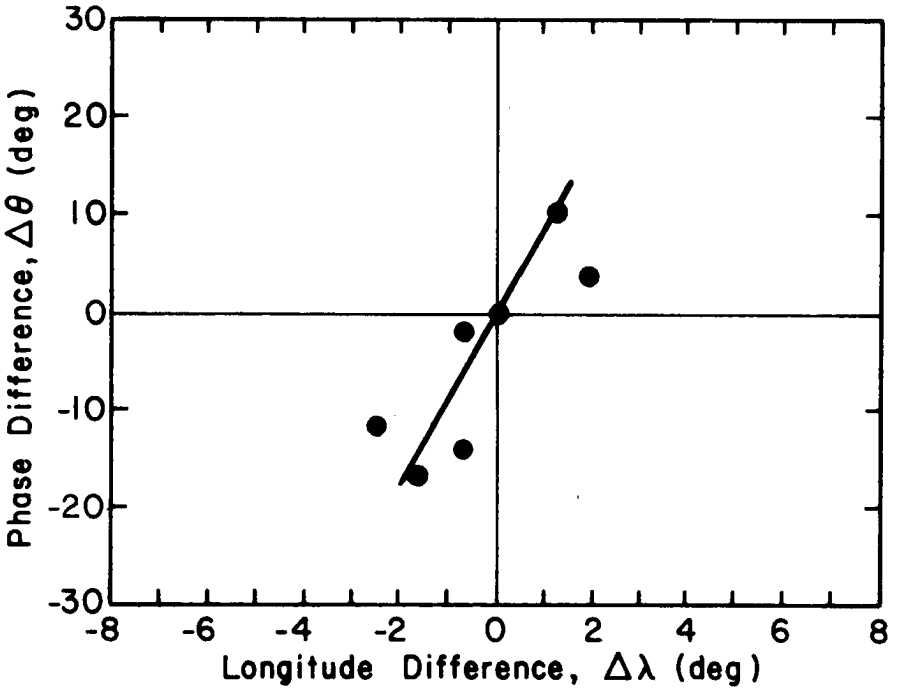

Fig. 23: Relation between the phase difference of the daily rainfall data ($\Delta\lambda$) and the longitude difference ($\Delta\lambda$) of the station pairs for the period range 2.58 - 4.21 days.

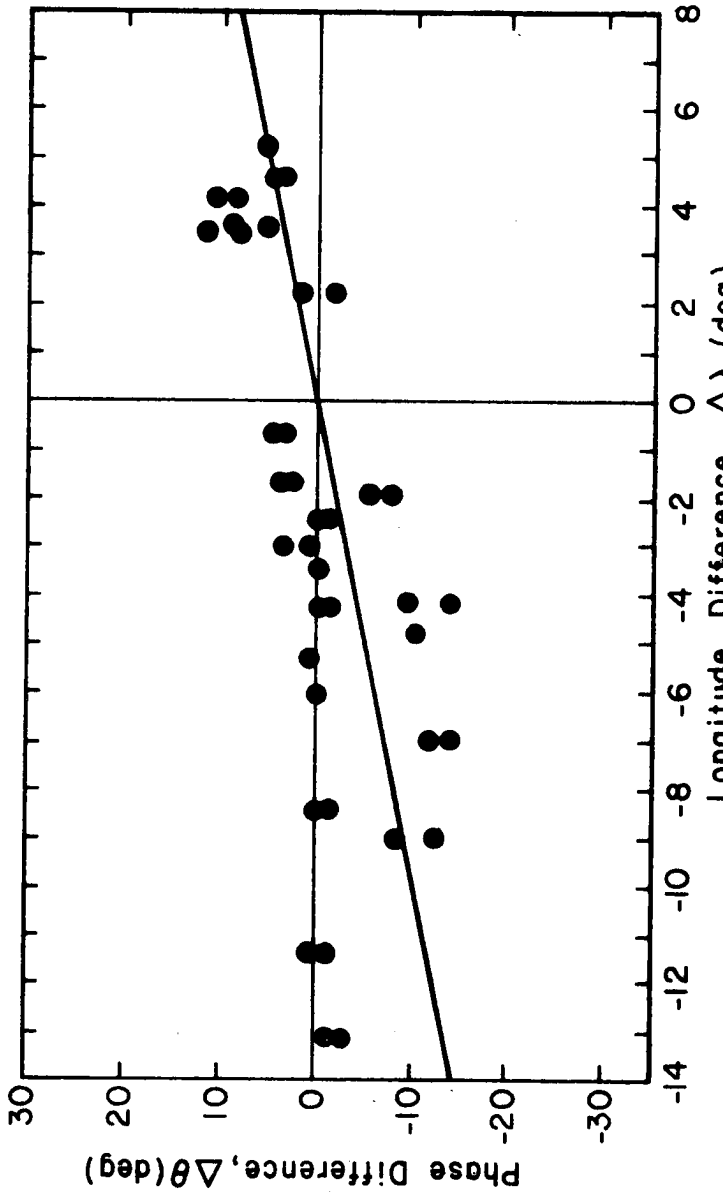

Fig. 24: Relation between the phase difference of daily rainfall data ($\Delta\theta$) and the longitude difference, $\Delta\lambda$ of the stations for periods equal to or greater than 40 days.

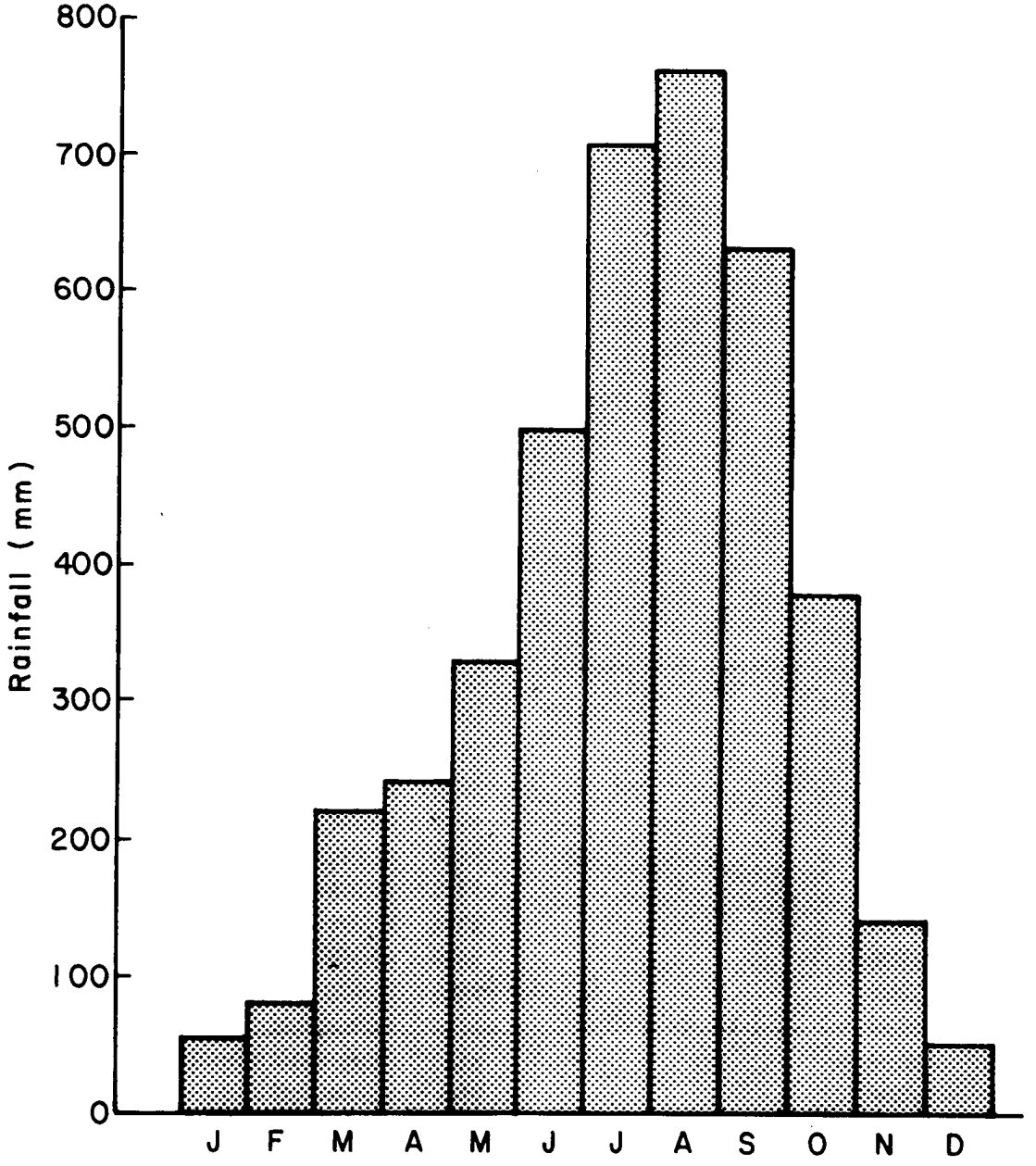

Fig. 25: Monthly mean rainfall for Douala, Cameroun, 1936-1969 (Mbele-Mbong, 1972)

BIBLIOGRAPHIC DATA SHEET	1. Report No. CSU-ATSP-222	2.	3. Recipient's Accession No.

4. Title and Subtitle

RAINFALL IN WEST CENTRAL AFRICA

5. Report Date: May, 1974

6.

7. Author(s): Samuel Mbele-Mbong

9. Performing Organization Name and Address

Department of Atmospheric Science
Colorado State University
Fort Collins, Colorado 80521

8. Performing Organization Rept. No. CSU-ATSP-222

10. Project/Task/Work Unit No.

11. Contract/Grant No. NSF GA-29147

12. Sponsoring Organization Name and Address

Atmospheric Science Section
National Science Foundation
Washington, D. C. 20550

13. Type of Report & Period Covered: Progress Report

14.

15. Supplementary Notes

16. Abstracts

An estimation of the relative importance of various factors to the rainfall in West Central Africa has been attempted. The factors considered were tropical waves, monsoon depressions, the position of the intertropical discontinuity (ITD) and the tropical easterly jet stream (TEJ) of summer. Eleven years (1954-1964) of daily rainfall amounts at 20 stations in Cameroun, Central African Republic, Congo, Gabon and Tchad were analyzed using spectral and cross spectral methods.

The spectral results revealed the presence, at nearly all stations, of wavelike oscillations with periods ranging from 2.03 to 10.25 days, and periods of about 40 days or longer. Oscillations with periods 2.58 to 4.21 days and those with periods 40 days or longer showed significant coherence magnitudes and propagated from East to West with approximate wave lengths of 500 to 2000 km, respectively. Oscillations with periods 2.58 to 4.21 days have been interpreted as cloud clusters, very likely of the "disturbance line" type which usually associate with easterly waves. Oscillations with period 40 days have been tentatively interpreted as major rain-generating disturbance perhaps of the monsoon depression type which are observed over the region in the summer months (June through September) when most of the rains fall. Preliminary indications are that the dominant factors in the rainfall in this part of Africa are the position of the ITD and the presence and speed oscillations of the TEJ.

17. Key Words and Document Analysis. 17a. Descriptors

Rainfall
Large-scale circulation
Disturbances
West Central Africa

17b. Identifiers/Open-Ended Terms

17c. COSATI Field/Group

18. Availability Statement	19. Security Class (This Report) UNCLASSIFIED	21. No. of Pages 126
	20. Security Class (This Page UNCLASSIFIED	22. Price